AD-A123 571 ALTERABLE MAGNETIC GRATINGS FOR FIBER OPTIC SWITCHING 1/1
(U) SPERRY UNIVAC ST PAUL MN DEFENSE SYSTEMS DIV
G F SAUTER ET AL. DEC 82 PX-14014 ARO-17201.2-EL
UNCLASSIFIED DAAG29-80-C-0134 F/G 17/2 NL

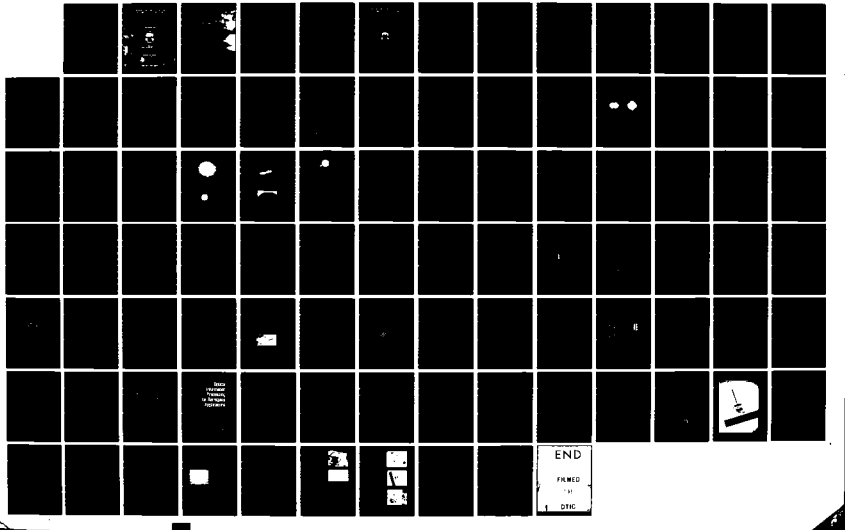

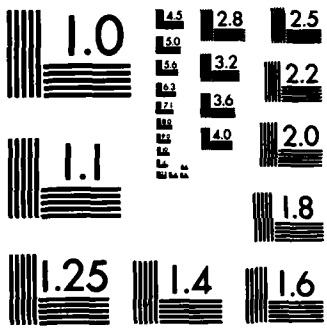

MICROCOPY RESOLUTION TEST CHART
NATIONAL BUREAU OF STANDARDS-1963-A

ALTERABLE MAGNETIC GRATINGS FOR FIBER OPTIC SWITCHING

FINAL REPORT

G. F. Sauter J. A. Krawczak G. L. Nelson F. G. Hewitt

DECEMBER 1982

U.S. ARMY RESEARCH OFFICE
Contract No. DAAG29-80-C-0134

SPERRY UNIVAC

PX 14014

THE FINDINGS IN THIS REPORT ARE NOT TO BE
CONSTRUED AS AN OFFICIAL DEPARTMENT OF
THE ARMY POSITION, UNLESS SO DESIGNATED
BY OTHER AUTHORIZED DOCUMENTS.

Unclassified

SECURITY CLASSIFICATION OF THIS PAGE (When Data Entered)

ARO 17201.2-EL

REPORT DOCUMENTATION PAGE		READ INSTRUCTIONS BEFORE COMPLETING FORM
1. REPORT NUMBER PX-14014	2. GOVT ACCESSION NO. AD-A123571	3. RECIPIENT'S CATALOG NUMBER
4. TITLE (and Subtitle) ALTERABLE MAGNETIC GRATINGS FOR FIBER OPTIC SWITCHING		5. TYPE OF REPORT & PERIOD COVERED Final July 1980 - Dec. 1982 6. PERFORMING ORG. REPORT NUMBER
7. AUTHOR(s) G. F. Sauter, J. A. Krawczak G. L. Nelson, F. G. Hewitt		8. CONTRACT OR GRANT NUMBER(s) DAAG29-80-C-0134
9. PERFORMING ORGANIZATION NAME AND ADDRESS Sperry Defense Systems P. O. Box 43525 St. Paul, MN 55164-0525		10. PROGRAM ELEMENT, PROJECT, TASK AREA & WORK UNIT NUMBERS 17201-EL
11. CONTROLLING OFFICE NAME AND ADDRESS U.S. Army Research Office Electronics Division, Box 12211 Research Triangle Park, NC 27709		12. REPORT DATE December 1982 13. NUMBER OF PAGES 84
14. MONITORING AGENCY NAME & ADDRESS (if different from Controlling Office)		15. SECURITY CLASS. (of this report) Unclassified 15a. DECLASSIFICATION/DOWNGRADING SCHEDULE

16. DISTRIBUTION STATEMENT (of this Report)

Approved for public release;
distribution unlimited.

17. DISTRIBUTION STATEMENT (of the abstract entered in Block 20, if different from Report)

NA

18. SUPPLEMENTARY NOTES

Further Journal and/or conference reporting of portions of this document are highly probable. Credit for sponsorship and copies of manuscripts will be given to Army Research Office. The findings in this report are not to be construed as an official department of the

19. KEY WORDS (Continue on reverse side if necessary and identify by block number)

Faraday rotation	fiber optics
stripe domain array	field alterable grating
garnet wafer	active star coupler
optical switch	nonblocking fiber optic switchboard

20. ABSTRACT (Continue on reverse side if necessary and identify by block number)

Optical mode switching of fiber light can enhance the capability of fiber optic communications systems by eliminating opto-electronic-opto converters at switching nodes and by performing the switching even on crosstalk-prone high data rate channels. During this program several aspects of the stripe domain alterable grating were studied in a fiber optic switch mode.

(cont.)

DD FORM 1 JAN 73 1473 EDITION OF 1 NOV 65 IS OBSOLETE

Unclassified

SECURITY CLASSIFICATION OF THIS PAGE (When Data Entered)

18.
Supplementary Notes Cont.

Army position, unless so designated by other authorized documents.

20.
Abstract cont.

Calculations and/or experiments revealed that a garnet epitaxial wafer containing a magnetic stripe domain grating functions as a diffraction type fiber optic switch when millimieter size integrable stripline drive coils are utilized to rapidly orient the grating. Random access switching in 140 nanoseconds was measured. This led to the realization that a high density fiber optic non-blocking PBX type switch is possible in which the input/output spaces contain hundreds of high data rate subscribers. A subspace of this nxm arrangement is the simple 1xm (m→20) switch for bus organized topclogies. Experiments with a centimeter size 1x4 model indicated that loss is 14 db. and crosstalk 41 db. at .85 microns. For 1.3 microns the garnet material was found to be virtually transparent. Along with the switching function wavelength demultiplexing by the grating was demonstrated.

Two different versions of a stripe domain active star coupler were conceived - one was actually demonstrated. In this case input fiber light could be switched between the 1 of m mode and the all of m conferencing mode in 2 microseconds.

For the sake of completeness a survey of fiber optic switches was made and suggestions for deployment stated.

ALTERABLE MAGNETIC GRATINGS FOR FIBER OPTIC SWITCHING

FINAL REPORT

G. F. Sauter J. A. Krawczak G. L. Nelson F. G. Hewitt

DECEMBER 1982

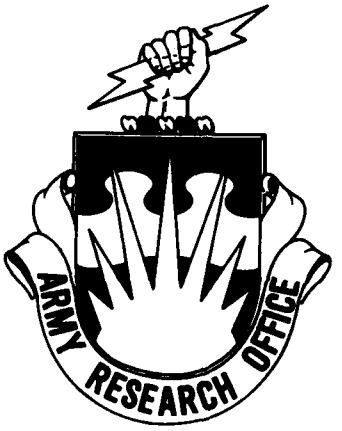

U.S. ARMY RESEARCH OFFICE
Contract No. DAAG29-80-C-0134

SPERRY UNIVAC
DSD
St. Paul, MN 55164

PX 14014

TABLE OF CONTENTS

PARTICIPATING SCIENTIFIC PERSONNEL

Dr. Gerald F. Sauter
Dr. Fred G. Hewitt
John A. Krawczak
Gary L. Nelson
E. James Torok

PUBLICATIONS

1. G. F. Sauter, R. W. Honebrink, J. A. Krawczak, "Alterable Grating Fiber Optic Switch," Applied Optics, Vol. 20 No. 20, 1981.

2. E. J. Torok, F. G. Hewitt, J. A. Krawczak, G. L. Nelson, "Manipulation Of Light With Magneto-Optic Stripe Domain Films," NASA Conference on Optical Information Processing for Aeorspace Applications, 1981.

3. Further publication is highly probable.

STATEMENT OF THE PROBLEM

Magnetic stripe domain garnet films were studied in the fiber optic switch mode. A fiber optic switch based on the new garnet technology has solid state nonvolatility, good optical properties at the important fiber wavelengths, wide temperature range, polarization independence, multimode or singlemode fiber capability, submicrosecond response, low switching energy, switchboard or bus topologies, strong or weak tapping of input fibers, active star coupling and physical dimensions compatible with fiber optic componentry. Thus such devices offer many opportunities for research in both fundamental properties and in applications to future Army communication systems.

In this contract garnet characterization was performed at fiber optic wavelengths, various switch configurations were constructed and evaluated for loss and crosstalk, dynamic response of the grating was studied, an active star coupler was conceived, demultiplexing was demonstrated and a switch survery was completed.

BACKGROUND

Magneto-Optic Beam Steering

Magneto-optic laser beam steering by means of the Faraday effect or the magneto-optic Kerr effect in stripe domains that occur quite naturally in transparent magnetic crystals has been shown to possess characteristics which tend to overcome or circumvent problems which limit other techniques.[1] The magneto-optic beam steering device can also be used to deflect incoherent or randomly-polarized light, and so can be used for passive steering (receiving) and fiber optics.[2,3]

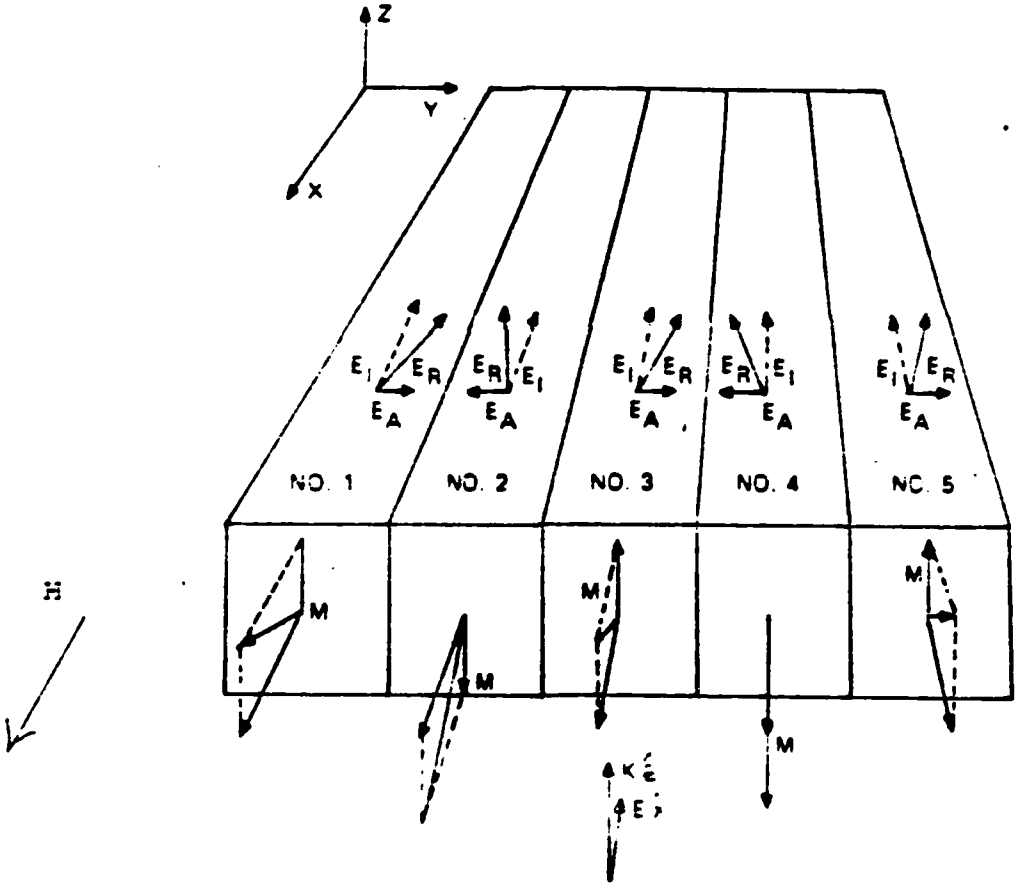

Figure 1. Magnetic Stripe Domains In a Platelet.

A magneto-optic light deflector based on the stripe domain phenomenon is inherently a wide angle, two dimensional low divergence deflector. In general, diffraction of a light beam occurs as a result of a periodic variation in the wave amplitude or phase across a wave normal surface. Magnetic stripe domains can introduce a periodic 180^{o} phase variation in a light beam. Consider an array of stripe domains in a magnetic platelet and a light beam propagating normal to the platelet as in figure 1. A stripe domain is a long, straight region of uniform width in which the magnetization vector is nearly constant. In an array of parallel stripe domains, the magnetization in every domain has one component which lies in the plane of the platelet parallel to the strip direction. This component has a constant magnitude everywhere in the array and causes the stripes to line up with the applied magnetic field. The other magnetization component which is normal to the plane of the platelet introduces the periodic phase variation in the light beam. This component points parallel to the z-axis in the even-numbered domains. Since the sense of the magneto-optic polarization rotation depends on whether the light propagates parallel or anti-parallel to the magnetization, this arrangement produces a differential Faraday rotation between light passing through the even-numbered domains and the light passing through the odd-numbered domains. The differentially rotated light beam has an electric component which is orthogonal to the incident electric vector polarization and which has 180^{o} alternations (parallel and anti-parallel to the y-axis) which match the periodic domain structure. In the far field region, this alternating vector adds constructively at angles Θ_n given by $\text{Sin } \Theta_n = n\lambda/2d$ where d is the width of the domain, λ is the light beam wavelength, and n is the order of the beam ($n = 0,1,3,5...$). The maximum intensity in the diffracted beams is attained when the Faraday rotation is $\pm 90^{o}$. In this special case, none of the transmitted light goes into the zero order beam, 81% of the light goes into the first order diffracted beams, 9% goes into the third order beams, and so on.

The direction and period of the magnetic grating are controllable by a magnetic field H that is applied in the plane of the film. Typically H is derived from two small Helmholtz pairs or stripline coil sets oriented perpendicularly so that any field direction in the plane is attainable by programming the coil currents. Required field intensities are around 100 gauss, similar to electron beam deflection intensities in CRTs. Figure 2 depicts the method of achieving solid state two dimensional light deflection with field driven stripe domains. In 2a an incident collimated beam is deflected by the grating according to the Bragg rule. The applied H field in 2b reorients the grating to the field direction. Deflected light tracks the reorientation, describing an arc in the image plane. As the intensity of the field increases (2c) the periodicity of the grating decreases while maintaining squarelike character, This drives the beam out to a higher deflection angle. Using the fields to deflect light results in random access or raster type scan in a polar coordinate space.

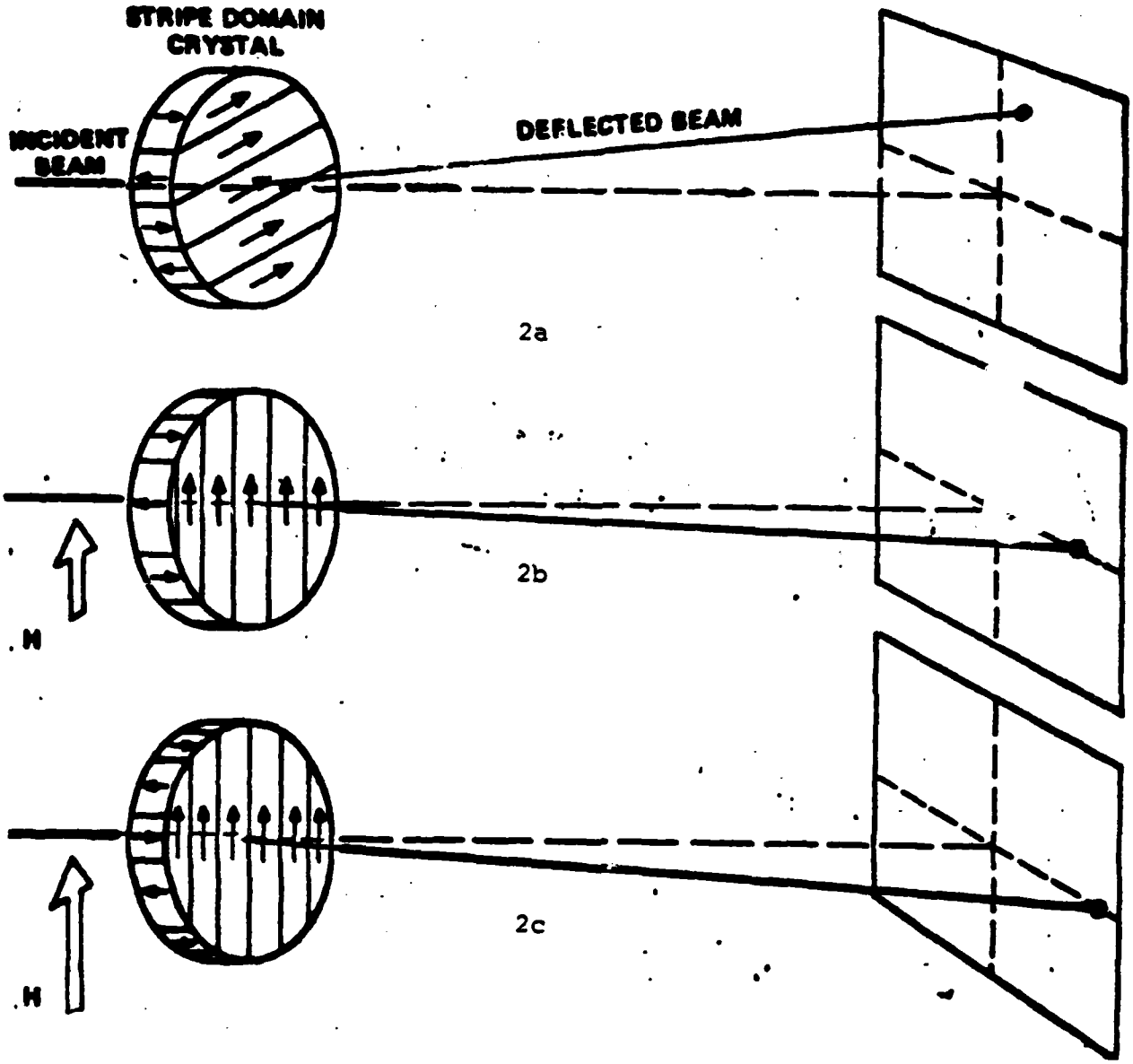

Figure 2. Two Dimensional Light Deflection With Magnetic Field Alterable Stripe Domains.

The rate at which a stripe domain deflector can slew the beam is the rate at which the stripe domains can be altered. This depends on the intrinsic properties of the stripe domain element and the rate at which the external magnetic fields used to control the stripes can be changed. The two basic switching modes for magnetic platelets are wall motion and magnetization rotation. While the speeds of both modes depend on the materials used and magnitude of the fields applied, switching in the latter mode occurs typically in ten nanoseconds while in the former mode it takes a few microseconds. Switching in 150 nanoseconds has been observed experimentally.

Materials

Although there are several candidate materials at wavelengths extending from .45 microns to 11 microns for which the stripe domain state is energetically favored, the most promising fiber optic material to date is bismuth doped rare earth iron garnet grown epitaxially on nonmagnetic garnet substrates. Epitaxial growth of bismuth garnet deflector films has evolved to the point where high quality samples are readily attainable using substrates and techniques developed for magnetic bubble memory devices.

Material requirements for stripe-domain magneto-optic crystals including bismuth garnet films are:

1) Large Paraday rotation to allow reasonable film thickness.

2) Low optical absorption for deflection efficiency and power handling.

3) Low coercivity (H_c) for low power requirements.

4) Normal anisotropy (H_k-crystalline, growth induced or strain induced) to produce stripe domains.

5) Low inplane anisotropy to allow rotational linearity.

6) Proper H_k to $4\pi M$ ratio to produce stripe domains.

7) High crystalline uniformity for low beam divergence and low scattering.

8) Good chemical, thermal and mechanical stability for environmental compatibility.

Applications

Applications for stripe domain light deflection include general purpose active and passive scanning of laser or ambient light, optical processing of extended images and high or low density fiber optic switchboards.

SUMMARY OF FINDINGS

Faraday Rotation Measurements

In a stripe domain phase diffraction grating the deflection efficiency is proportional to

$$\sin^2 F(\lambda)t$$

where $F(\lambda)$ is the Faraday rotation of the material and t the thickness of a particular wafer.[4] Typically F is a monotonically decreasing function as λ moves into the infrared from the visible.

The Faraday rotation of bismuth garnet samples including the new large lattice films was measured at several wavelengths. The data in figure 3 shows Faraday rotation on conventional gadolinium and large lattice scandium bismuth garnet. Data at 1.3, 1.15 and .8 microns was acquired as part of this contract. Recently samples have been grown on neodymium large lattice constant wafers and some rotation data obtained. This is contained in figure 4, where rotation is plotted against lattice size. An approximate doubling in rotation is seen relative to films grown on GGG. Since efficiency goes with the square of rotation a factor of 4 or better efficiency has been realized. Enhanced rotation occurs when increasing amounts of bismuth are incorporated in the film. Increasing the lattice size allows more bismuth to stably enter the film promoting further increases in rotation and ultimately efficiency. For instance, at .8 microns a 3G based film 40 microns thick has 5% efficiency. If the same film had been placed on the largest available lattice garnet, the efficiency would approach 20% provided that optical absorption does not increase. This is presently being explored.

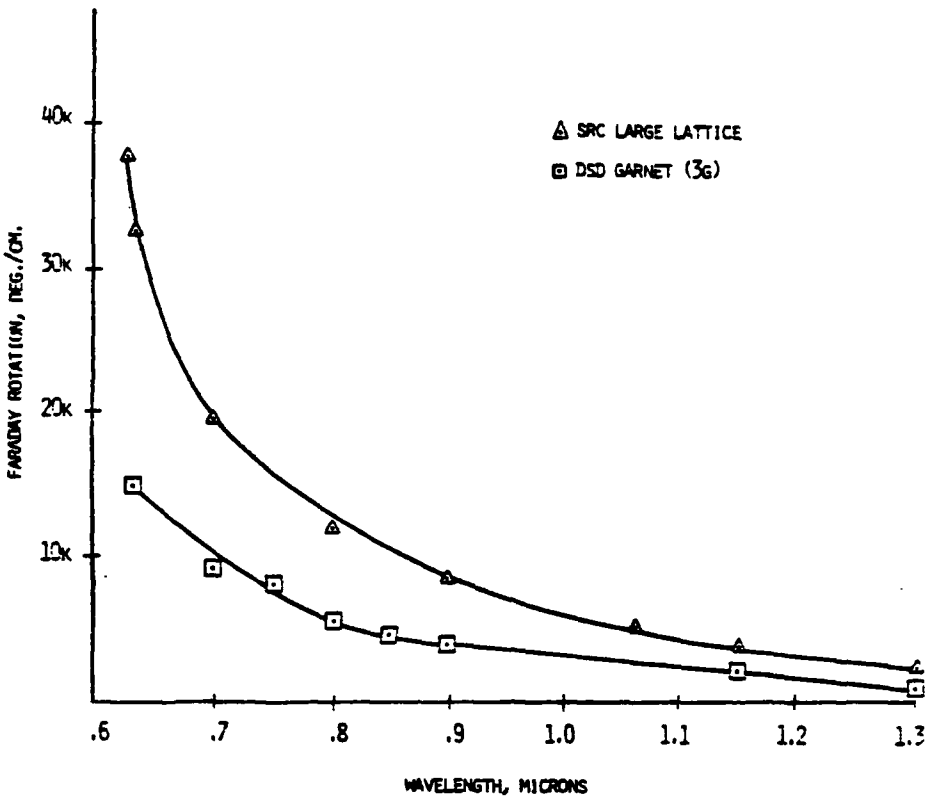

Figure 3. Faraday Rotation Spectra Of Bismuth Garnet.

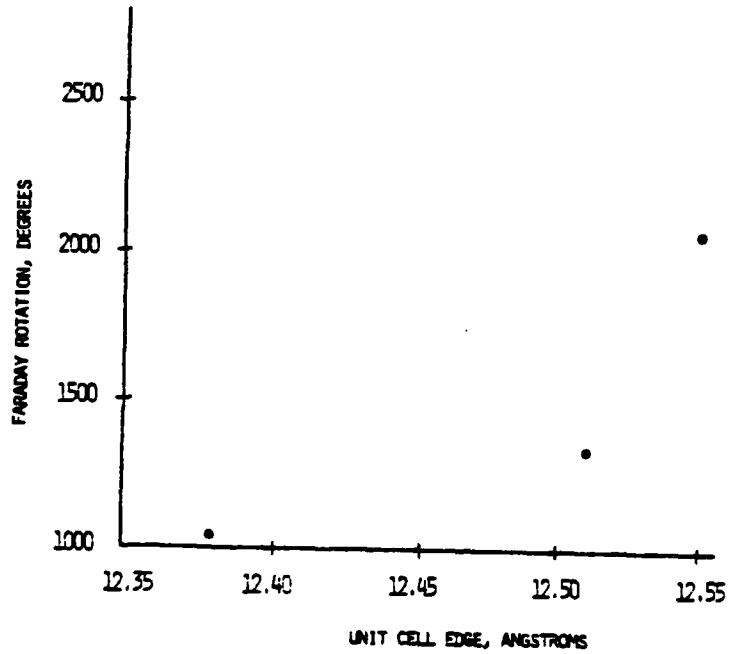

Figure 4. Lattice Constant Dependent Faraday Rotation In Garnet.

Stripe Domain 1X4 Fiber Optic Switch

The basic fiber optic garnet switch model is seen in figure 5. A single input fiber is attached to a gradient index (grin) lens which collimates the input light. The collimated beam is deflected by the stripe film and then focused on the output face of the output grin lens some radial distance from the optic axis. Output fibers bonded to the output lens capture deflected light when fields Hx and Hy are energized. The radial distance of the output fibers on the lens face can be determined from the grin rod ray matrix given as

$$\begin{vmatrix} r \\ \zeta \end{vmatrix} = \begin{vmatrix} \cos \sqrt{A}\, Z & \frac{1}{n\sqrt{A}} \sin \sqrt{A}\, Z \\ -n\sqrt{A} \sin \sqrt{A}\, Z & \cos \sqrt{A}\, Z \end{vmatrix} \begin{vmatrix} r_i \\ \phi \end{vmatrix}$$

with r & ζ the output radius and beam emergence angle, A the gradient constant of the lens, n the lens index, Z the lens length, and r_i and ϕ the input radius and angle.[6] A garnet film diffracts first-order light according to the Bragg rule so that

$$\Theta = \sin^{-1} \frac{\lambda}{\Lambda}.$$

A common grin lens with a 0.21 NA input fiber collimates the input light to a diameter of 0.56 mm; thus, $r_i(max)$ = 0.56 mm. From data sheets for a Nippon Sheet Glass Selfoc™ lens we find that n_o = 1.55, $\sqrt{A}$ = .242/mm, and Z = 6.5 mm. Then on solving the matrix for r and ζ we obtain for the maximal rays:

$$r = 2.67 \sin^{-1} \frac{\lambda}{\Lambda} \text{ mm}$$

and

$$\zeta = 0.21 + 0.0022 \sin^{-1} \frac{\lambda}{\Lambda} \text{ radians}.$$

Selecting λ/Λ such that $\sin^{-1} \lambda/\Lambda = 10^{o}$, we arrive at r ≈ 0.46 mm and ζ ≈ 0.21 radians. The spot size on the output face of the grin lens is found from

$$\frac{1.22\lambda}{\text{lens NA}} \approx \frac{1.22\mu}{0.37} = 3.4\mu.$$

Therefore, output fibers of small core size are adequate as long as the fiber acceptance angle is 12° or more. This is easily satisfied by commonly available fibers. The final design required four output fibers to be polished and bonded perpendicular to the output lens output face with core centers a distance of 0.46 mm from the lens axis. Implementation of the design was by placing four 125-micron diameter fibers along the inside circumference of a capillary tube of inside diameter equal to 1.1 mm, epoxying the fibers, and polishing the fixture on a wheel. The assembly is shown in figure 6. It was then incorporated into the apparatus of figure 7 for making loss and crosstalk measurements. Incident light through the input fiber was steerable to any of the four output fibers by coils H_x and H_y driven by a programmable sin/cos current supply.

One garnet sample with a deflection angle of 10° at 0.633 micron was placed in the apparatus in order to determine coupling efficiency. Neglecting Fresnel losses at the multiplicity of interfaces, which would be largely eliminated by antireflection films, it was found that available deflected light could be coupled to the core modes of the output fibers with less than 1 dB coupling loss. Crosstalk was evaluated by switching input light to one of the four output fibers, then moving the photodetector to the other nonselected fibers and measuring the amount of stray light coupled into them. Almost all of this stray light is the result of zeroth-order, undeflected light.

Table 1 is a listing of the accumulated data, with fiber numbers corresponding to figure 6. Each crosstalk value has been normalized to the level of first-order signal coupled to the selected fiber.

TABLE 1. CROSSTALK MATRIX

SELECTED FIBER	OBSERVED FIBER			
	1	2	3	4
1	-	-24 dB	-24 dB	-24 dB
2	-15 dB	-	-21 dB	-21 dB
3	-21 dB	-17 dB	-	-21 dB
4	-21 dB	-18 dB	-18 dB	-

Because some of the crosstalk levels are less than desirable, a method was devised to significantly reduce crosstalk with only 3 dB insertion loss penalty. Since nearly all of the crosstalk is derived from the zeroth order and the zeroth-order polarization

is instantaneously orthogonal to the first order, a polarizer in the input side of the garnet film conditions the input light so that an analyzer on the output side of the film absorbs or diverts zeroth-order light. Experiments with this technique reduced crosstalk to better than -40 dB. If the switch is utilized with a polarized input source, such as a laser diode at 0.85 micron and a short pigtail fiber, then the 3 dB penalty would not be incurred.

To be useful as a fiber optic switch, garnet films must have sufficient optical efficiency between 0.8 and 0.9 micron. Present data links can operate with less than 100 microwatts of coupled fiber power for megabit rates over kilometer lengths. Thus, the magneto-optic coupling coefficient, optical absorption, and the first-order deflection efficiency of bismuth garnet was measured at 0.81 micron. The usable Faraday rotation is 3000°/cm and the optical absorption is 370 dB/cm. Films can be easily made 40 microns thick, so that efficiency expectations for a mirrored sample are about 7 percent. The best sample available exhibited 4 percent efficiency when a laser diode at 0.82 micron was used as a source. The deflected power was found to be 100 microwatts per spot. Using beam recombination of the two first-order spots, even higher deflected power can be obtained.

One method of obtaining beam recombination in the stripe domain fiber optic switch is to combine the first-order spots in a fiber asymmetrical coupler, as shown in figure 8, where the output lens and fibers associated with only one switch position are included. It has been reported that by properly choosing the relative diameters of the combining fiber and the switch fibers, it is possible to achieve beam recombination with as little as 0.11 dB loss.[7]

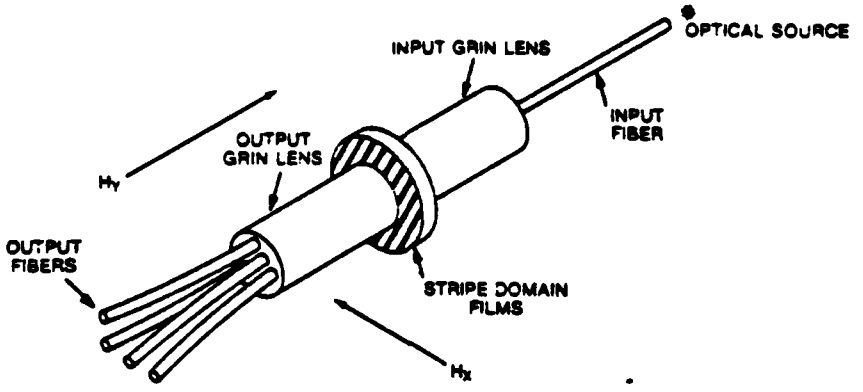

Figure 5. Stripe Domain 1xm Switch.

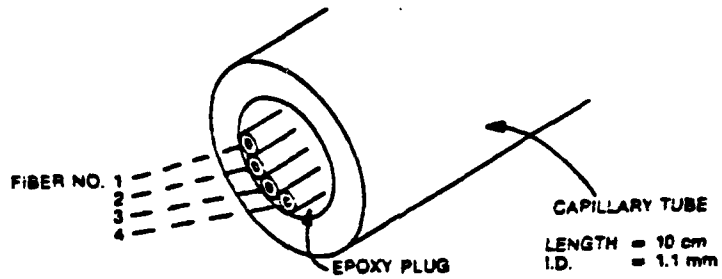

Figure 6. Output Fiber Arrangement.

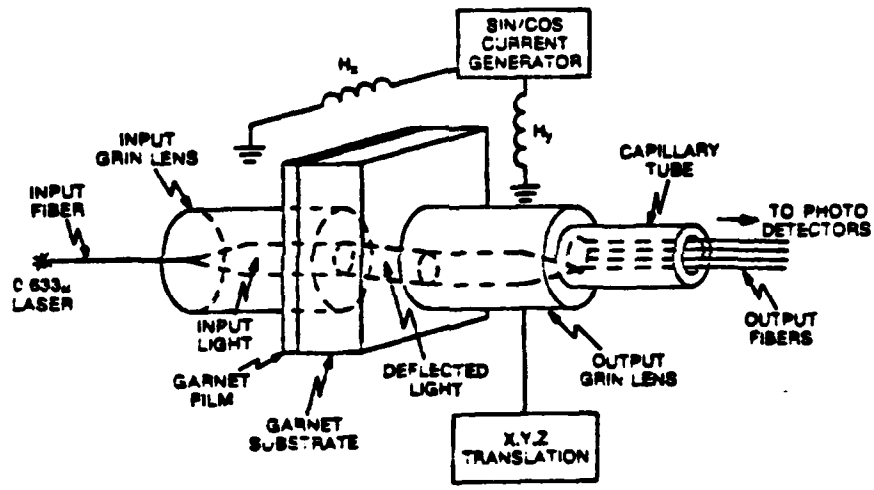

Figure 7. Fiber Optic Switch Apparatus.

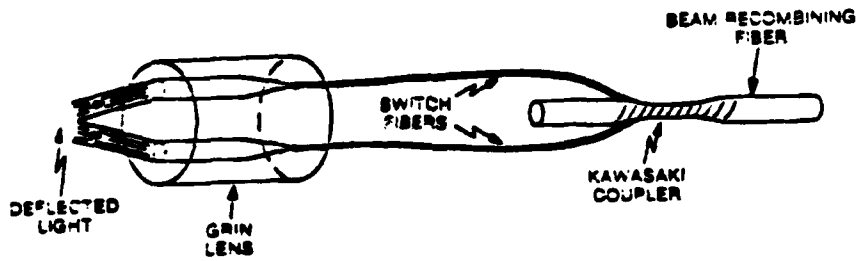

Figure 8. Beam Recombination.

Stripline Switching Of Garnet Deflector Wafers

Stripline driving was used to explore the minimum switching time of garnet stripe domain films. Past high speed attempts to switch films had been performed with small coils and had yielded inductance limited response-the best (fastest) near two microseconds. A stripline approach was taken so that a more ideal, impulse response measurement would be obtained and also to explore whether striplines are capable of driving deflector films as this is a more desirable approach.

The experimental apparatus constructed included the stripline itself, drive electronics, and deflected beam optical monitoring capability. The one millimeter wide stripline was cut from 25 micron copper sheeting and placed against a single sided garnet wafer as shown in figure 9. A silver reflecting film .05 microns thick was previously evaporated onto the garnet film in a narrow band approximating the stripline. In this way an incident .633 micron laser beam would pass through the substrate/garnet film and be reflected at the evaporated mirror, and in the same way the deflected beams would exit back towards the source. This provided a simple means of optically monitoring the response of the film to the magnetic field impulse from the stripline. A final element in the sample/drive assembly was a mumetal magnetic keeper somewhat larger then the 1" sample diameter and .5 mm thick. This was periodically included in the "assembly" by mechanically holding the mumetal against the back of the sample. This effectively halved the stripline current required to drive the garnet with no loss of response speed relative to no keeper at higher currents.

The electronics used to drive the stripline is shown in figure 10. A 555 time circuit configured as a monostable element is used to drive an SCR which discharges capacitor C_s through the stripline. The amplitude of the current pulse is controlled by varying V_s, the voltage C_s is charged to. The current pulse width is controlled by varying the value of C_s. The RC time constant of C_s and the stripline dc resistance approximately determines the pulse width. In operation, the drive pulse voltage was monitored by looking across the stripline and the current monitored with a CT-1 Tektronix current probe. To minimize parasitic effects, the electronics was constructed with a copper ground plane and all leads, particularly the C_s/SCR/stripline loop, as short as possibe.

Two approaches to monitoring the deflected beam were taken. In initial experiments, the magnetic grating was disordered by moving a large permanent magnet near the sample. The effectiveness of a particular drive pulse was then judged by whether the grating was reconfigured aligned to the stripline field. This was shown by the location, divergence and movement of the deflected spots. The later approach involved monitoring the deflected spot with a photodetector, and the disappearance and reappearance of the deflected

spot on the detector as the stripe domain grating responded to the drive pulse. The difficulty with this approach was obtaining adequate sensitivity and fast response with the detector to insure that detector response was not the measured variable. Detector response was determined separately for a given experimental setup before garnet measurements were made. This was done by attenuating the direct laser beam to approximate the sample's deflected spot intensity and then using a Lasermetrics model 5002 electro-optic modulator to switch the beam. The resulting output, with the detector thus illuminated, provided its response to compare with deflector response measurements.

Initial efforts, where the sample behavior was monitored by eye, demonstrated that stripline switching is a viable technique for driving a garnet light deflector element. In these experiments, the stripe domain grating was disarrayed with a large permanent magnet as mentioned earlier, and various pulse widths and amplitudes applied to the stripline. Results indicate that pulses in the submicrosecond range with amplitudes of a few amps can produce a stripe domain grating under the stripline that deflects the laser beam with divergence nearly as low as when a saturating field from a large permanent magnet is applied. This validated the stripline approach and indicated a rough minimum pulse width of 50 nanoseconds for reasonable currents (under 8 amps). The low beam divergence obtained (implying very uniform grating) indicated that the sample was being saturated by the pulse, but the complete response time, including grating formation after the pulse, was not yet determined.

At this stage the deflected beam monitoring capability was added so that the grating behavior could be "timed". The experimental procedure was an interation of: choose a load resistor for the photodector giving as fast a response as possible while still providing usable signal levels, measure the detector response using the electro-optic modulator, simultaneously display stripline voltage drop, current probe output, and detector output on an oscilloscope, photograph the display with the detector both shielded from and exposed to the deflected beam, extract the measured response, and compare to the measured detector response. Several iterations were made before achieving a measured deflector response slower than the measured detector response. This result is shown in figure 11. This shows that in 150 nanoseconds the deflected beam can be switched off of the detector, moved through the film's radial field of view (10^{o} at .633 microns for this sample), and retraced to the detector position. The sample measured produced a deflected beam with an angular width of approximately 5 milliradian at the .633 micron wavelength. This results in 35 resolvable spots along the radial direction. Therefore the overall grating response can be described as 150 nanosecond, random access switching between spots in the field of view and an average switching time of two nanoseconds between adjacent spots in a radial scan.

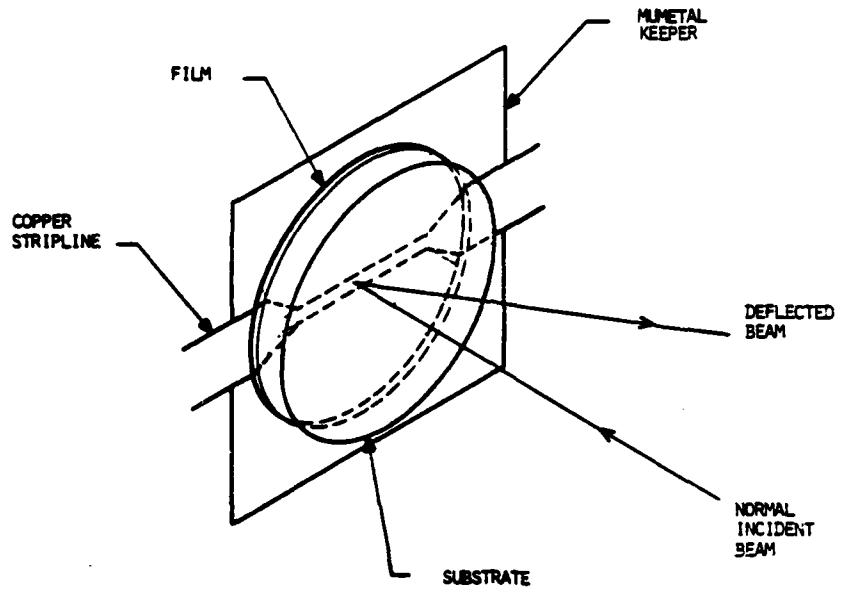

Figure 9. Single Stripline Switching Configuration.

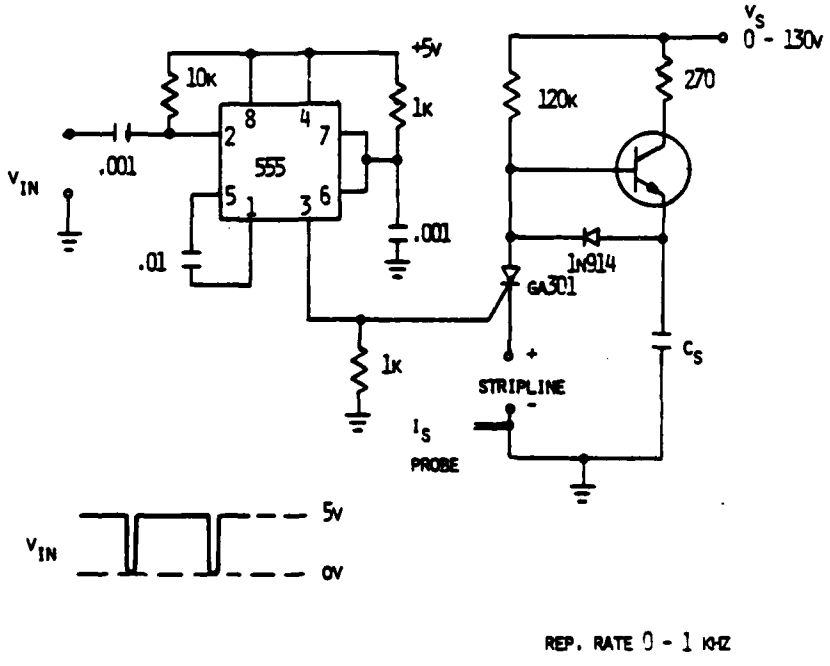

Figure 10. Single Stripline Drive Electronics.

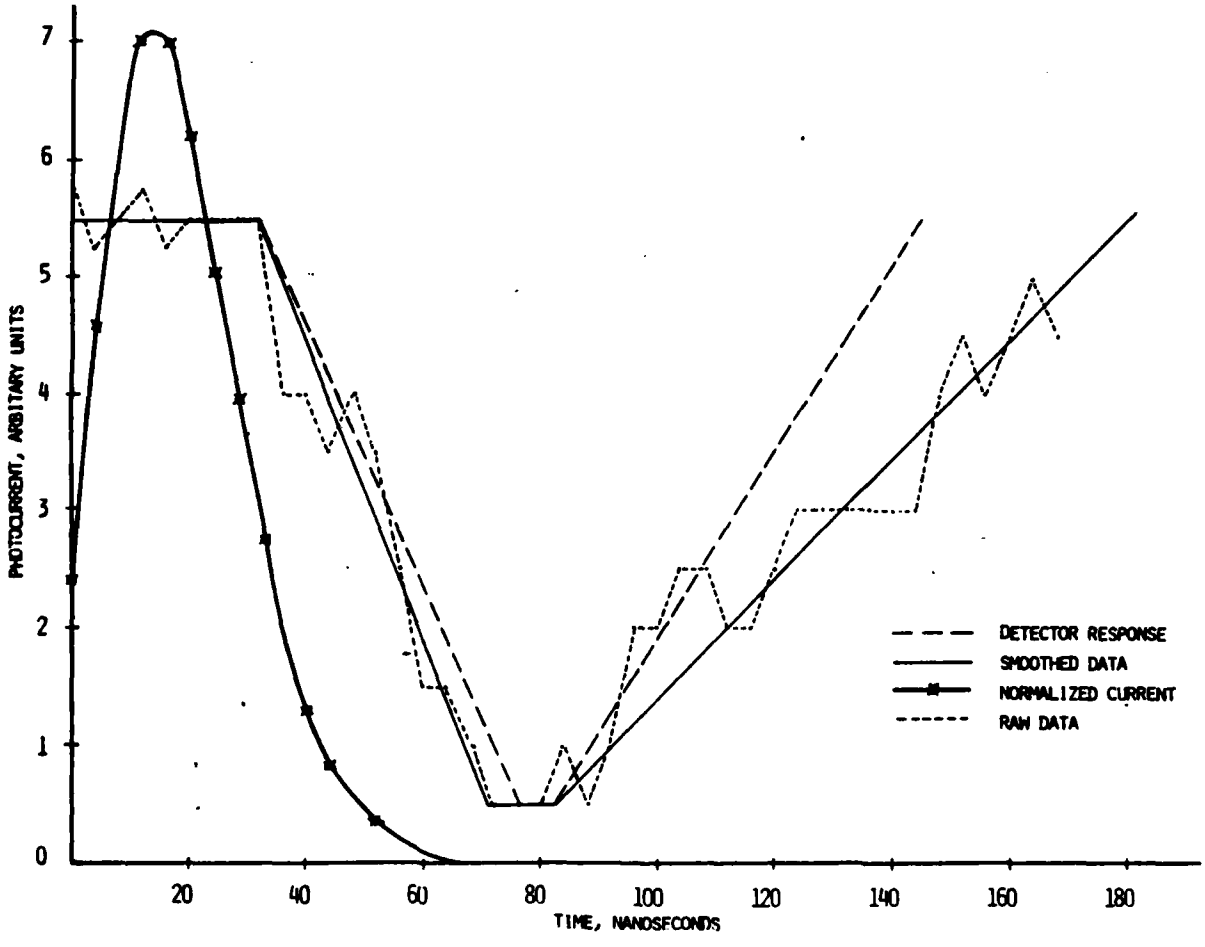

Figure 11. Single Stripline Data.

In order to reduce the pulse current height of 8 amps for the required switching field of 100 oersteds over a fiber lens aperture, multiple stripline circuits were designed. Figure 12a shows one such circuit, enlarged by 10X for pictorial reasons, that provides a one dimensional in-plane magnetic field underneath the central linear array of seventeen striplines. The circuit is unusual in that current flows in the same direction in each stripline. A second set of lines oriented at 90^{o} to the first (12b) provides an orthogonal field in the plane of the material. Thus, by programming current levels in each set a field in any direction in the stripe domain plane is possible.

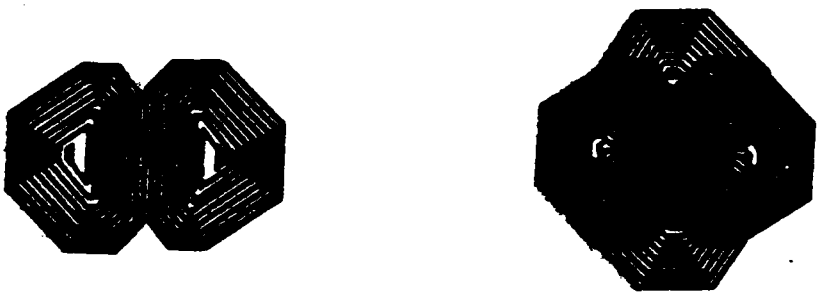

(a) (b)

Figure 12. 10X Enlargement Of Stripline Coil Sets.

To ascertain the field strength available from this arrangement a simple two-stripline model was considered as shown in figure 13. From Ampere's Law the line integral around a stripline yields a magnetic field in the plane of strength

$$H_x(x) = \frac{I}{2\pi w}\left[\tan^{-1}\frac{1+\alpha}{\beta} + \tan^{-1}\frac{1-\alpha}{\beta}\right]$$

where I is the line current, w is the width of the striplines, $\alpha = x/2w$ and $\beta = y/2w$. For n lines in parallel an appropriate sum must be taken for the field at any point. However by considering the field from only two adjacent lines a solution with better than 5% accuracy is gotten. For the model of figure 12 $H_x(x)$ at the bottom of a typical garnet film (y = 25 microns) is plotted in figure 14. If a metallic or ferrite keeper is placed

above the striplines the field values approximately double. Thus, a 2 amp current pulse in these lines is sufficient to switch a stripe domain array. The nonuniformity of $H_x(x)$ can be improved by inserting a spacer between the film and the striplines or by changing the spacing between the lines. However, for some switching configurations it is only necessary to overcome magnetic coercivity to reorient the array. Then the nonuniformity is of little or no consequence.

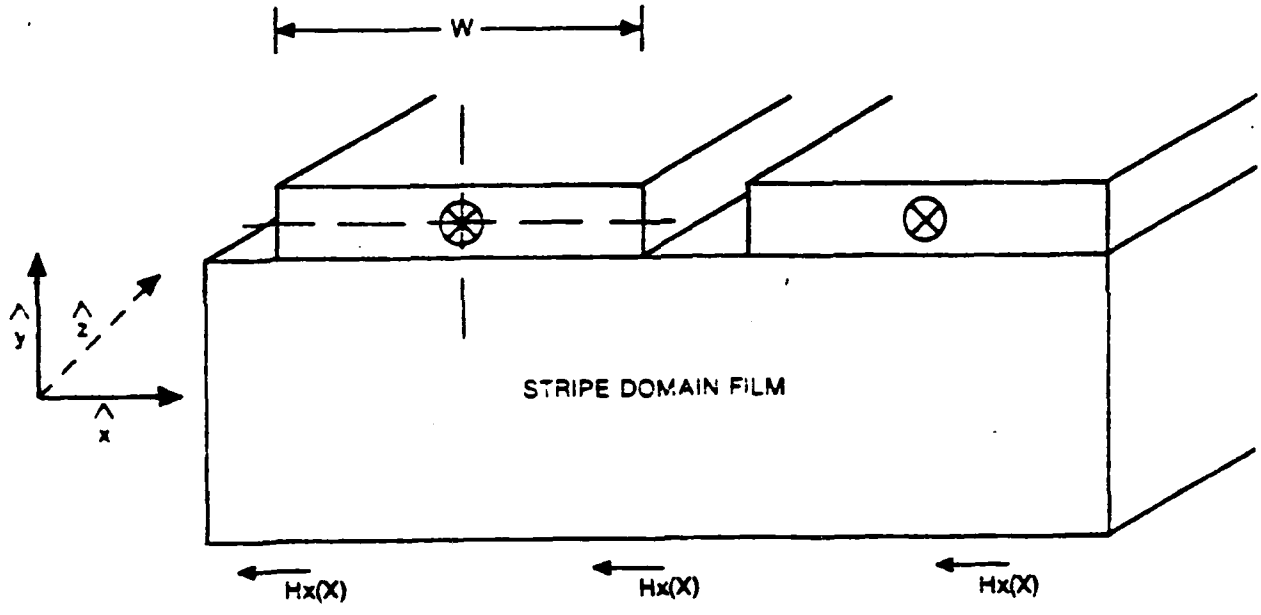

Figure 13. Two Stripline Model For Field Strength Calculations.

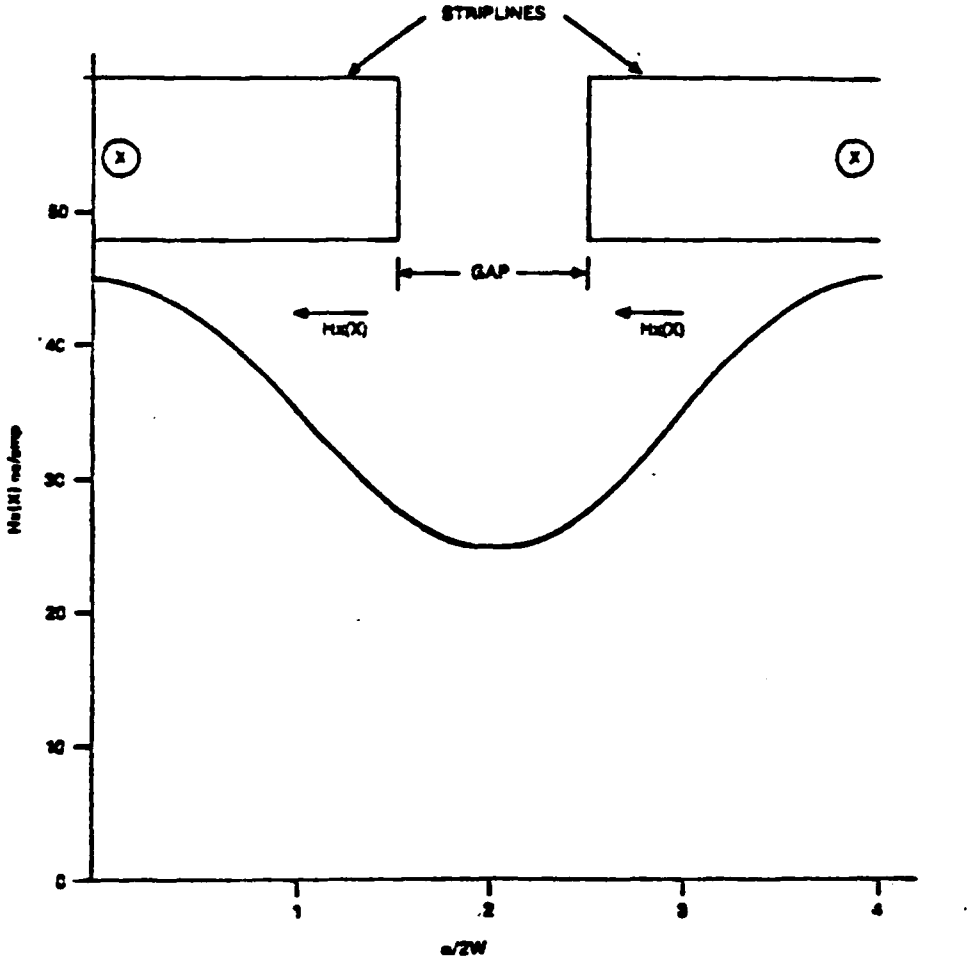

Figure 14. In Plane Field From Two Adjacent Striplines Carrying Equal Currents.

Samples of these coils were fabricated on Kapton^{T} overlays using photolithographic processes. The width of the individual lines is 75 microns and the active area is two millimeters in diameter, the diameter of a typical Selfoc lens. Two drive current circuits were designed based on laser diode pulsers. The first circuit is shown in figure 15. A pulse transformer is used to pass either a positive or negative pulse to the integrated coil depending on the SCR that is gated. Figure 16 presents a variation that removes the pulse transformer. In this version the coil current direction is determined by simultaneously selecting one of two pairs of SCRs. Again, magnitude is controlled by ΔV.

Using these circuits with stripline coils and typical garnet wafers it was possible to rotate the grating through 360° with no more than two amp current pulses of one μsec. duration. The switching energy is approximately 15 microjoules. At 1000 switches per second the average coil dissipation is about 20 milliwatts.

These small coil sets are particularly attractive for use in a fiber optic stripe domain switchboard. A common garnet wafer size is 7 cm. in diameter. This wafer could accommodate 100 stripline pairs to make a very compact 100 by 100 totally optical mode switchboard with all inputs simultaneously communicating to any permutation of the 100 output fibers. Alternatively, in a simple 1xn type switch the coils could reduce the package size to nearly that of the fiber optic connectors used to interface the input and output fibers.

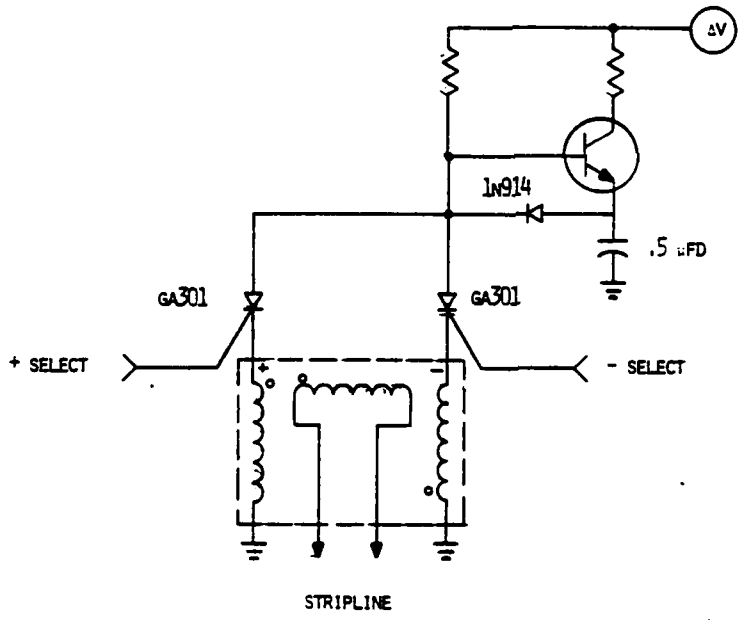

Figure 15. Multistripline Drive Circuit.

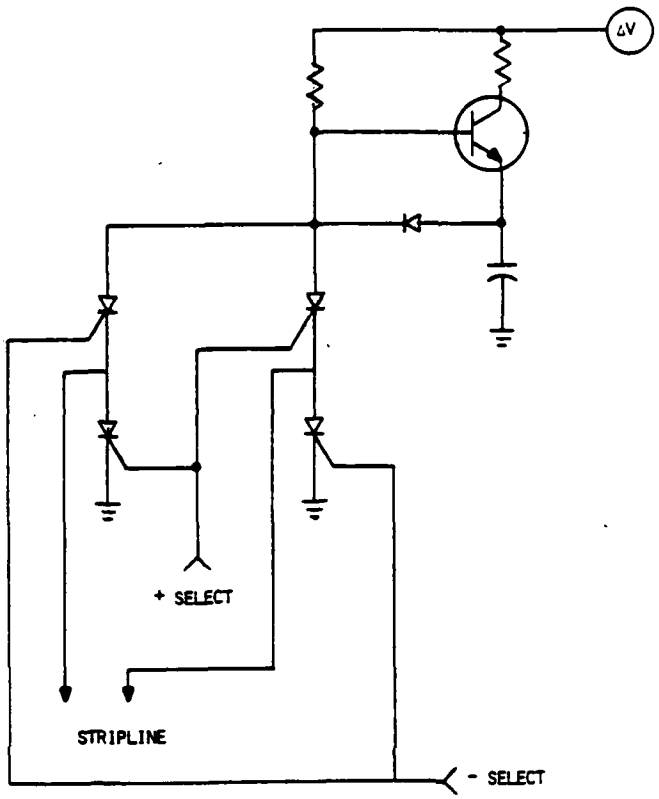

Figure 16. Transformerless Multistripline Drive Circuit.

Active Star Coupler Mode

A significant achievement of this contract was the conception and demonstration of an active star coupler using stripe domain garnet. In general form an active star coupler maps input light to one, some or all output fibers on a star in a controllable way. The systems potential of such a device is attractive. Partial or total conferencing among subscribers is possible. Secure transmission is assured for messages destined to a specific subscriber.

An apodized linear phase diffraction grating with constant periodicity can function as an optical switch by rotating the grating in some fashion. Then the angular spectrum of the output is discrete in the radial coordinate and pseudo-discrete in the azimuthal coordinate in that the grating can be moved incrementally in azimuth. A grating that is configured into radial form with constant periodicity has an angular spectrum that is again discrete in radial spatial frequency but continuous in azimuth. Such a grating is depicted in figure 17 where there is constant periodicity near the center. Collimated light normally incident on this type of grating diffracts into thin annuli at radii relative to the optic axis given by

$$r = d \tan\left(\sin^{-1}\frac{m\lambda}{\Lambda}\right)$$

where d is the far field distance from the grating, m the order number, λ the optical wavelength and Λ the grating period. First order diffraction (m = 1) is shown in figure 18. In a fiber optic system output fibers would be positioned to intercept light around the annulus. A mechanical grating of this variety would be difficult to fabricate because of the requirement for constant periodicity.

Normally a stripe domain array is configured as a linear grating. In-plane magnetic fields can rotate the grating as well as alter the periodicity. A second mode that is accessible with in-plane fields is that of a radial grating with constant periodicity. Figure 19 shows apparatus for inducing such a grating into a garnet wafer. A pulsed point magnetic pole oriented perpendicular to the plane of the stripe domain array provides the appropriate field geometry to establish the radial grating. Experiments were conducted with this apparatus. It was seen that the grating could be altered from linear to constant period radial with a single current pulse in the solenoid of 10 microsenconds duration. Figure 20 is a resultant photograph of an induced radial grating with constant periodicity. Truncated stripe domains that form to minimize magnetostatic energy are responsible for the constant periodicity.

It was also observed that the ferrite pole tended to short circuit the in-plane fields that restore and operate the linear grating. This was overcome by fabricating a integrated, stripline coil that supplies a symmetric field along all radii from the center. The integrated coil is seen in figure 21, a 10X enlargement. Between the center of the coil and the perimeter, the planar field just under the conductors has the same form as the linear coils discussed in the previous section. Here though, the spatial coordinate is r and the field is symmetric in azimuth. Samples of this coil were fabricated on kapton overlays and found to switch the grating in 5 microseconds with one amp of current. There was no difficulty from interactions between this coil and the linear grating coil set, as was experienced with the point pole.

A more versatile active star coupler that is based on the stripe domain fiber optic switchboard concept is schematized in figure 22, a 1X9 coupler. This coupler can provide conferencing between an input fiber and any subset of the output fiber set. In figure 21 the input fiber power is divided equally by a 1 to 9 binary phase grating coupler. The transform lens and an array of planar gradient lenses act as a telescope in reverse to image the splitter onto an array of stripe domain switches that are independently controllable. A 1 to 1 star occurs when all stripe domain elements are rotated to the same orientation. Then switched light from each element is focused on one output fiber. A 1 to q ($q<9$) star is configured when the controller steers input light to the desired subset of output fibers. For instance if the desired output subset is $\{a_3 a_5 a_6\}$ then 3 of the switches would be oriented to a_3, 3 to a_5 and 3 to a_6. The case of 1 to 9 is achieved when each switch is oriented to a unique output fiber. As yet this concept has not been examined in detail nor have experiments been conducted.

In terms of fiber optic systems what have been shown are fiber optic switches that offer dynamically the option of either a secure one to one communications link or a one to many conferenced link. This is the essence of active star coupling.

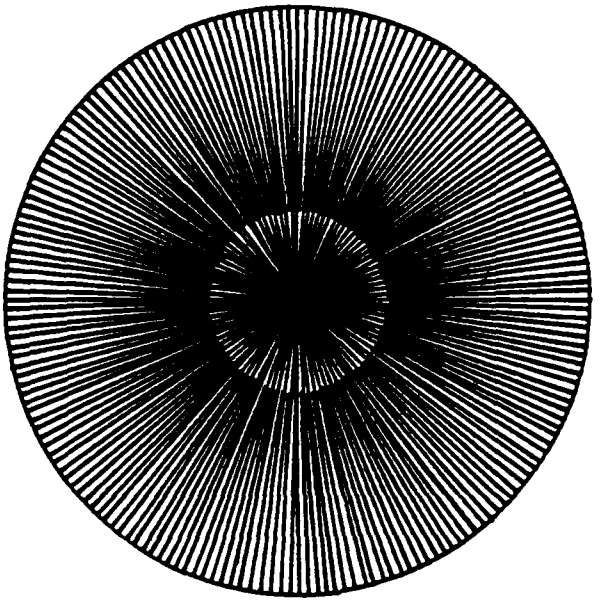

Figure 17. Constant Period Radial Grating.

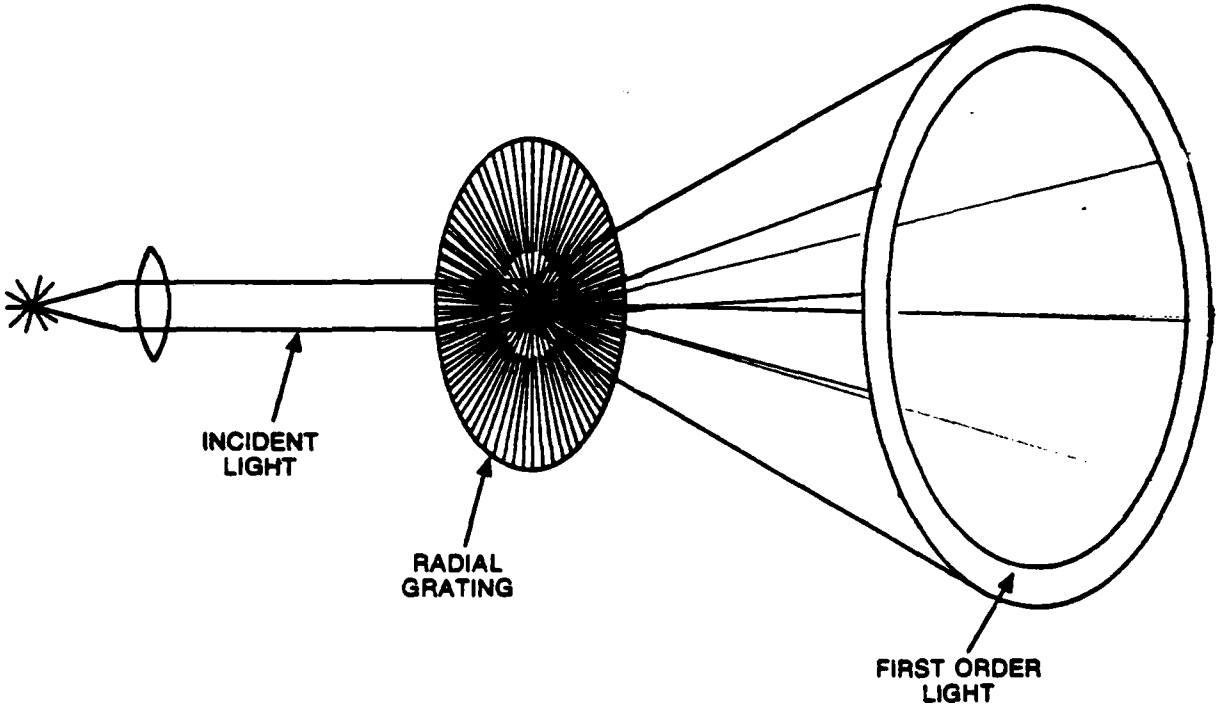

Figure 18. First Order Angular Spectrum Of A Radial Grating.

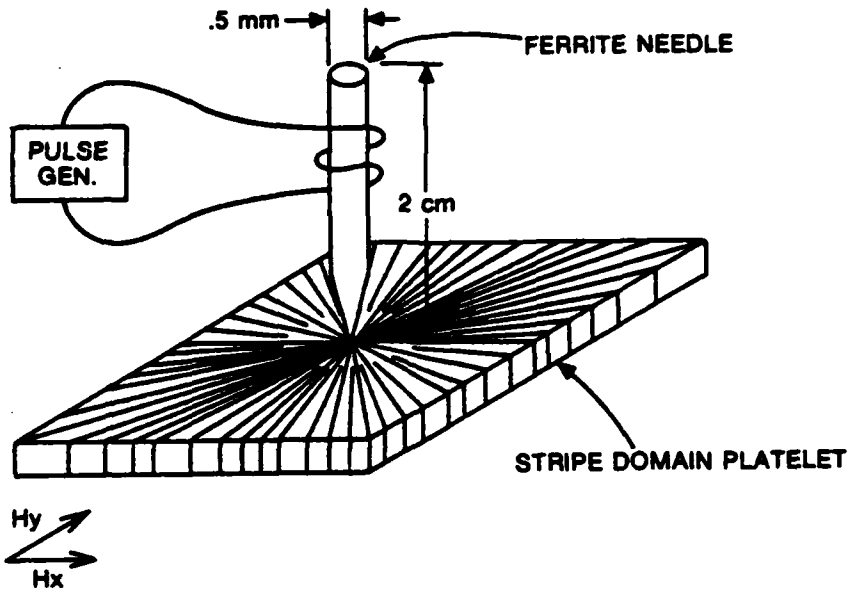

Figure 19. Stripe Domain Radial Grating Generator.

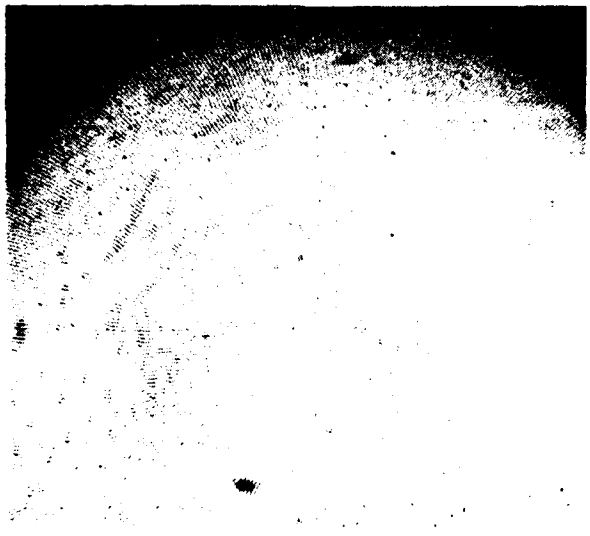

Figure 20. Induced Radial Grating In Garnet.

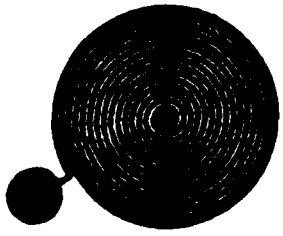

Figure 21. 10X Magnification Of Integrable Stripline Coil For Radial Grating Generator.

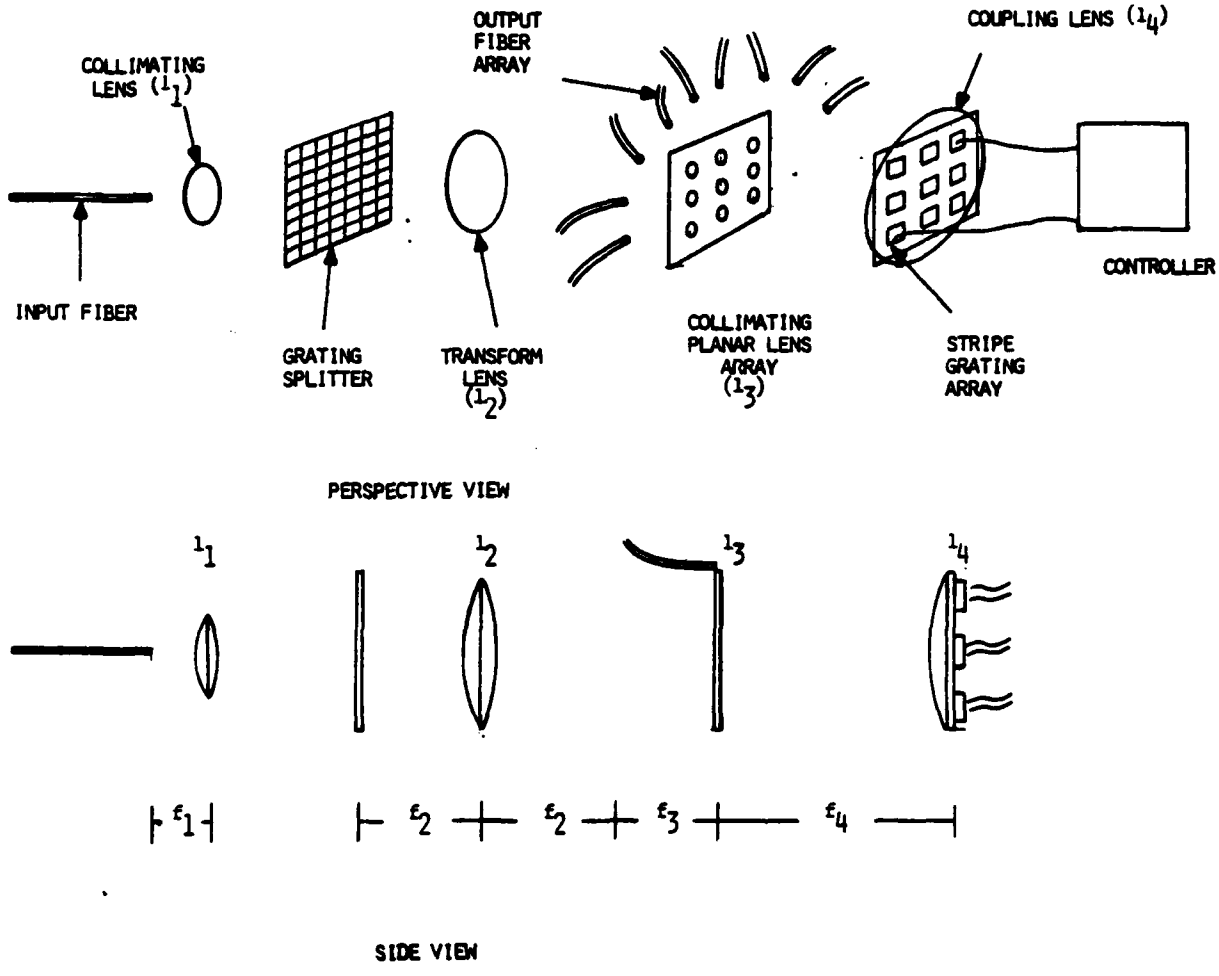

Figure 22. Switchboard Active Star Coupler.

Wavelength Demultiplexing With Garnet Gratings

Gratings have been suggested for wavelength multiplexing and demultiplexing in fiber optics.[9] Since stripe domain arrays are phase gratings, wavelength sensitivity is obtained along with the switch function in a system.

Investigations of the demultiplexing capability of garnet based gratings were facilitated with the apparatus of figure 23. Collimated, multiwavelength light was deflected by the grating according to the rule

$$\sin \Theta = \frac{m\lambda}{\Lambda},$$

where Θ is the deflection angle, m the order number, λ the optical wavelength and Λ the grating period. For switching purposes m = 1. A selfoc lens in close contact with the wafer focused the deflected light at a distance r from the axis given by

$$r \approx \frac{\phi \sin \sqrt{A}\, Z}{n \sqrt{A}},$$

where ϕ is the launch angle, $\sqrt{A}$ is the quadratic gradient constant, Z the lens length and n the index of refraction of the lens.

Then $$r \approx \frac{\sin^{-1} \lambda/\Lambda \sin \sqrt{A}\, Z}{n \sqrt{A}}.$$

A fiber positioned by a translator at r intercepts light of wavelength λ.

The wavelength resolution of the grating/lens combination is determined by the diameter of fibers, typically no less than 125 microns. By taking a variation on r it is found that

$$\Lambda = \left[\left(\frac{\delta\lambda}{n\sqrt{A}\ \delta r}\right)^2 - \lambda^2\right]^{\frac{1}{2}}.$$

For instance, using data on Selfoc lenses (n = 1.55, $\sqrt{A}$ = .242 mm^{-1}) along with δr for two touching fibers it is seen that a grating just splits wavelengths at .8 microns and .9 microns if grating period Λ is about two microns. Although garnet films can be grown with this fine of a grating they are inefficient.

At the time the experiment was conducted, sources at .633 microns and 1.06 microns along with a good quality stripe grating film at Λ = 3.4 microns were available. For this arrangement, δr = 370 microns at the output face of the Selfoc lens. Experimentally it was observed that δr was close to 330 microns or within 10% of the predicted value. Actual data is presented in figure 24. Also shown are the loci of rotation for the switching function of the grating at the two wavelengths. Crosstalk measurements indicated -10 db. at the .633 micron position and -20 db. at the 1.06 micron position. With a 3 db. loss penalty the crosstalk could be improved substantially by incorporating a polarizer and analyzer into the experiment. Then zero-th order crosstalk is essentially eliminated this way.

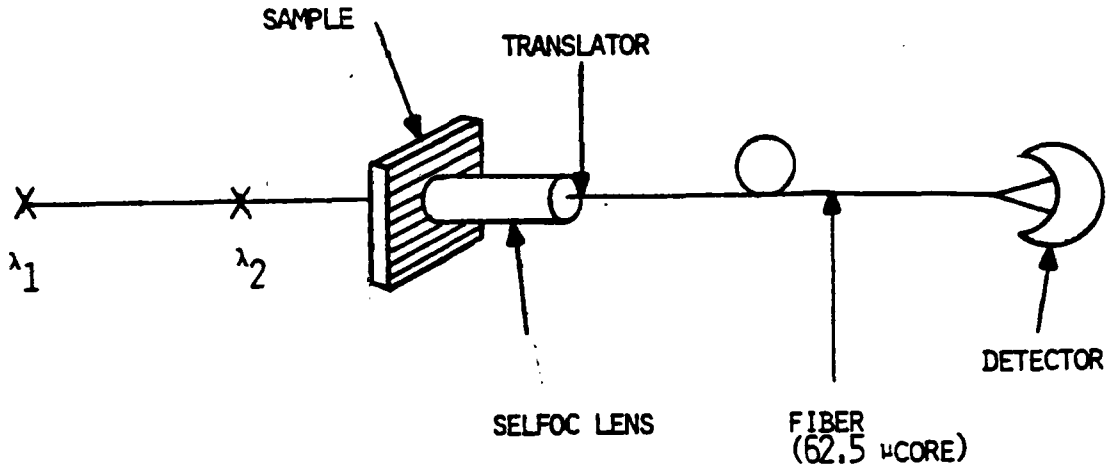

Figure 23. Two Wavelength Apparatus.

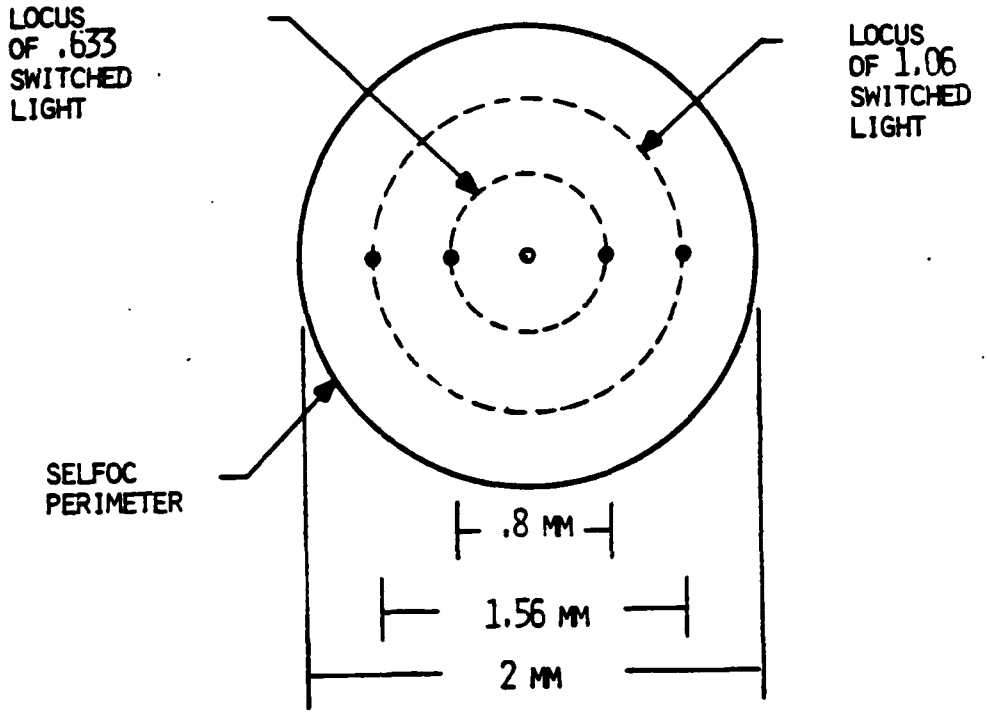

Figure 24. Two Wavelength Splitting/Switching.

Grating Efficiency Improvement With Antireflection Coatings

One of the loss mechanisms in garnet wafers is due to the high index of refraction. Typically the substrate index is near 1.9 while the epitaxial stripe film index is about 2.3. Fresnel reflection loss is given by

$$R = \left(\frac{n - n_{air}}{n + n_{air}}\right)^2 .$$

The loss per surface is 9.6% for the substrate and 15.5% for the film. When two uncoupled surfaces are considered the total reflection loss is 18.3% for the substrate and 28.6% for the film. Of course if the wafer surfaces are highly parallel etalon activity is possible, reducing or increasing the loss in a complex manner.

In order to reduce reflection losses and eliminate etalon modes it is necessary to deposit quarter-wave plates on the air/crystal interfaces. A single quarter-wave plate on a substrate has a reflection loss of

$$\frac{n^2_{\lambda/4} - n_{air}\, n_c}{n_{air}\, n_c + n^2_{\lambda/4}} ,$$

where n_c the crystal index. This follows the numerator to 0 so that the optimum index occurs when

$$n_{\lambda/4} = \sqrt{n_{air}\, n_c} = \sqrt{n_c} .$$

For garnet n_c is either 1.9 or 2.3 so that $n_{\lambda/4}$ = 1.38 and 1.52 respectively. Fortunately MgF_2 with n = 1.38 and 7059 glass with n = 1.53 are available. Variations over the entire fiber spectrum are mainly in the third decimal place. These two compounds should reduce reflection loss to near 0 when deposited on garnet films or substrates.

Single layer quarter wave plates of 7059 glass were electron beam deposited on epitaxial garnet films. At .81 microns the reflection loss was measured to be 3% or nearly an order of magnitude lower than uncoated samples. Thickness or index variations can account for the greater than 0 reflection.

The D.C. Term In The Angular Spectrum Of The Grating

Systems issues dictate the efficiency of a stripe domain grating used for fiber optic switching. In a bus organized configuration it is advantageous to have weak tapping of the bus at each switch point to allow signal energy to propagate with low attenuation around the bus. In a star arrangement with long fibers maximum signal strength switching is desirable. For a data system that has but few subscribers and short fiber links, weak tapping may be sufficient. Then the d.c. component in the grating's angular spectrum can be utilized for other purposes such as providing switch position select data or even switching power itself in the case of remote deployment.

Deflection of light with magnetic stripe domains has the potential for either strong or weak coupling at the switch point.

The maximum theoretical deflection efficiency into the first order is shown in figure 25. High efficiency at interesting fiber wavelengths is evident. In order to obtain these efficiencies with present materials it is necessary to operate garnet wafers in the multipass mode, using resonant or nonresonant cavity feedback techniques. If the wafer is placed in the external cavity of a three mirror diode laser, then high frequency self pulsations of the diode are reduced as well as increased grating efficiency obtained.[10]

In the case where little optical power is lost in attenuation (short fibers) the d.c. component possesses sufficient energy to actually switch the grating. Present garnet wafers require approximately 30 microjoules and can switch in less than one microsecond. A one milliwatt beam of optical power made available to a 50% efficient photovoltaic converter supplying power to 60% efficient electronics can switch the grating 10 times per second without any power supplies. Alternatively, the photovoltaic cell can be used to trickle charge a small battery set that accompanies the switch.

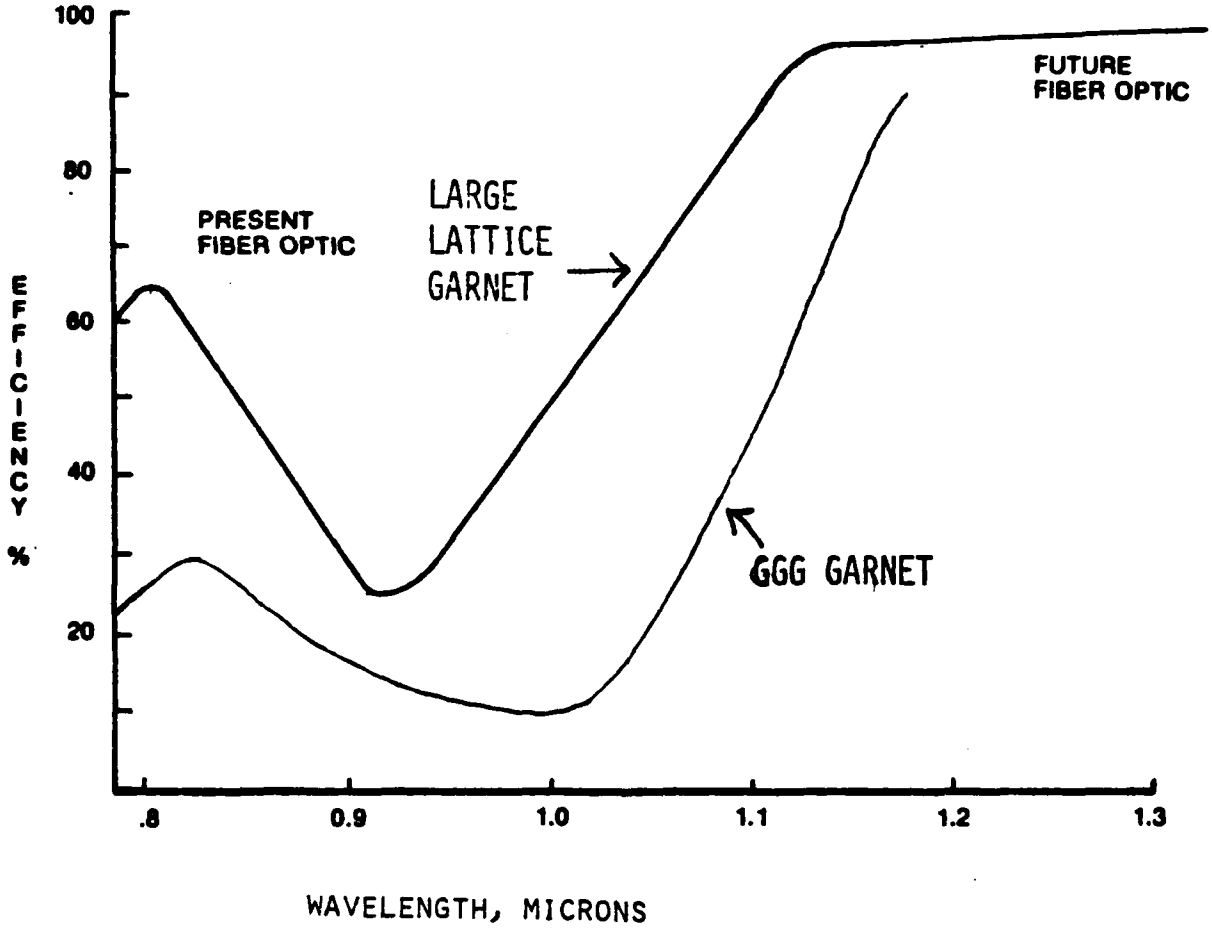

Figure 25. Theoretical Efficiency Spectra Of Garnet, Stripe Domain Gratings.

OPTICAL SWITCHES FOR COMMUNICATIONS SYSTEMS

Introduction

Low transmission losses and attractive wide bandwidth capacity of fiber optic cables have been the driving force in the development of fiber optic communications systems. There are additional advantages for military applications. These include small size and weight, potentially very low cost, and freedom from electromagnetic interference, including nuclear EMP. A large number of components and devices would be required for all optical systems. They would include optical fibers, wave guides, sources, detectors, modulators, transducers, couplers, switches, connectors, splices, amplifiers, memories, limiters, oscillators, discriminators, and gates. In present optical systems only transmission is optical. Regeneration, amplification, and modulation are largely electrical.

Progress in the development of optical switches suggests that switches may be the next component to be widely incorporated into optical communications systems. The value of optical switches can be seen by a brief consideration of optical systems without switches. The simplest optical fiber communication system is a transmitter-fiber cable-receiver. The use of transceivers in place of the transmitter and receiver allows for two way communications.[11]

Consider a simple communications systems consisting of four terminals. They could be connected by individual fiber cables as shown in figure 26. Introduction of an electronic switching unit (switchboard) could reduce the number of fiber cables as shown in figure 27. As terminals are added to the system; either the number of cables will rise rapidly, or the number of optical-electrical conversions will increase.

Another technique to connect terminals is to use couplers-devices which split the optical signal into fixed ratios. This technique allows each terminal to communicate with all other terminals in the system. Two systems using couplers are shown in figure 28. In 28A each terminal is connected to a fiber optic bus by means of a three way coupler. In 28B all terminals are connected to a single multiway coupler. A disadvantage of optical coupler systems is the loss due to signal splitting at the couplers. Because of the optical splitting losses, systems employing couplers usually are restricted to relatively short distances. Another disadvantage is the restriction on line sharing. Sharing must be either time or band. Also, encryption is necessary to secure sensitive data.

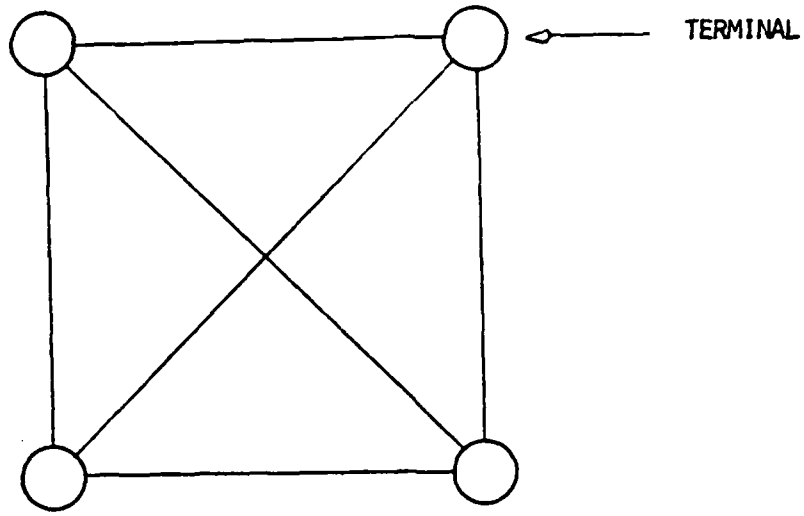

Figure 26. Four Port Optical Network.

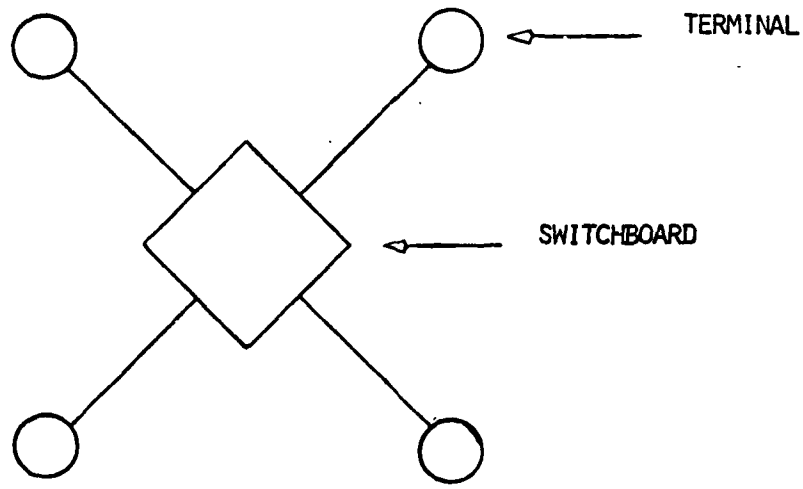

Figure 27. Four Port Optical Network With Controller.

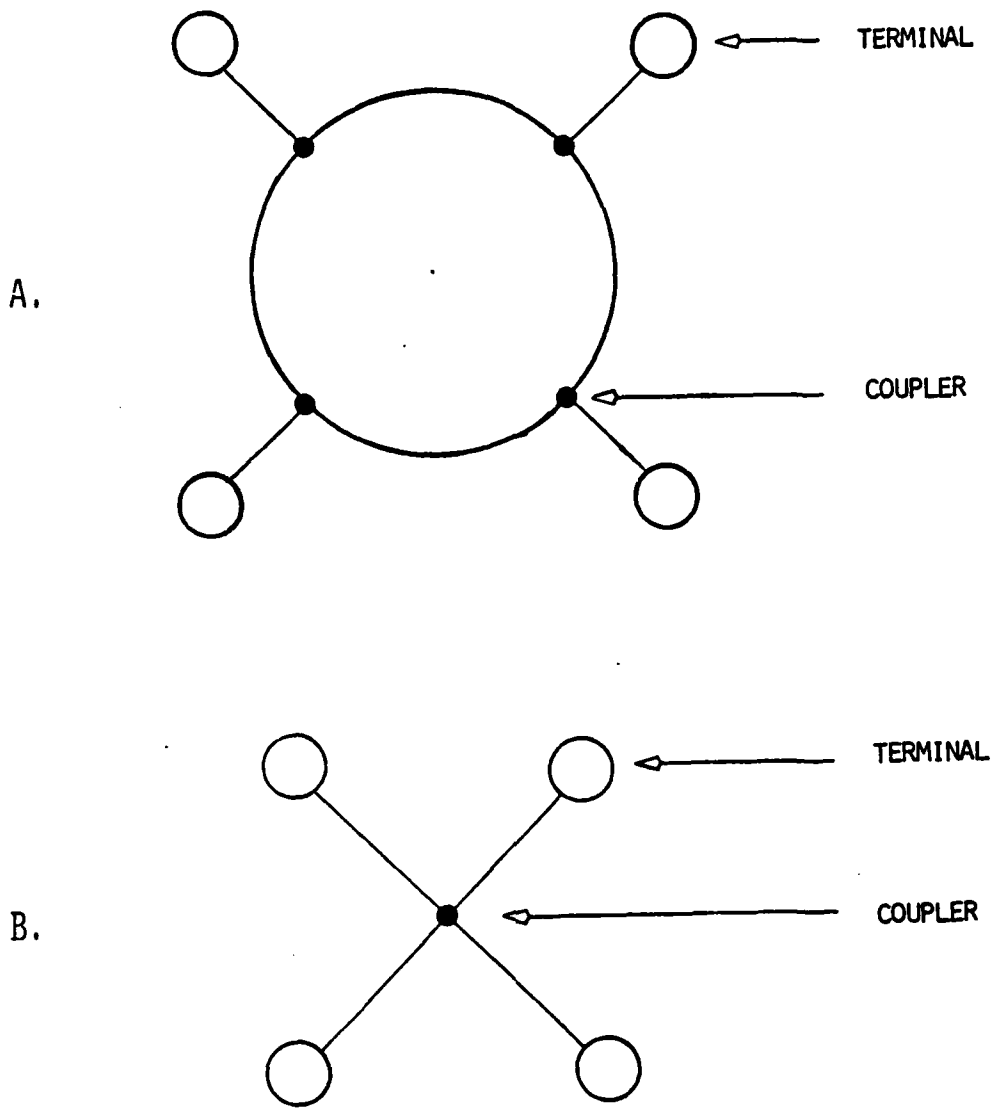

Figure 28. Four Port Optical Network With Couplers.
A. Ring Topology B. Star Topology

The simplest optical communication system is implemented by making all terminal to terminal connections by individual cables as shown in figure 26. However, as the number of terminals increases the number of cables increases very rapidly. Line sharing as shown in figure 27 can be accomplished by means of electronic switchboards at the expense of increasing the number of optical-electrical conversions and of restricting data rates to levels tolerable by electronic switches. Optical couplers as shown in figure 28 can decrease the number of optical-electrical conversions at the expense of signal splitting and line sharing. The role of optical switches can be seen by replacing the optical couplers in figure 28 with optical switches. The obvious advantages of optical switches are retaining line sharing without increasing optical-electrical conversions and without signal splitting.

Although optical switches offer these important advantages, they are not without problems. For example, insertion loss could be high enough to void the advantage of eliminating signal splitting. Some of the other characteristics of optical switches which should be considered are optical crosstalk, blocking status, switching speed, wavelength response, mode and polarization response, directionality, linearity, control power requirements, peak signal power, range of signal power, reliability, size and shape, weight, environmental stability and cost.

Near term systems applications will be dominated by multimode fiber optic cables. Polarization sensitive switches are less desirable in use with multimode fibers since they can incur an automatic 3 db. insertion loss. In the longer term, multimode fibers have an apparent disadvantage: they are incompatible with the large number of singlemode optical switches that are being developed to route signals between pairs of points in a multi-terminal system.

The next several sections will briefly describe some optical switches which have been demonstrated. The examples will include mechanical, piezoelectric, electro-optic, magneto-optic, and thermo-optic. The examples include type II, III, and IV switches. No examples of type I switches will be presented since an open: closed switch can be implemented in any technology.

Basic Switch Types

Switches may be divided into four classifications: (Type I) the two terminal open/closed switch; (Type II), the multiterminal switch with one unique terminal; (Type III), the multiterminal switch with all terminals having equal status; and (Type IV), the multiterminal switch with two sets of terminals in which no connections are made within the two sets.

The two terminal switch (1:1) has very little use in communications systems. However, many other switches can be functionally replaced by a network of two terminal switches. These replacement networks would probably exhibit a number of unfavorable characteristics. For example, the problem of coordinating the network of switches may require a specialized controller.

The second type of switch is the multiterminal switch with one unique terminal (1:N). This type is sometimes referred to as a traveling switch. In this type of switch the unique input terminal is connected to some function of the other output terminals. The most common arrangement is to make connection with only one of the other terminals. Other possibilities are to make connections to a subset of terminals as in an active star. Electromechanical switches used in communications systems typically have ten or more output terminals and sometimes have as many as five hundred. Any number of outputs can be implemented by means of a tree network in which each output terminal is connected to the input terminal of a switch. The output terminal of each subsequent level is similarly connected to other input terminals of other switches until the desired number of output terminals is achieved. Such tree networks can be constructed even from simple 1:2 switches.

The third type of switch is the multiterminal switch in which all terminals have equal status (N:(N-1)). There is no single terminal which is unique and therefore designated as the input terminal. This type of terminal is usually not found in communications switch catagories. In this type of switch any one of the terminals is connected to some function of the other terminals. The simplest function being connection of any pair. When one pair of terminals is selected for connection, other terminal pairs may incidently be connected.

The fourth type of switch is the multiterminal switch with two separate sets of terminals in which connections are only made between the separate set of terminals and not within the sets (N:N'). This type of switch is sometimes referred to as a coordinate or crosspoint switch. The common implementation of this switch is to make a connection between one terminal of one of the two separate sets and one of the terminals of the other set. When one connection is made, other connections may be made independently in some switch implementation or incidently in other switch implementations.

Mechanical Switches

The first mechanical switch example is a type II switch which uses optical fibers in a square bore glass tube. Two output fibers are fastened to opposite corners in the square tube and exit out of one of its ends. The single input fiber enters from the other end of the square tube and has a nickel sleeve a short distance from the end of the fiber. The input is switched between the two output fibers by means of a magnetic field which pulls the nickel sleeve into one of the corners of the square tube.

Another example of a type II switch uses the double internal reflection of a prism.[12] A 1:2 switch would have three planar parallel optical fibers with the middle fiber as the common input as shown in figure 29. The prism has two positions, each of which connects to one of the two output fibers.

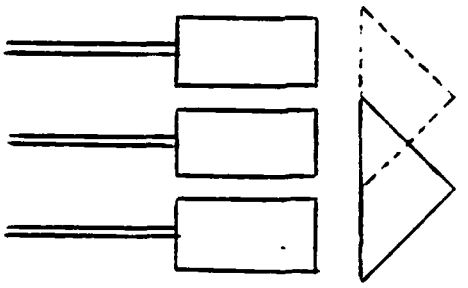

Figure 29. Moveable Prism Optical Switch.

A third example of a type II switch is shown in figure 30. A common input fiber is attached to the axis of a Selfoc lens. A series of output fibers are attached at the same end of the Selfoc lens in a circular pattern. A mirror is mounted at an off normal angle on the shaft of a rotator. The output fiber to which the input is reflected will therefore depend on the angular position of the rotator.[13]

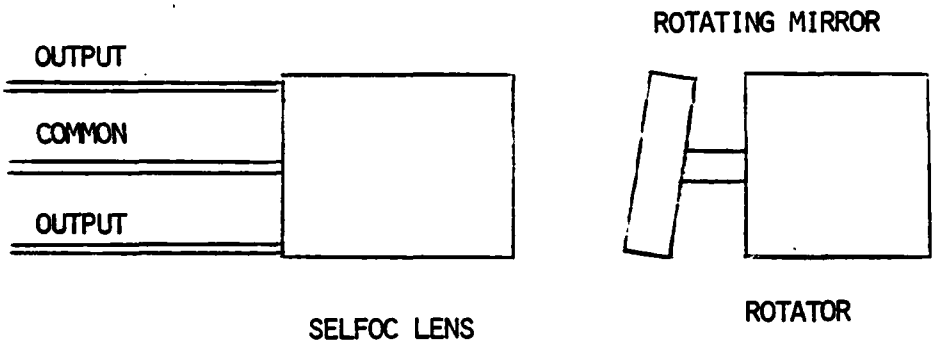

Figure 30. Rotating Mirror Optical Switch.

An example of a type III mechanical switch is shown in figure 31A. The optical fibers are arranged in a plane pointing at a concave mirror.[14] The light signal diverging from an optical fiber will be focused by the concave mirror and reflected in a direction determined by the orientation of the mirror. The mirror can be rotated about an axis through the center of the mirror and normal to the plane of the optical fibers. Switch positions are indicated by the direction of the mirror optical axis. The switch connects pairs of optical fibers and figure 31A is in position D connecting fibers 2 and 4. Figure 31B is a table showing switch positions with the associated optical fiber connections. In position C two sets of optical fibers are connected, and in switch positions B & D optical signals are reflected back into the same optical fiber.

If it is desirable to eliminate the simultaneous connection of two sets of optical fibers, the optical fiber spacing can be modified as shown in figure 32. In this arrangement the signal from one of the optical fibers (2) is reflected back into itself in switch position B. If it is desirable to eliminate this self connection the optical fiber arrangement shown in figure 33 can be used.

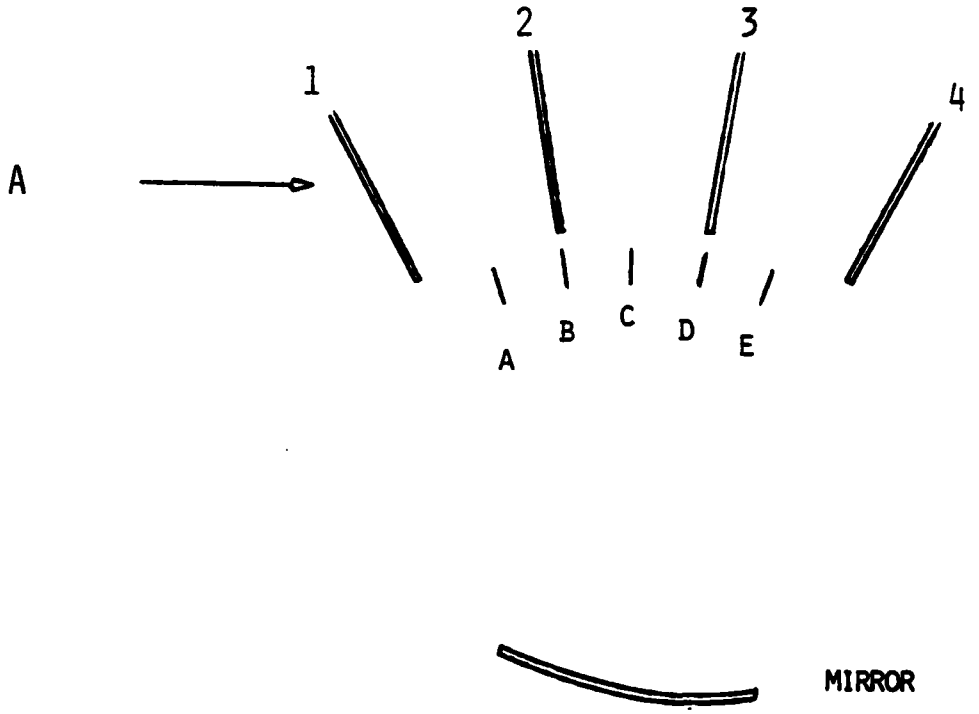

	SWITCH POSITION	OPTICAL CONNECTIONS
	A	1,2
	B	1,3 & 2,2
B	C	1,4 & 2,3
	D	2,4 & 3,3
	E	3,4

Figure 31. Mechanical Active Star Optical Switch.

A

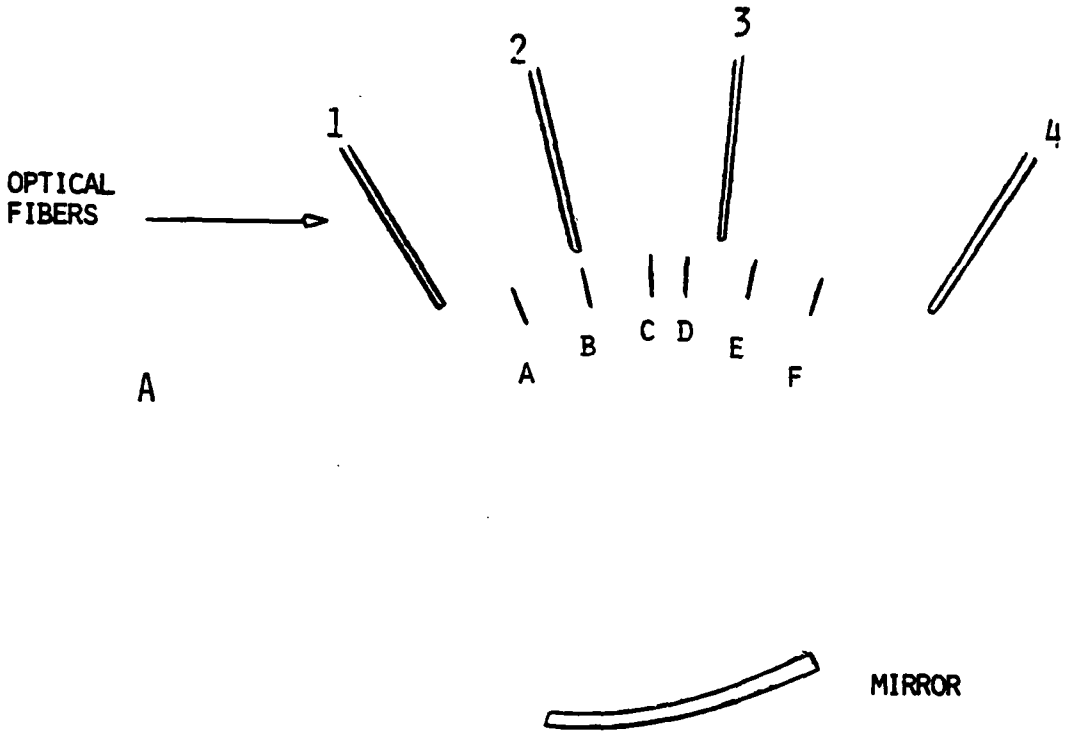

B

SWITCH POSITION	OPTICAL CONNECTIONS
A	1,2
B	1,3 & 2,2
C	2,3
D	1,4
E	2,4
F	3,4

Figure 32. Concave Mirror Optical Switch Restricted To Single Pair Subsets.

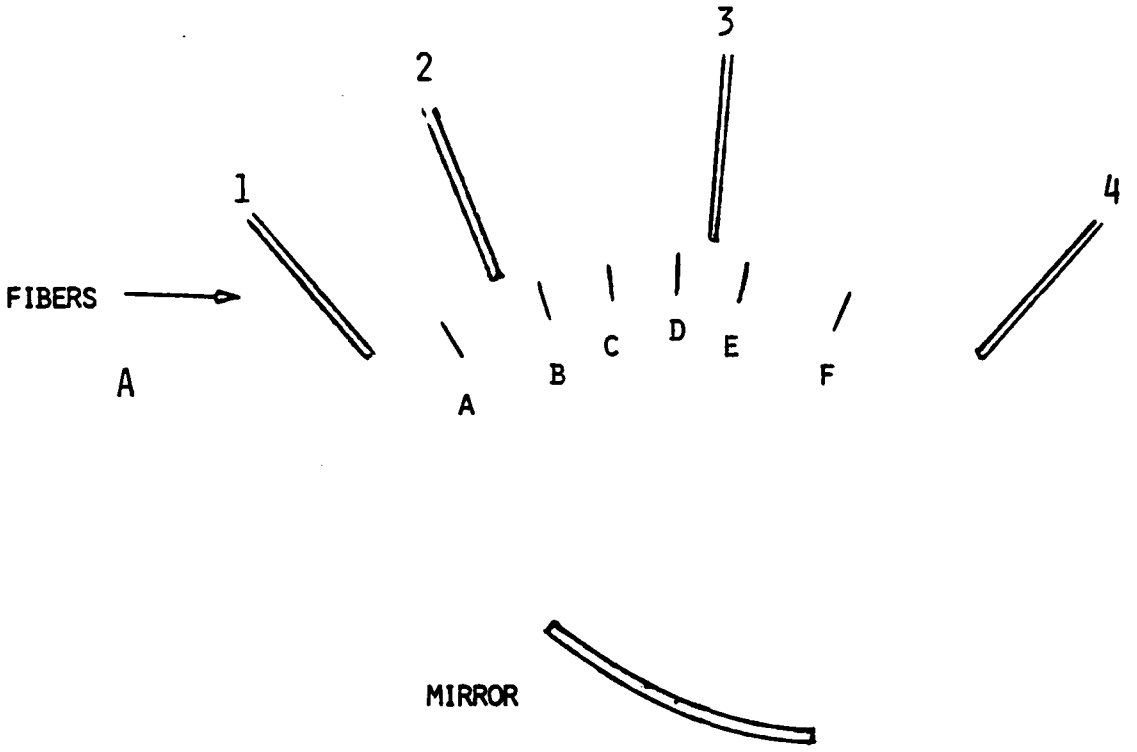

	SWITCH POSITION	OPTICAL CONNECTIONS
	A	1,2
	B	1,3
B	C	2,3
	D	1,4
	E	2,4
	F	3,4

Figure 33. Concave Mirror Optical Switch With Feedback-Free Restriction To Single Pair Subsets.

A mechanical implementation of a type IV switch (2:2) is shown in figure 34. When a rhombus prism is moved into the two light beams of figure 34A they are interchanged as shown in 34B. An array of these 2:2 switches can be used to make an N:N switch.

Another type IV mechanical optical switch that has been developed by American Time Products[15] is an in-line fiber optic bypass switch. In its normal operating mode the switch allows passage of two parallel optical signals, the output of one switch path being the input to the node input detector and the output of the other path being the node-regenerated or reconstructed optical signal as shown in figure 35A. In the other mode the switch serves to provide direct transfer of the incoming optical signal to the next network node (35B). The transfer of the collimated optical beam is accomplished with a high-precision coil-driven slide having two mirrors mounted at 45^{o} to the input light beam. (35C).

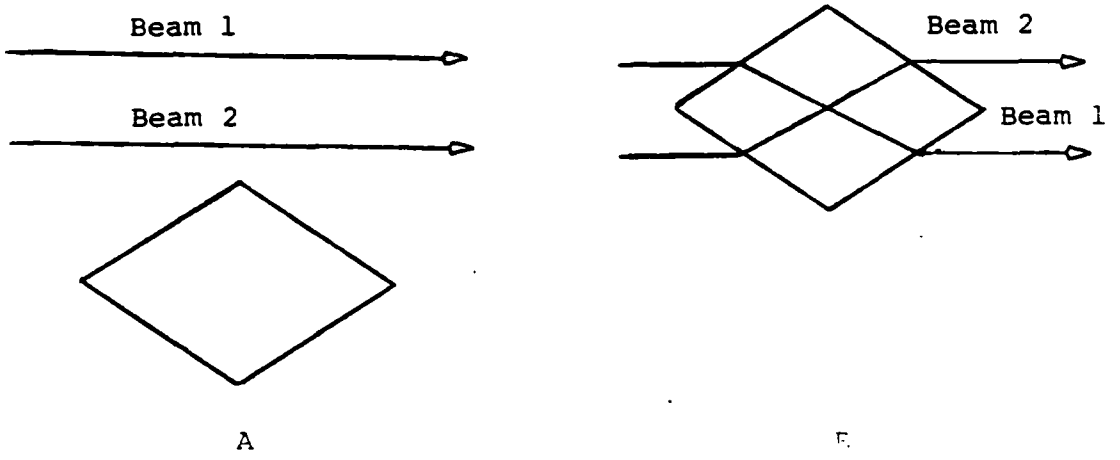

Figure 34. Two-Port Crossover Switch.

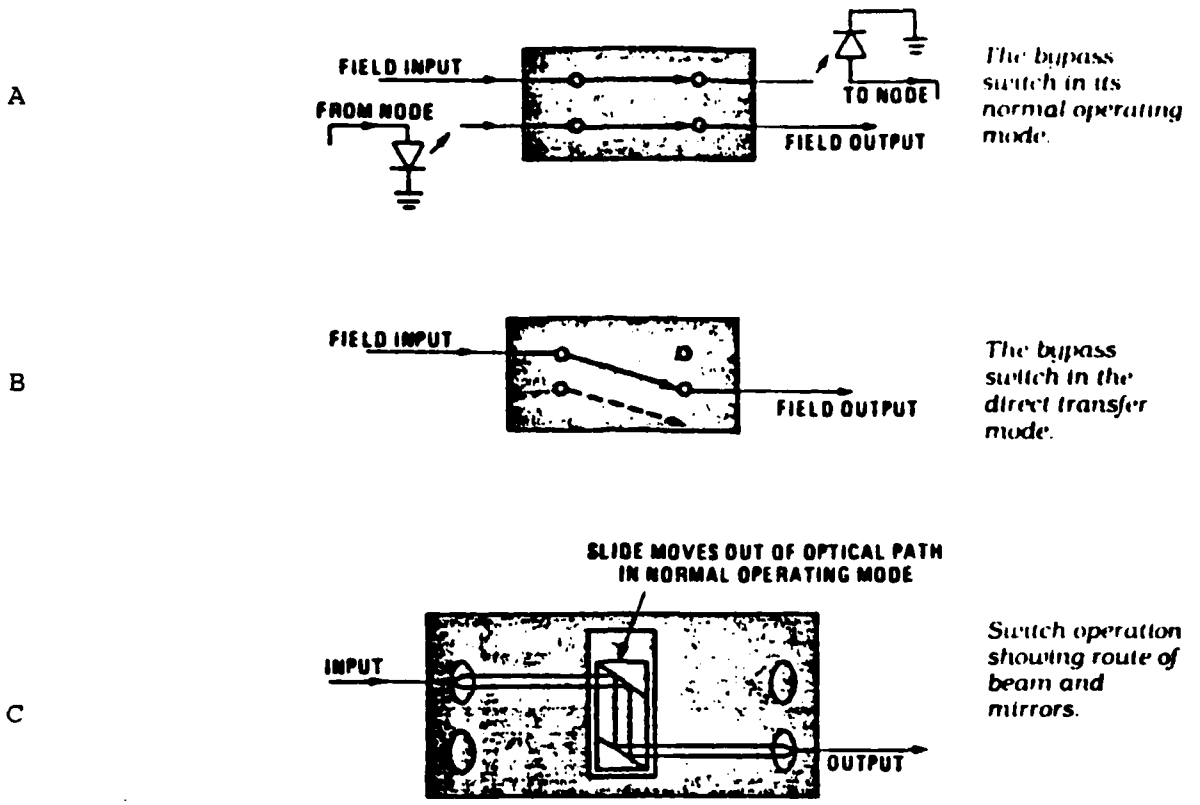

Figure 35. Four-Port Optical Bypass Switch.

A novel total internal reflection switch shown in figure 36 has been implemented by NTT Jbaraki Electrical Communication Labortory in Japan.[16] A low refractive-index channel is made in an SiO_2-Ta_2O_5 sputtered film with CO_2 laser irradiation. The decrease in refractive index of up to 2% results in a total internal reflection angle of over 11°. The total internal reflection is spoiled by contact of a gadolimium gallium garnet chip brought into contact with the switch area by means of an electromagnet. The gadolinium gallium garnet increases the effective refractive index of the channel more rapidly than the surrounding film area thereby decreasing the critical angle for total internal reflection. A switching angle of 22.5° and extinction ratio of 12-16 db. were obtained at 0.633 micron wavelength.

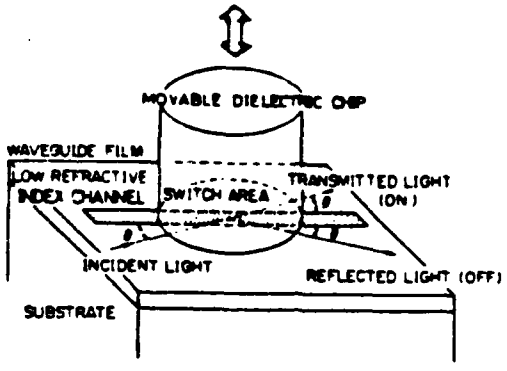

Figure 36. Total Reflection Optical Waveguide Switch.

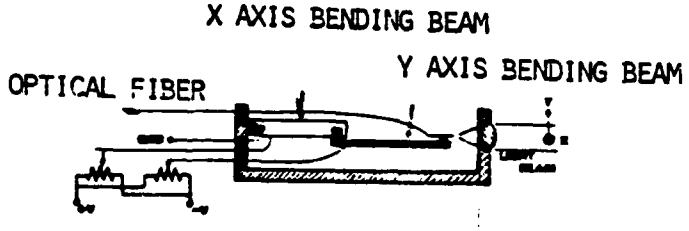

Figure 37. Piezoelectric Bending Element For A 16 X 16 Optical Switchboard.

Piezoelectric Switches

Arel Control Systems, Ltd. of Israel has demonstrated a 16:16 type IV switch which employs piezoelectric steering of optical fibers.[17] The emitting end of the input optical fiber is mounted on the free end of two piezoelectric bending beams as shown in figure 37. One voltage controlled beam bends in the X direction, the other in the Y direction. The output of the fiber is collimated by a lens to one of a 4X4 array of detectors. An array of 16 independent input deflectors are used.

Electro-Optic Switches

A well developed electro-optic technology is a type II switch which utilizes birefringence and the Pockels effect. One element of the switch is a Pockels cell operating on the longitudinal electro-optic Pockels effect. Application of the so-called half wavelength voltage to the cell will cause the polarization of the transmitted optical beam to be rotated through 90^{o}. The other element of the switch is a birefringment crystal such as calcite. The optical path through the birefringment crystal depends on the plane of polarization which is controlled by the Pockels cell as shown in figure 38. The input beam must be polarized in the proper plane with respect to the Pockels cells. A series of n switches can be used to switch a fiber optic input into one of 2^{n} output fibers.

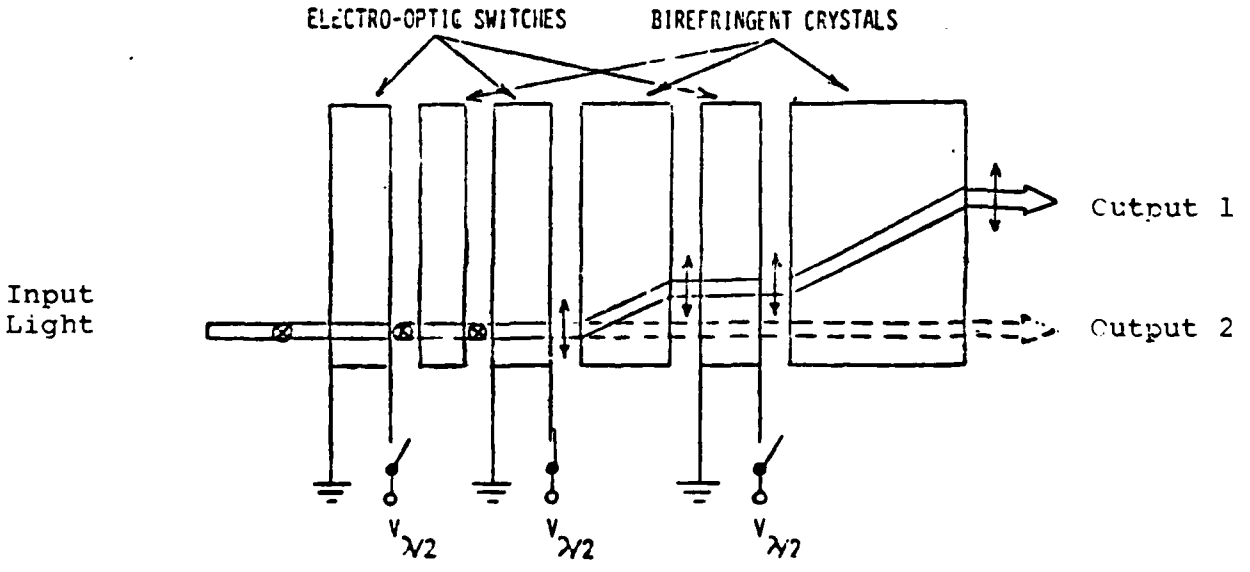

Figure 38. Pockels Cell Optical Switch.

The polarization loss can be eliminated by separating the input into orthogonal polarizations and passing them separately through two parallel switches before recombination. An interesting 2X2 type IV switch incorporating this concept has been developed by Sumitomo Electric Industries, Ltd. of Japan.[18] The input beams are separated and recombined by four part birefringent prisms as shown in figure 39. The pockels cell consists of six layers of $Bi_{12}SiO_{20}$ in order to reduce the operating voltage. With an applied voltage of 590 volts, an extinction ratio of more than 29 dB was obtained at a wavelength of 0.83 microns. The insertion loss is 3.9 dB and the switching time is about 7 microseconds.

An optical switch can be made using the interface between glass and a liquid crystal. Total internal reflection of the P component of polarization can be "frustrated" by applying a voltage across the liquid crystal layer. A 4X4 type IV switch using this concept has been constructed by Sperry Research Center.[19] As shown in figure 40 the switch has similar input and output halves. The input light beam is internally reflected from one side of the input prism to the other until it impinges on a transparent electropair that has an applied voltage to allow transmission into the coupling prism. The output half is rotated 90° to form the matrix configuration. This requires a half-wave plate between the switch sections so that the plane of polarization will also be rotated 90°. All switch combinations can be made simultaneously.

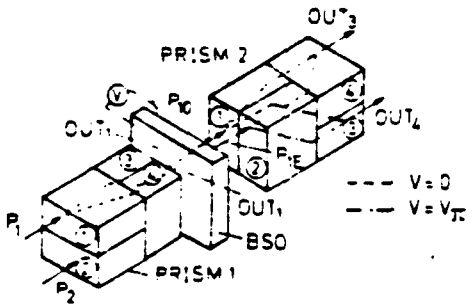

Figure 39. Multimode Polarization Independent Solid State Optical Switch.

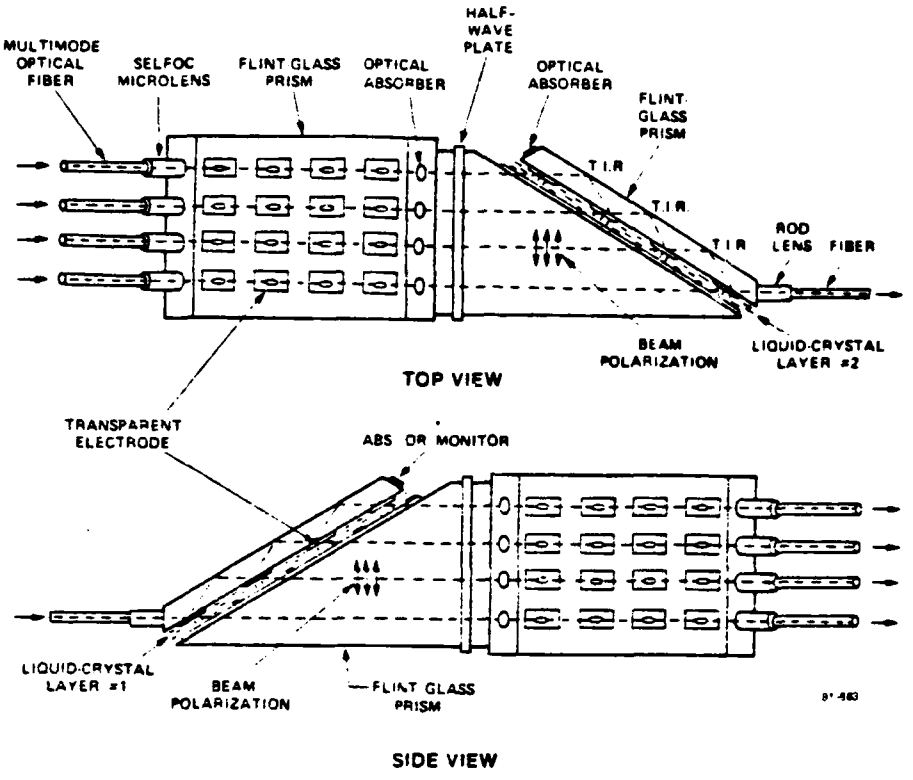

Figure 40. Nonblocking 4X4 Liquid State Optical Switch.

This liquid crystal switch demonstrated optical crosstalk of -44 to -53 dB and an insertion loss of as low as 6 dB with an average value of 15 dB. With the 40 volt addressing voltage, the turn-on time is 0.6 milliseconds and the turn-off time is 4.0 milliseconds.

A novel electro-optically controlled directional-coupler switch has been demonstrated by the University of Sheffield in England.[20] A gold metal film deposited on a $n\text{-}n^+$ GaAs epitaxial layer forms a strain induced refractive index in the vicinity of the film edge. The edge waveguide so formed supports one TE and one TM polarized mode. The propagation constant of the TE mode may be altered by inducing a small refractive index change through the electro-optic effect. Two such edge-guided modes brought into close proximity in a slot structure form a highly synchronous directional-coupler switch which can be electro-optically controlled. Using a wave length of 1.15 micron an isolation of 15 dB in the cross-over state has been achieved.

A 1X3 type II switch has been demonstrated at Osaka University in Japan.[21] A 3-branched waveguide formed by Ti-diffusion in Z-cut $LiNbO_3$ is shown in figure 41. In the absence of an applied

voltage, the refractive-index distribution is uniform in the cross section of the main input guide. The optical power carried by the E^z_{io} modes, therefore, should localize in the center part of the main guide and be fed mostly into the center branch B. When an appropriate positive voltage is applied, the side of the main guide toward the A branch has a higher index than the other parts, and thereby, the optical power is confined in region A and fed into branch A. A negative voltage switched the optical power into branch C. At a wavelength of 0.63 micron, the extinction ratio was nearly 10 dB at an applied voltage of ±25 volts.

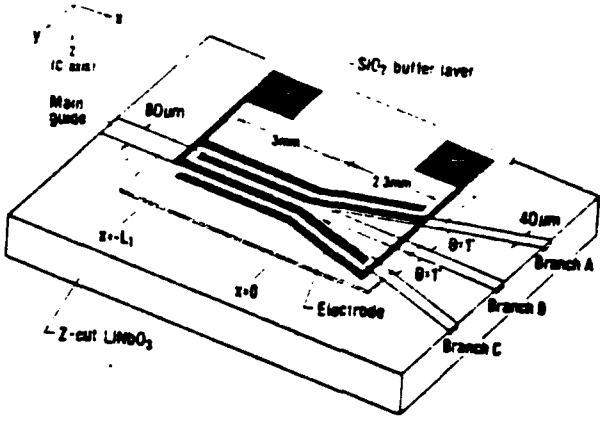

Figure 41. Four-Port Multimode Waveguide Optical Switch.

A 3X3 type IV switch based on total internal reflection has been demonstrated at Carnegie-Mellon University.[22] The switch element is crossed waveguides formed by Ti-diffusion in Y-cut $LiNbO_3$ as shown in figure 42. The area of the waveguide intersection has twice the refractive index change as the waveguide channels. Waveguide width is typically 20 microns. Intersection angles of 1.0^o, 1.5^o, and 2.0^o were tested. A pair of parallel metal electrodes having 5 micron separation are deposited at the center of the intersection region. Voltage applied to the electrodes switches the beam into the cross channel by total internal reflection. At a wave length of .63 microns in the fundamental mode drive voltages were from 5 to 11 volts with extinction ratios of 15.7 to 17.5 dB. The measured insertion loss is around 1.3 dB per intersection.

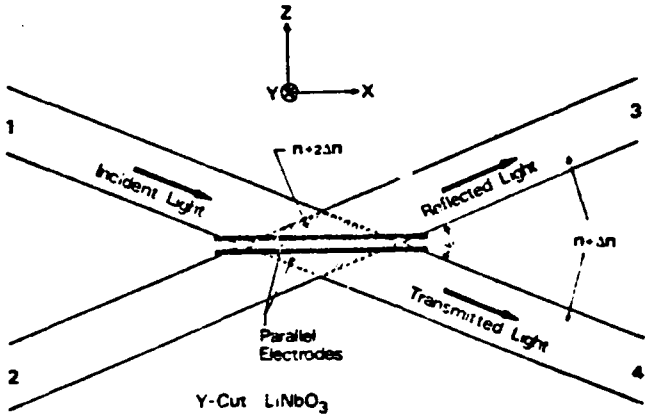

Figure 42. Multimode Waveguide Optical Switch.

A number of multimode switching devices have been developed at Sperry Research in which both waveguide path and switching control are achieved by means of the electro-optic effect.[23] Figure 43 shows how a single electro-optic channel is formed in a C-cut wafer of $LiNbO_3$. Approximately 400 volts across a 75 micron thick crystal produces a 10^{-3} change in index which is sufficient to guide light that diverges by $\pm 1.7^{\circ}$ in the crystal. An electrically controlled directional coupler shown in figure 44 was fabricated from a 54 micron thick C-cut platelet of $LiNbO_3$. The branch, 1° from the main channel tapers to zero width in the interaction region with a gap of 75 microns. If electrical excitation is applied only to the main channel, the lower index of the crystal in the interelectrode gap acts as a barrier that rejects incident light back toward the main-channel axis. If both branch and main-channel electrodes are excited, the barrier is removed and the switch acts as a 3 dB directional coupler at a level of 450 volts.

Devices were also made with C-cut $LiTaO_3$ in which guide channels are created by two lower-index stripe barriers created electro-optically. A 4-to-1 optical multiplexer using this double stripe geometry is shown in figure 45. The multiplexer has electrodes on top and bottom surfaces to create a main channel, four branch channels and four gates to couple branch channels to the main channel. Demultiplexer action can be produced by sequentially

removing one inhibit voltage at a time from the four gate electrodes, to produce a junction that permits about half the light to propagate down the corresponding branch channel. Branch angle switching of 10^{o} required 400 volts.

The double stripe geometry was also used in the optical crosspoint switch shown in figure 46. Because these waveguides intersect at 3.6^{o}, much of the $\pm 1.8^{o}$ confined input light can be switched into the crossguide. With a voltage of about 500 volts, about 10% of the multimode light is deflected into the cross channel. A 2X2 optical matrix switch of four crosspoints, showed -7 dB switching to an output channel and an optical signal-to-crosstalk ratio of 14 dB.

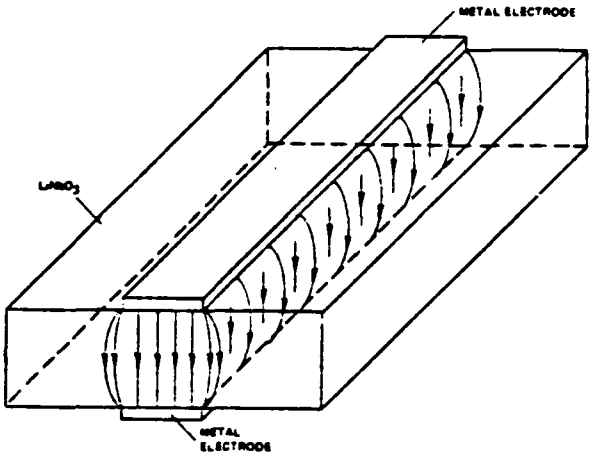

Figure 43. Guide Field Geometry.

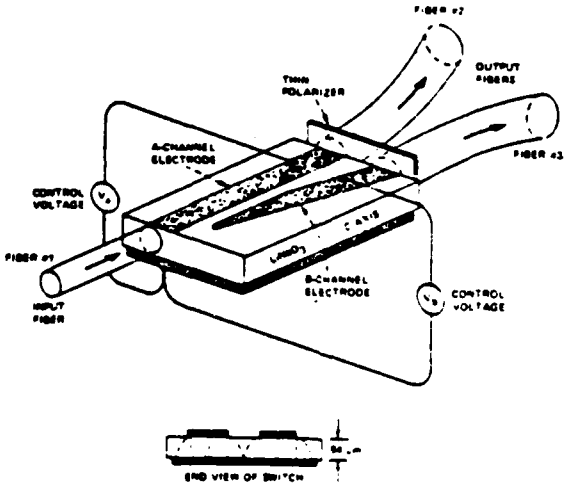

Figure 44. Three Port Multimode Optical Waveguide Switch.

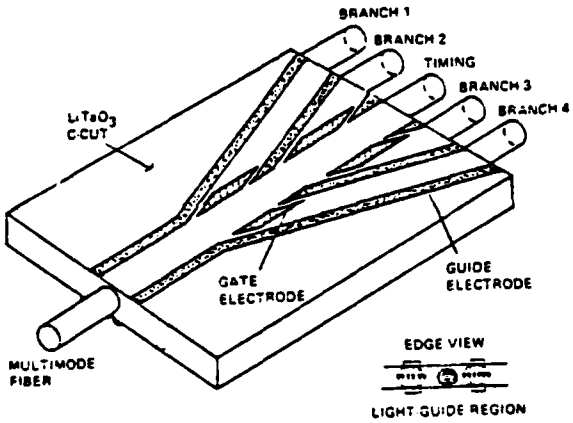

Figure 45. Four-to-One Multimode Optical Multiplexer -Demultiplexer.

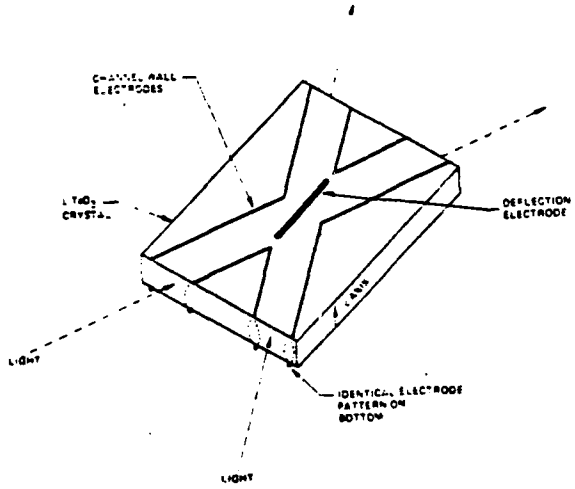

Figure 46. Four-Port Optical Crosspoint Switch.

Magneto-Optic Switches

A waveguide magneto-optic 1X2 switch or modulator has been demonstrated by Bell Telephone Laboratories.[24] The experimental arrangement is shown in figure 47. A $Y_3Ga_{1.1}Sc_{0.4}Fe_{3.5}O_{12}$ is grown on a {1,1,1} $Gd_3Ga_5O_{15}$ substrate with easy axis parallel to the film. Two prism film couplers are used to couple light into and out of the film. Between the two couplers, a small serpentine electrical circuit is placed closely in contact with the film. The magneto-optic effect of the film causes light traveling in the film to convert from the TM to the TE mode. As the current in the circuit increases and decreases at the radio frequency, M tilts toward or away from the direction of light propagation. This motion of M increases or decreases the magneto-optic effect which serves as the coupling between the TM and TE modes. The two modes are separated by the birefringence of the rutile output coupling prism. Light from a 1.152 micron laser was modulated up to 80 MHz. Light was switched between the two wave guide modes by applying a magnetic field as small as 0.2 oersteds.

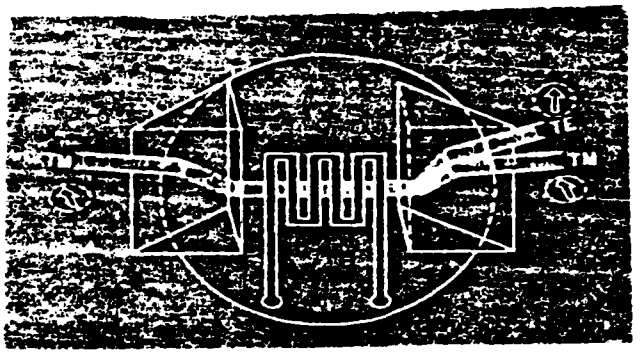

Figure 47. Waveguide Magneto-Optic Switch.

A 2X2 magneto-optic switch using Faraday rotation has been developed by Fujitsu Laboratories in Japan.[25] The switch is shown in figure 48 and consists of input and output prisms, a half-wave plate to rotate the input light beams 45°, cylindrical lenses to couple into, a switchable Faraday rotator with 45° rotation, and a switchable semihard control magnet which is not

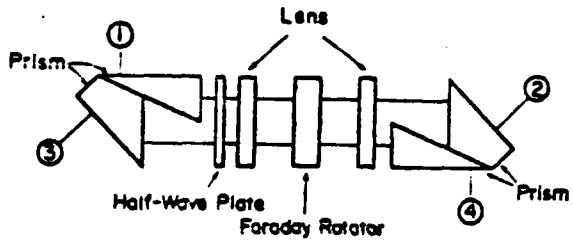

Figure 48. Polarization Independent Multimode Optical Switch.

shown in the figure. The prisms are a combination of two birefringent rutile prisms which are used for polarization separation to eliminate the 3 dB loss for multimode fiber input. Separation is achieved because the P-polarization is transmitted at the Brewster angle and the S-polarization is totally internal reflected due to the difference in their refractive indicies. The Faraday rotator is a 50 micron thick single-crystal plate of YIG. The switching field for this Faraday rotator is less than 100 Oersteds. At a wavelength of 1.3 microns the insertion loss was 1.5 dB and the crosstalk was -32 dB. Switching time is 20 microseconds at 3 volts and 500 milliamps.

Thermo-Optic Switches

A 1X2 thermo-optic switch has been demonstrated at Osaka University in Japan.[26] It is based on the temperature dependence of the refractive index and is shown in figure 49. The Y branch waveguide structure was fabricated by K^+ ion exchange in a soda-lime microscope slide. The input waveguide expands to a 60 micron width before the split into two output branches. With no input to the heaters the optical power is split between the two output branches. When a voltage is applied only to heater A, the input beam is then confined in the higher index region underneath heater A, and thereby more optical power is diverted into branch A while less power is fed into branch B. At a switching level of 30 volts the turn on time is about 1.2 milliseconds and the turn off time is about 1.6 milliseconds. Crosstalk was -12 dB or less.

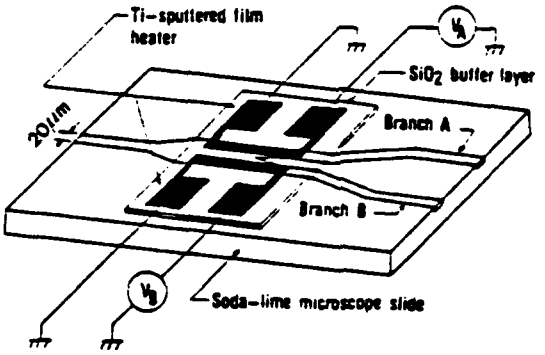

Figure 49. Three-Port Multimode Thermo-Optic Switch.

The Stripe Domain Switch

The stripe domain switch utilizes the diffraction of light by a grating structure whose line spacing and direction are controlled by a magnetic field. The grating is formed by magnetic stripe domains in a ferrimagnetic film having high Faraday rotation and low optical absorption. There is a normal component of the magnetization which alternates in adjacent stripes and operates, by means of the Faraday effect, as a phase grating. Increasing the applied magnetic field causes an increase in the grating spatial frequency, which causes diffraction through a larger angle. The stripes orient themselves along the direction of the applied field so that the diffraction can be controlled in two dimensions. When the applied magnetic field is removed the stripes relax to a normal minimum spatial frequency which determines the minimum diffraction angle. The stripe domain switch is multimode and is not polarization dependent.

The most obvious application of stripe domain technology as an optical switch is a type II switch with a single input fiber attached normally to the stripe domain film as shown in figure 50. Output fibers are arranged in a circular pattern at the minimum deflection angle. A pulsed magnetic field can be applied to switch the input signal to any one of the output fibers. This fundamental arrangement can be modified in a number of different ways.

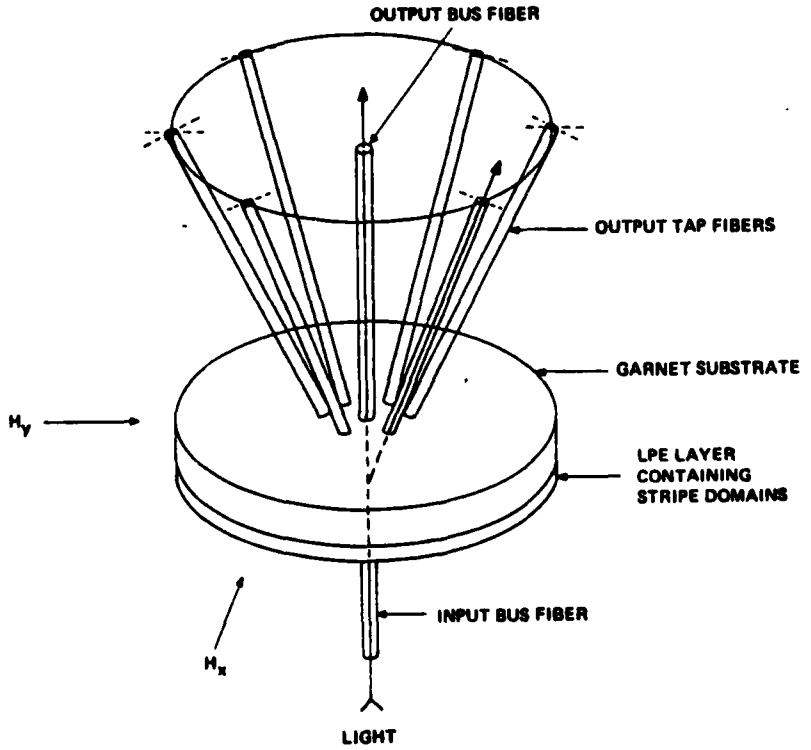

Figure 50. Stripe Domain Fiber Optic Switch.

One modification is to increase the number of outputs by the addition of one or more circular arrays of optical fibers at higher deflection angles. These higher deflection angles require a constant magnetic field to maintain the proper spatial frequency of the grating. The stripe domain phase grating produces a diffraction pattern which has the odd order beam on both sides of the zeroth order beam. The relative intensity of the beams is a function of several variables with the possibility of suppressing the zeroth order beam. Both first order beams can be used to provide switching into two output fibers. Another arrangement is to put an output fiber on axis to provide for a bus output, with the device acting as a tap switch. In addition straight uniform stripe domains, other stripe domain configuration are possible. One of the most interesting stripe patterns is a series of concentric circular domains. This pattern produces a circular diffraction pattern which can be used to switch the input into all the outputs at a particular diffraction angle in another version of an active star coupler.

The stripe domain deflector can also be used to implement a type III switch as shown in figure 51. This switch is similar to the switch in figure 31 with the rotating mirror replaced by a stripe domain film with a mirror on the back side so that it operates in a reflection mode. Another difference is that Selfoc lens are attached to the optical fibers so that the light beam will be parallel for diffraction from the grating. In figure 31 the diverging light from the fiber is focused by the concave mirror. The stripe domain spacing (d) required for first order diffraction is given by:

$$d = \frac{\lambda}{4 \sin \frac{1}{2} \Delta} \quad \frac{1}{\cos \gamma}$$

where λ is the wavelength, Δ is the diffraction angle and γ is the angle that a line bisecting the diffraction angle makes with the normal (see figure 51). The factor $1/\cos \gamma$ is plotted in figure 52 and shows that for small values of γ, the grating spacing varies only slowly with γ. The smallest grating required is for diffracting the beam from fiber 1 to fiber 5 in figure 51. The largest grating spacing is for the closest fiber pair. To minimize the required range for the grating spacing, the closest fiber pair should be placed near the grating normal as in figure 51. The fiber input locations shown in figure 51 were selected so that all terminal pairs could be connected without incidently connecting other terminal pairs.

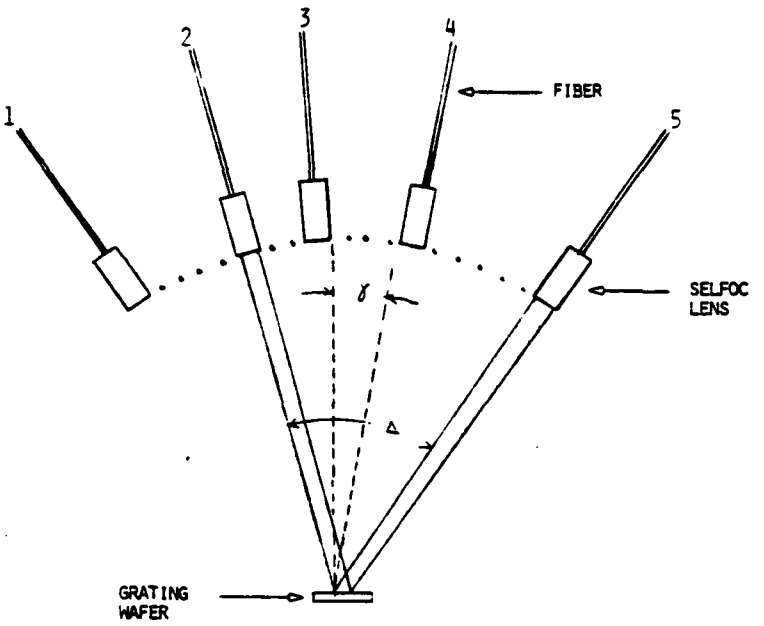

Figure 51. Active Star Mode Fiber Optic Switch.

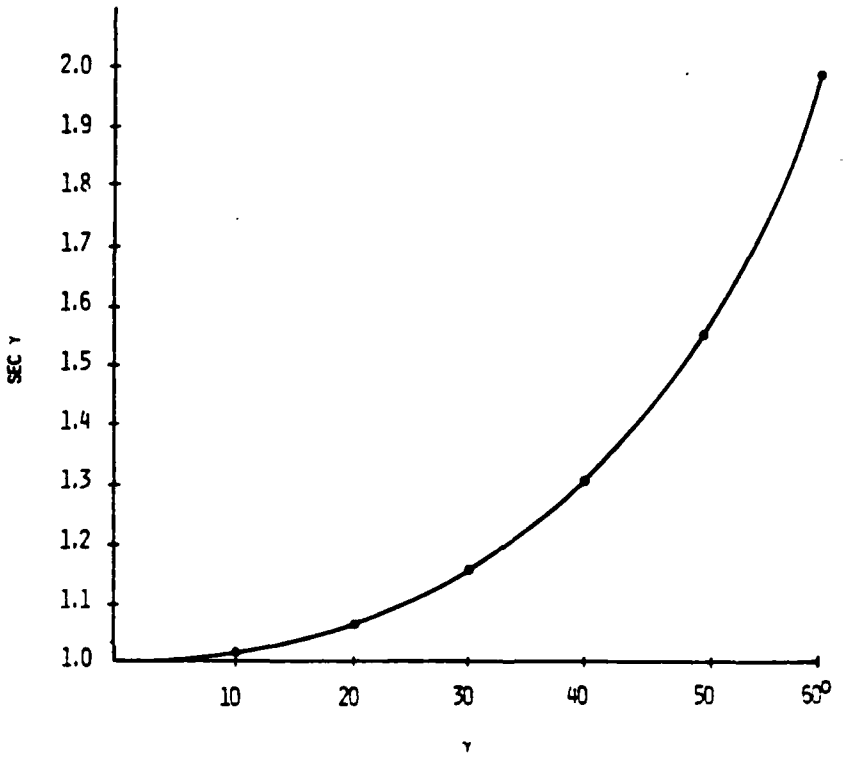

Figure 52. γ vs. secγ.

Finally, the stripe domain technology can be used to implement a type IV switch as shown in figure 53 which depicts a 4:4 configuration. A Selfoc lens on the end of each input fiber collimates the widely diverging light from the fiber tip. The light from a given Selfoc lens falls on one and only one deflector element which steers it through an output lens to one and only one output fiber. This switch can have up to 10^4 input lines and 10^4 output lines in two dimensional arrays, all operating simultaneously. Two inputs can be switched to the same output which can be of interest if the two optical signals are at different wavelengths.

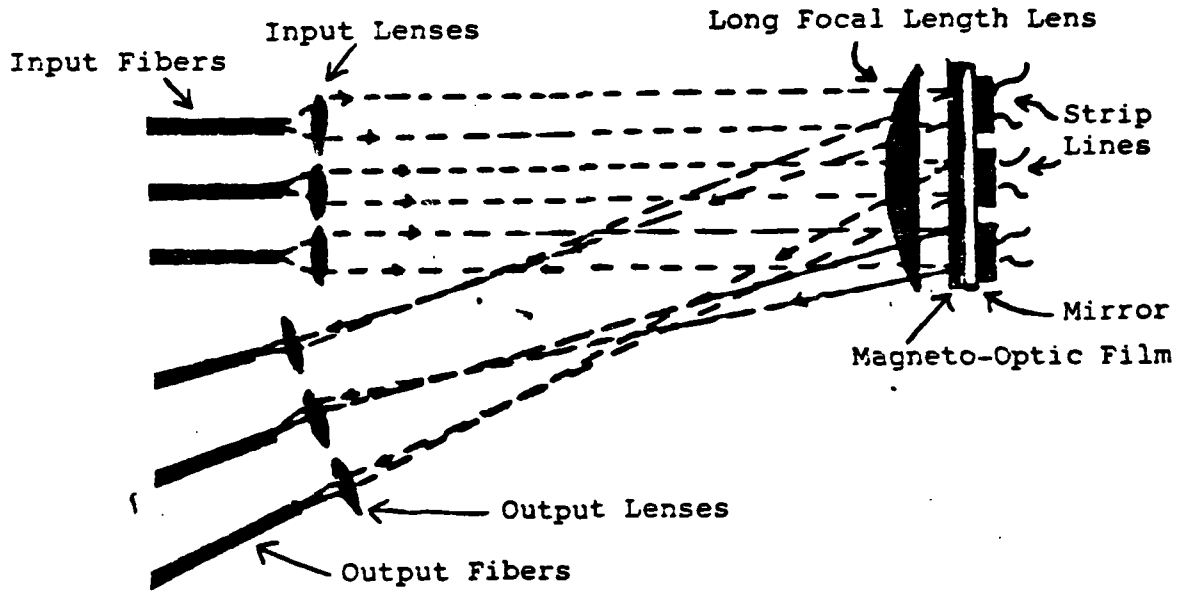

Figure 53. Stripe Domain High Density Circuit Switchboard For Fiber Optics.

This switch will not work well backwards because light emerging from the end of an output fiber will in general have too large a beam divergence to fall on a single deflector element. Therefore a second array of input fibers with Selfoc lenses and output fibers is required for two way communication, although the same deflector elements can be used.

The incorporation of this switch into a system of the type shown in figure 53 is illustrated in figure 54, where the four terminals are connected in addition by a redundant switchboard. Figure 55

illustrates two such star systems connected by an internode fiber bus. Repeaters are shown for completeness on both the switchboard models. As in any communications system the need for repeaters would depend on details of deployment.

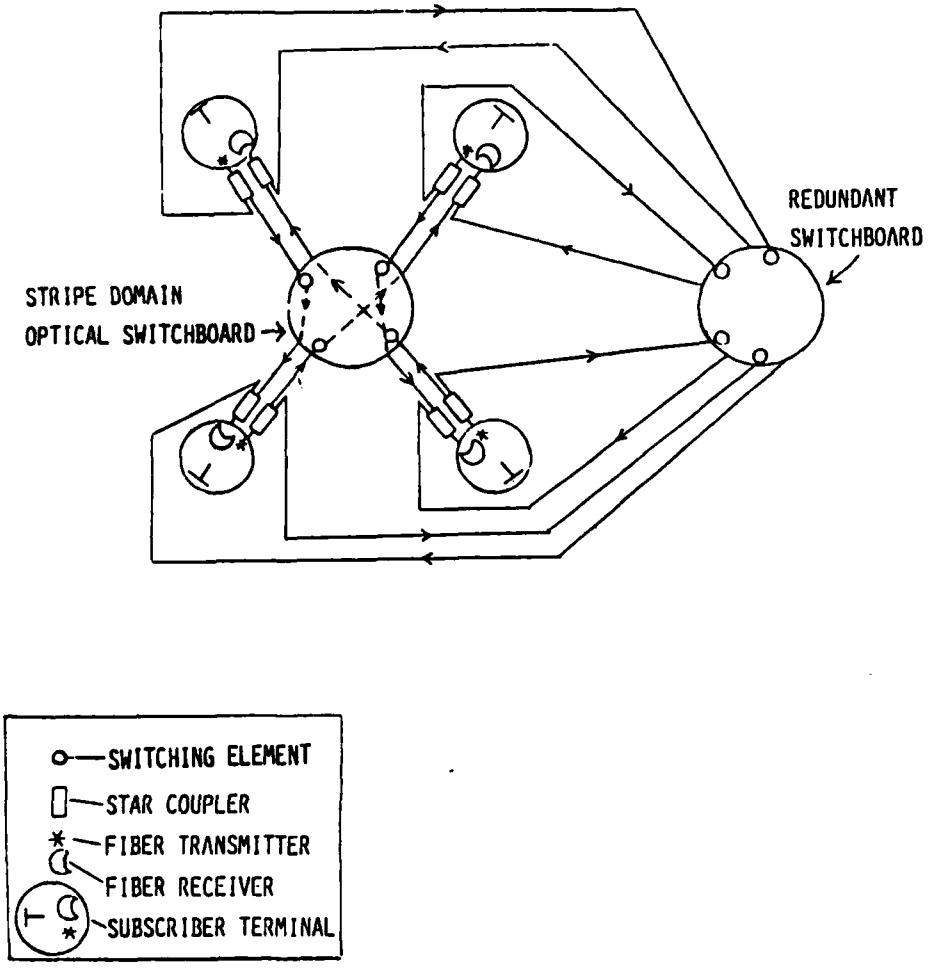

Figure 54. Stripe Domain Star Topology Optical Switchboard With Redundancy.

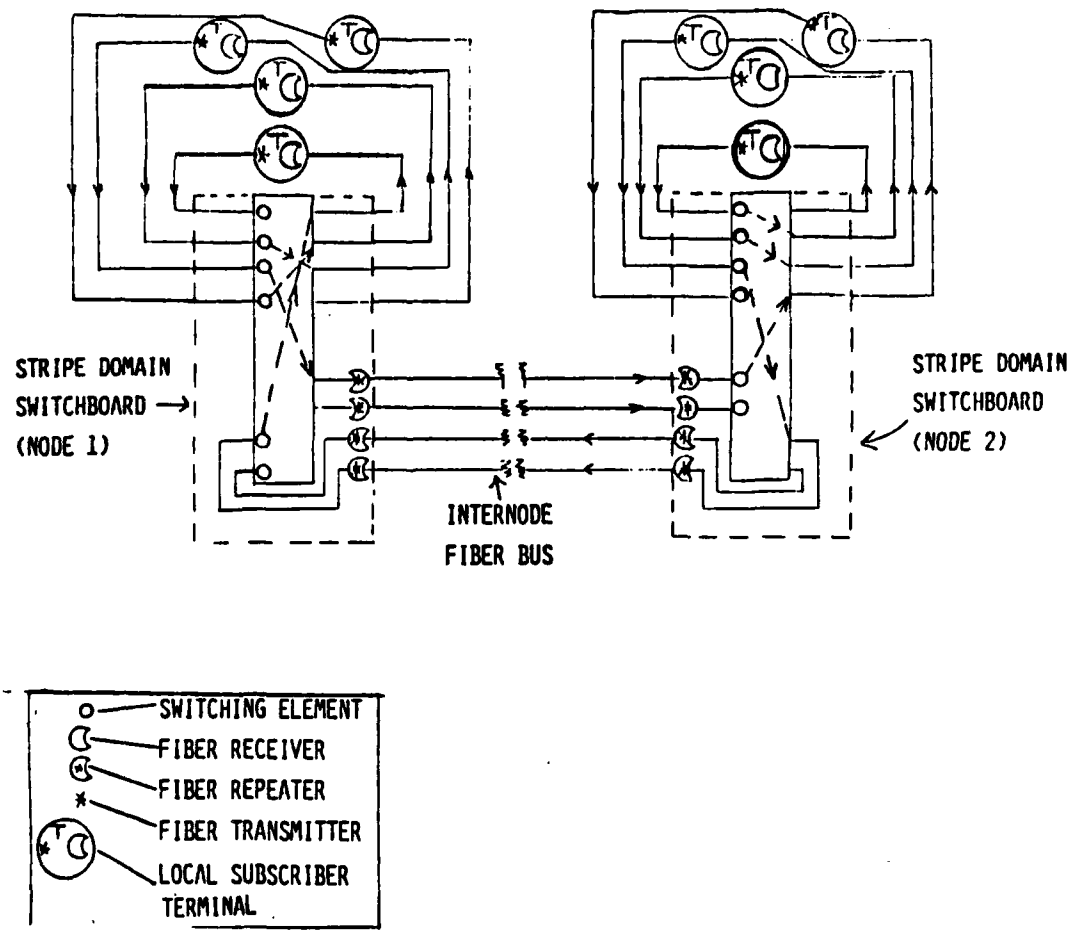

Figure 55. Stripe Domain Two Node Optical Switchboard System.

Conclusions

The magnetic stripe domain technology is a fundamentally simple solid state device that can be used to implement a wide range of all optical switch types with the potential for low cost. The technology does not require device cascading which can lead to large accumulative signal losses. A comparison is shown in figure 56. It has the capability of multiple simultaneous outputs and can be used with a data bus in a tap mode. In general it is a two way communication switch all though some implementations render it a one way device. Because of its very high switching speeds, it can also incorporate signal modulation and multiplexing. The dispersive characteristic of the magneto-optic grating allows the possibility of wavelength separation.

One of the problem areas is the optical absorption of the magneto-optic garnet film which limits device efficiency. This problem is being reduced by the development of garnet materials with low optical absorption and by multipass techniques in which the light beam is reflected back and forth through the deflector film many times. There are also other materials such as EuO which might prove suitable candidates for this switching technology.

Comparison For The Case
Of A 128 Input 128 Output
Switchboard

	Magneto Optic	Binary 1X2
Number of Stages	1	2
Components	128 input lenses 128 integrated deflector elements 1 coupling lens	32,258 switches and 256 stars

Figure 55. Stripe Domain and Binary Optical Switches.

BIBLIOGRAPHY

1. T. R. Johansen, D. I. Norman and E. J. Torok, "Variation of Stripe-Domain Spacing in a Faraday Effect Light Deflector," Journal of Applied Physics, Vol. 42 No. 4, P. 1715, 1971.

2. E. J. Torok, F. G. Hewitt, J. A. Krawczak, G. L. Nelson, "Manipulation of Light With Magneto-Optic Stripe Domain Films," NASA Conference on Optical Information Processing for Aerospace Applications, 1981.

3. G. F. Sauter, R. W. Honebrink, J. A. Krawczak, "Alterable Grating Fiber Optic Switch," Applied Optics, Vol. 20 No. 20, P. 3566, 1981.

4. G. B. Scott and D. E. Lacklison, "Magneto-Optic Properties and Applications of Bismuth Substituted Iron Garnets," IEEE Transactions on Magnetics, Vol. MAG-12 No. 4, P. 292, 1976.

5. G. L. Nelson and W. A. Harvey, "Optical Absorption Reduction in $Bi_1Lu_2Fe_5O_{12}$ Garnet Magneto-Optical Crystals," Journal of Applied Physics, Vol. 53 No. 3, P. 1687, 1982.

6. "Theory of the Selfoc ^{R} Lens" in Selfoc Handbook, pub. by Nippon Sheet Glass of America, P. 13, 1981.

7. D. C. Johnson, B. S. Kawasaki and K. O. Hill, "Fused Biconical Tapered Fiber-Optic Devices : Applications to Data Buses," Fiber and Integrated Optics, Vol. 3 Nos. 2 & 3, P. 263, 1980.

8. U. Killat, C. Clausen, G. Rabe, "Binary Phase Gratings for Couplers Used in Fiber Optic Communication," Fiber and Integrated Optics, Vol. 3 Nos. 2 & 3, P. 221, 1980.

9. W. J. Tomlinson and G. D. Aumiller, "Optical Multiplexer for Multimode Fiber Transmission Systems," Applied Physics Letters, Vol. 31 No. 3, P. 169, 1977.

10. Y. Suzuki, T. Sato, "7 G bit/s Coherent Pulse Generation In An Actively Mode-Locked GaAlAs Diode Laser," Electronics Letters, Vol. 18 No. 19, P. 821, 1982.

11. T. Ozeki, T. Uematsu, T. Ito, M. Yamamoto, and Y. Unno, "Half-Duplex Optical Transmission Link Using an LED Source-Detector Scheme," Optics Letters, Vol. 2, No. 4, P. 103, 1978.

12. K. Kaede, in 1978 Nat. Conv. Record (I.E.C.E., Japan) paper 861.

13. T. Tanaka, S. Ishizuka, H. Serizawa and Y. Tsujimoto, "A New Form of Optical Transmission System Using 1X6 Optical Switch," Fiber and Integrated Optics, Vol. 4 No. 1, P. 1, 1982.

14. R. A. Soref, W. B. Spillman, Jr. and M. Kestigian, "Fiber-Optic Switching Techniques," Proceedings of the National Electronics Conference, Vol. 33, P. 188, 1979.

15. T. C. Odderstol, "A Bypass Switch Gets in Line," Photonics Spectra, P. 41, December 1982.

16. H. Terui and M. Kobayashi, "Total Reflection Optical Waveguide Switching Through Dielectric Chip Motion," Applied Optics, Vol. 20, No. 18, P. 3152, 1981.

17. H. Laor, Technical Digest, Seventh ECOC, Copenhagen, 1981.

18. S. Iguchi, H. Goto, M. Kato, S. Takeuchi, Y. Kuhara, K. Tada, and T. Nakahara, "Development of Electrically Controlled Optical Switch," J. Opt. Commun. Vol. 1 No. 1, P. 22, 1980.

19. R. Soref, "4X4 Electo-Optical Matrix Switch for Fiber Optic Networks," SRC-RP-81-90, Nov. 1981.

20. T. Benson, T. Murotani, P. Robson, and P. Houston, "A Novel Flecto-Optically Controlled Directional-Coupler Switch in GaAs Epitaxial Layers at 1.15 μm," IEEE Trans. on Electronic Devices, Vol. ED-19, No. 9, P. 1477, 1982.

21. K. Mitsunaga, K. Murakami, M. Masuda, and J. Koyama, "Optical $LiNbO_3$ 3-branched Waveguide and its Application to a 4-port Optical Switch," Applied Optics, Vol. 19, No. 22, P. 3837, 1980.

22. C. Tsai, B. Kim, and F. El-Akkari, "Optical Channel Waveguide Switch and Coupler Using Total Internal Reflection," IEEE J. Quantum Electron., Vol. QE-14, P. 513, 1978.

23. D. McMahon, "Multimode Optical Switching," Laser Focus, P. 46, March 1979.

24. P. Tien and R. Martin, "Switching and Modulation of Light in Magneto-Optic Waveguides of Garnet Films," Appl. Phys. Lett., Vol. 21, No. 8, P. 394, 1972.

25. M. Shirasaki, H. Takamatsu, and T. Obokata, "Bistable Magneto-optic Switch for Multimode Optical Fiber," Applied Optics, Vol. 21, No. 11, P. 1943, 1982.

26. M. Haruna, and J. Koyama, "Thermo-optic Deflection and Switching in Glass," Applied Optics, Vol. 21, No. 19, P. 3461, 1982.

MANIPULATION OF LIGHT WITH MAGNETO-OPTIC STRIPE DOMAIN FILMS

SPERRY UNIVAC
DEFENSE SYSTEMS

NASA Conference Publication 2207

Optical Information Processing for Aerospace Applications

Proceedings of a NASA conference
held at Langley Research Center
Hampton, Virginia
August 18-19, 1981

NASA
National Aeronautics
and Space Administration

**Scientific and Technical
Information Branch**

1981

MANIPULATION OF LIGHT WITH MAGNETO-OPTIC STRIPE DOMAIN FILMS

E. J. Torok, F. G. Hewitt, J. A. Krawczak, G. L. Nelson

Sperry Univac, DSD, St. Paul, Minnesota

Work sponsored in part by the Army Research Office (ARO), Research Triangle Park, North Carolina.

ABSTRACT

Magnetic diffraction grating materials are currently being developed to provide a simple means of deflecting light in a two-dimensional, solid-state fashion. The most promising material, for several applications, appears to be bismuth substituted iron garnet films in epitaxial form. Calculations indicate that deflection efficiency greater than 60% is possible in the near-infrared region of the spectrum. Within the field of view of the deflector, measurements predict that 10^5 resolvable spots can be expected. Applications include 1) general purpose deflection of free laser light, 2) image processing of extended sources such as transparencies, 3) programmable lensing, and 4) fiber optic matrix switching.

MAGNETO-OPTIC LIGHT DEFLECTOR

The active component of this deflector is a dynamically alterable, solid-state phase diffraction grating that is the energetically favored domain structure of properly configured magnetic materials. A description of the deflector follows.

Diffraction of a light beam occurs as a result of periodic variations in the wave amplitude or phase across a wave normal surface. Magnetic stripe domain arrays can introduce a periodic 180^0 phase variation in an incident optical field, through magnetic birefringence. A stripe domain is a long, straight region of uniform width in which the magnetization is nearly constant. Typically, the width can vary from .5 micron to 30 microns or more while the length can extend to several centimeters.[1] Stripe domains in a given sample may or may not have equal width, depending on sample properties and on imposed magnetic fields.

Consider a linear array of stripe domains in a magnetic platelet as depicted in figure 1. Adjacent stripes have $\hat{z}$ components of magnetization that are antiparallel and usually have a continuous component in the x y plane. Because of the Faraday effect the E_x and E_y components of an incident optical field suffer clockwise rotation in odd-numbered stripes and counterclockwise rotation in even-numbered stripes. This differential rotation provides an electric component that is orthogonal to the incident polarization and has 180^0 alternations (parallel and antiparallel to $\hat{y}$) that match the spatial period of the domains. The process operates uniformly for all incident polarizations, including random.

In the far-field emerging light adds constructively at angles θ_n, given by

$$\sin \theta_n = \frac{n\lambda}{\Lambda} ,$$

where n is the order number, λ the incident wavelength, and Λ the grating period. In the special case where each stripe has the same width, even orders are suppressed. Magnetic apodization at the transitions between even and odd stripes discourages higher orders, as well.

The n^{th} odd-order power diffraction efficiency for a square phase grating is found from

$$\frac{I_n}{I_o} = \frac{4}{n^2\pi^2} e^{-\alpha(\lambda)t} \sin^2 F(\lambda)t ,$$

with α the optical absorption coefficient, t the material thickness, and F the Faraday rotation.[2] Figure 2 shows the potential total efficiency of several candidate crystalline deflector materials in the visible and infrared region of the spectrum, based on reported values for F and α.[3-6]

In order to alter the grating in a solid-state dynamic fashion, reliance is made on the strong coupling of the material magnetization and applied magnetic fields either coplanar with, or perpendicular to, the stripe domains. There are several ways in which a magnetic grating can be field programmed to deflect light. A perpendicular field changes the stripe width, periodicity, or both, causing linear deflection and perhaps a shuffling of light amongst the various allowed orders. If the field is applied in the plane, and collinear with the domains, then the stripe width varies with H^{-1}, increasing the diffraction angle with increases in field intensity. Finally, if the field is applied to a general direction in the plane, the grating is reestablished collinear to the field, resulting in azimuthal deflection. For some materials the field strength necessary to cause deflection in the annular field of view is less than that required for Lorentz deflection of electron beams in CRTs. Thus, microsecond switching speeds are possible with watt level electrical power.

GARNET

Of the deflector candidates contrasted in figure 2, rare earth iron garnet is presently the preferred material for a variety of reasons. It is readily obtainable as epitaxial films up to 100 microns thick grown on gadolinium gallium garnet, commonly employed as magnetic bubble memory substrates. Stable stripe domain arrays of sufficient quality to provide 10^5 resolvable spots in the annular field of view have been observed. Curie points to 550°K insure that the magnetization is nearly constant over a wide temperature range, including room ambient. The applied fields required to manipulate the stripe domains are on the order of 100 oe., derivable from computer controlled Helmholtz pairs or strip lines in close proximity to the crystal. With bismuth doping the Faraday rotation can reach 50,000°/cm in the visible and 12,000°/cm in the near-infrared.[7] The optical absorption exhibits a local minimum at the .81 micron fiber-optic wavelength and a large window of near-zero absorption at wavelengths greater than 1.2 microns. Calcium doping has been successfully used to reduce the absorption at important wavelengths.[8] From experimental data obtained with

a Faraday hysteresigraph and a spectrophotometer on thin epitaxial samples it is possible to calculate the maximum deflection efficiency of thick samples or of thin samples operated inside an optical resonant cavity. The calculation has been done and the results are shown in figure 3. Work is currently under way to experimentally evaluate these expectations and to develop the necessary crystal growth facilities to exploit the potential of bismuth garnet for light deflector applications.

APPLICATIONS

Agile light deflectors based on magneto-optics offer unique solutions to a number of optical switching and processing problems. Obvious applications include laser radar at 1.06 microns and 10.6 microns, focal plane array scanners, and optical communications between moving platforms. Because stripe domain arrays can be plastically deformed by spatially varying fields, adaptive optic processing of images of extended objects can also be performed. In guided wave communications, bismuth garnet, in its present form, serves quite well as a high fanout fiber optic switch.

Adaptive Optics

In a stripe domain grating the periodicity, stripe width, and orientation need not be constants over the aperture. Spatially varying magnetic fields can be utilized to locally modify the deflection of incident light from pointlike sources or from extended sources such as collimated beams or transparencies. By properly tailoring the grating, dynamically alterable compressors or expanders and image rotators can be generated.

One-dimensional compressors or expanders are constructed from the domain pattern that has the basic spatial modulation seen in figure 4a. Both the stripe density and grating orientation are functions of local field. This would be useful for correcting image distortions.

Gratings obtained by converting the linear array of a film with some in plane magnetic component, into the radial array of figure 4b, provide a means for continuous distortionless image rotation if the grating has the appropriate radial stripe density gradient. A geometric optic analysis reveals that the gradient is such that the stripe density is inversely proportional to radius. Then the impressed image rotation angle, B, is found to be

$$B = \tan^{-1} \frac{s\lambda}{2c} ,$$

with s the distance to the post grating image plane and c a quantity that depends on field magnitude and stripe widths. In addition, the image experiences a magnification of sec B. Continuous rotation occurs with intensity changes in the field.

In order to initialize the grating to a radial mode it is necessary to bring a point pole into approximate contact with the film surface. The symmetry in the pole's field causes the grating to assume the desired form but with constant stripe density.

In practice the pole can be supplied by a polished ferrite needle. The inplane field that develops the proper stripe density was found to match the tangential field produced by an extended magnetic polepiece. Thus, it has been possible to observe both the rotation and the scaling properties of the radial domain image processor. Rotations to near 90^{o} were recorded. Since the required polepiece is available in ferrite form, high speed rotation is expected.

Arrays formed from domains that are concentric annuli about a fixed center may act like a Fresnel zone plate; i.e., collimated light focuses on the zone axis when the domain widths satisfy the pertinent Fresnel relations. If the incident light impinges on just a sector of this array as in figure 4c, focusing occurs off the optic axis. In either case, dynamic control of the domains implies dynamic lensing. Most likely, garnet materials for this application are of the bubble type because they have only a perpendicular magnetization component.

Fiber Optic Switch

Useful deflection efficiency at the present fiber optic wavelengths, along with magnetic control of the intrinsic grating in garnet films is the basis for a multiport fiber optic switchboard as seen in figure 5. Information-bearing light, propagating in any or all of the elements of the input fiber 2-dimensional matrix is collimated by gradient index lenses (GRIN). Light from a given fiber lens falls on just one deflector element which steers it to one fiber in the focal plane of the output lens. The switchboard has high fanout with just a single level of optical switching. Greater than 100 X 100 input or output arrays can be accommodated.

Figure 6 shows a basic version of a fiber optic switch that utilizes only the inner circumference of the deflector field of view. Input bus light is tapped by selected output fibers that are arranged at the appropriate positions on the I/O face of a GRIN lens. This version provides a set-and-forget feature; i.e., once the orientation of the stripes has been established by the field coils to direct input light to the selected tap, all coil current can be removed until another tap fiber selection is required.

Meaurements and observations to date indicate that the switch has a number of other desirable features. It is insensitive to incident polarization, making it particularly attractive for fiber optics. Crosstalk can be held to < - 20 db. with a fanout of 10. Physical size can be as low as 1 cm^{3} as shown in figure 1, a working model of a 1 X 3 switch. Field coil switching is approximately 1 watt with microsecond select time. As a diffraction grating it satisfies the reciprocity theorem and is dispersive, allowing two-way operation of multiwavelength carriers. These attributes provide significant systems potential.

One useful systems device is an optical switch that can access just one output or simultaneously access all outputs, on electrical command. It was demonstrated that the basic stripe domain fiber optic switch can accomplish this because of its adaptive optic capability. With reference to figure 4b, if the stripe grating is switched to the constant periodicity radial format discussed under adaptive optics, the deflection space is a thin annulus at the same deflection angle as for the linear grating. Since the tap fibers are arranged to intercept light at this angle, they are uniformly illuminated with the light propagating in the bus fiber. Thus, all tap fibers are

simultaneously selected. This can be implemented by placing a point magnetic pole on the optic axis, just behind the mirror. Switching between single select and the multiselect star coupler mode should occur in microseconds.

Because of its high fanout the garnet fiber optic switch may have use as a residue arithmetic adder for optical computing. Figure 8 is a schematic of a possible modulo 5 adder in which input fiber light represents one addend and the grating selected output represents the other.

SUMMARY

Magnetic stripe domain arrays in bismuth iron garnet epitaxial films are alterable in orientation and grating constant with externally applied magnetic fields generated by high speed deflection circuitry. Optical radiation, incident upon the grating, is thus diffracted in a two-dimensional solid-state fashion. Favorable deflection efficiencies and local control of the grating suggest a number of applications. Further work may lead to compact devices that are applicable to robotics and optical processing.

REFERENCES

1. Johansen, T. R.; Norman, D. I.; Torok, E. J.: Variation of Stripe Domain Spacing in a Faraday Effect Light Deflector. JAP, Vol. 42, No. 4, Mar. 1971, 1715.

2. Scott, G. B.; Lacklison, D. E.: Magneto-optic Properties and Applications of Bismuth Substituted Iron Garnets. IEEE Trans. on Mag., Vol. Mag-12, No. 4, July 1976, 292.

3. Fleming, D. L.; Lund, R. E.: Magneto-optic Bubble Domain Spatial Light Modulator. SPIE, Vol. 128, 1977, 230.

4. Dimmock, J. O.; Huorwitz, C. E.; Reed, T. B.: Infrared Transmission Magnetic Birefringence and Faraday Rotation in EuO. APL, Vol. 14, No. 2, 15 Jan., 1969.

5. Ahn, K. Y.; Suits, J. C.: IEEE Trans. on Mag., Vol. MAG-3, Sept., 1967.

6. Shafer, A. W.; Torrance, J. B.; Penney, T.: Correlations of Infrared Absorption, Conductivity, and Stoichiometry in EuO. Magnetism and Magnetic Materials, C. D. Graham, Jr. (ed.), AIP, 1971.

7. Soref, R. A.; Kestigian, M.: Development of Liquid Crystal and Magnetic Stripe-Domain Multimode Optical Switches. Rome Air Development Center, Report SRC-CR-80-25, 1980.

8. Nelson, G. L.; Harvey, W. A.: Optical Absorption Reduction in $Bi_1Lu_2Fe_5O_{12}$ Garnet Magneto-Optical Materials, JAP, February 1982. (To be published)

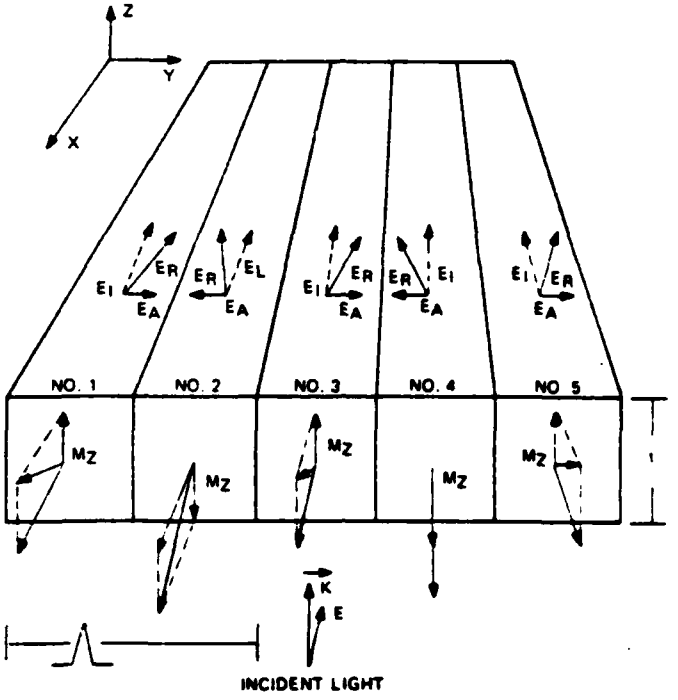

Figure 1.- Magneto-optic diffraction grating.

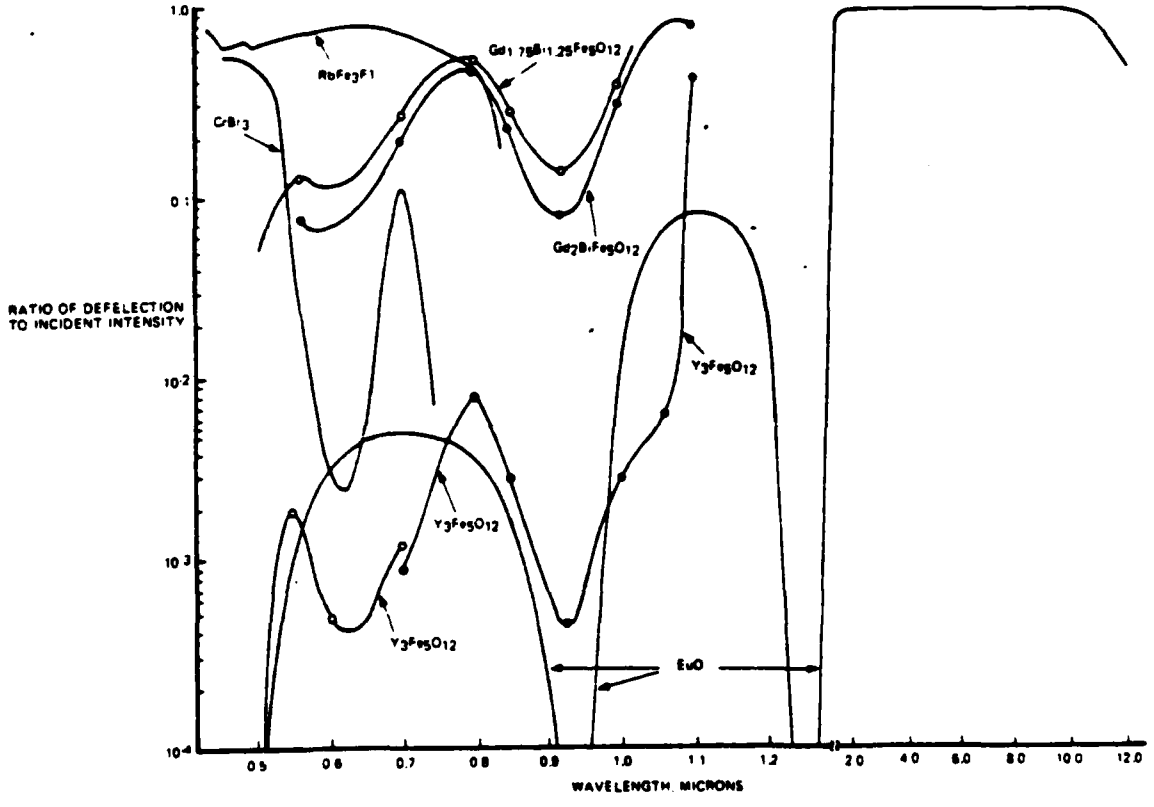

Figure 2.- Calculated diffraction efficiency of stripe domain materials.

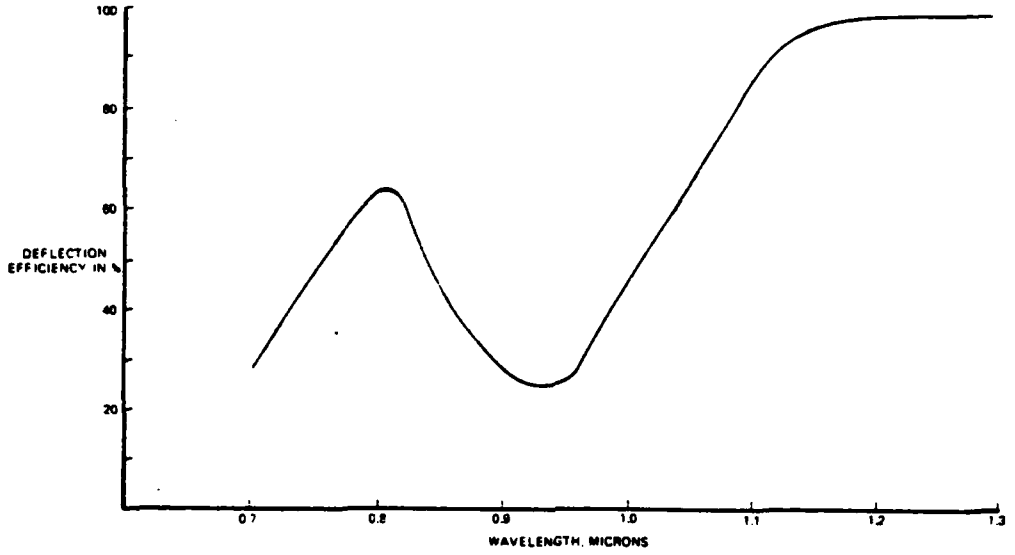

Figure 3.- Calculated diffraction of optimized garnet film.

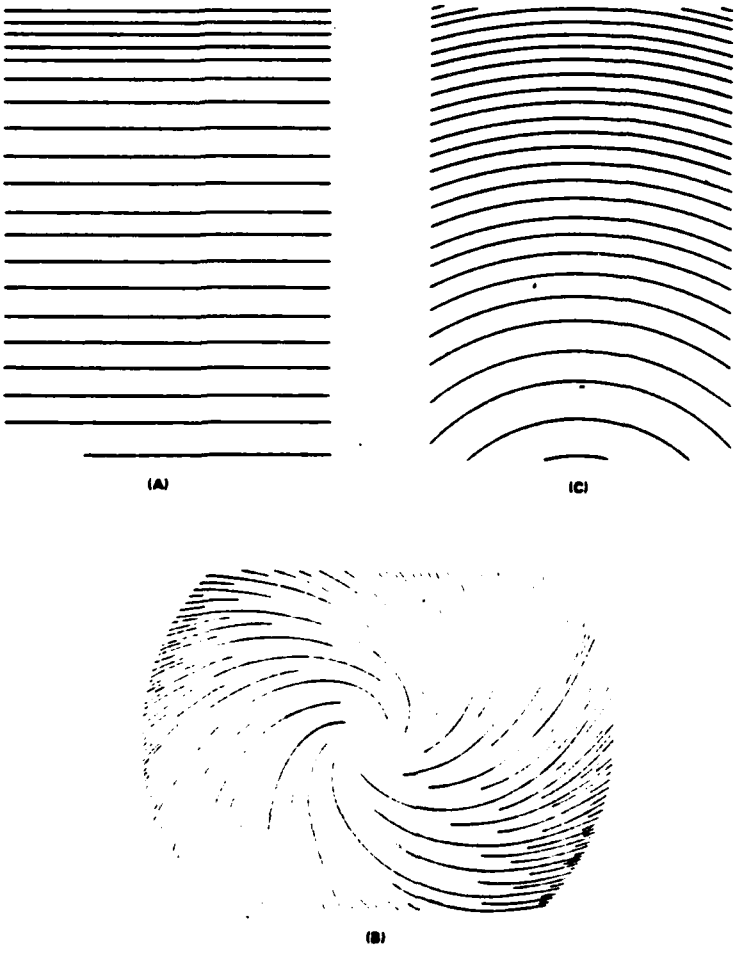

Figure 4.- Adaptive optic configurations. (a) Compression/expansion. (b) Image rotator (c) Fresnel zone plate.

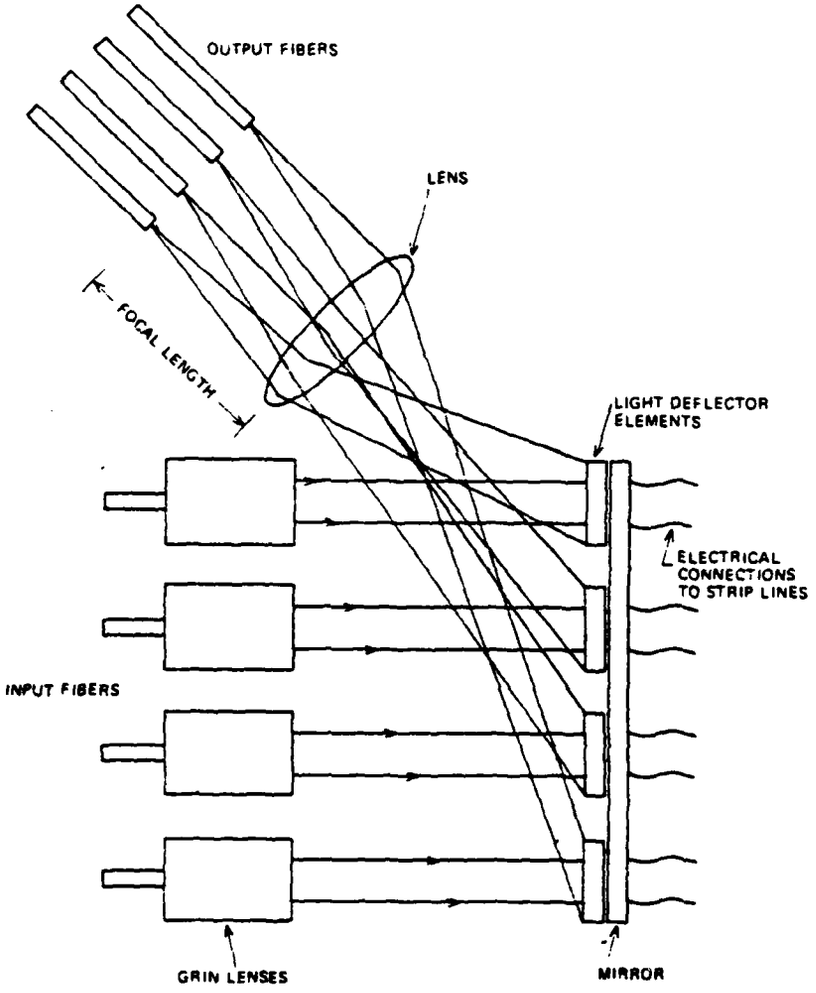

Figure 5.- N X M swithboard.

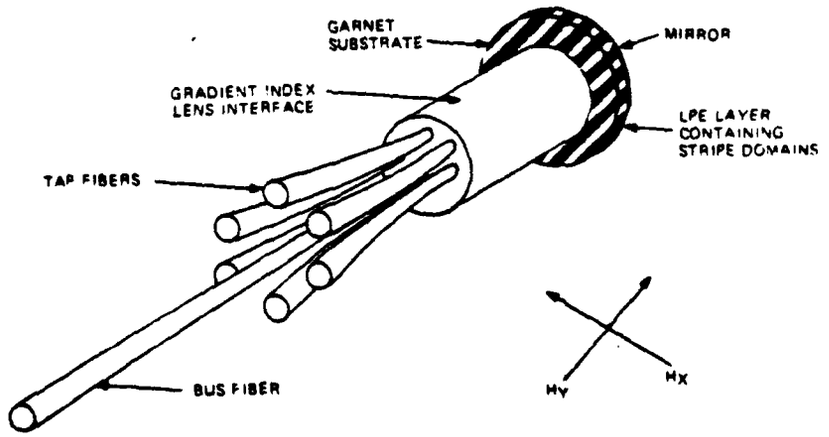

Figure 6.- Fiber optic switch.

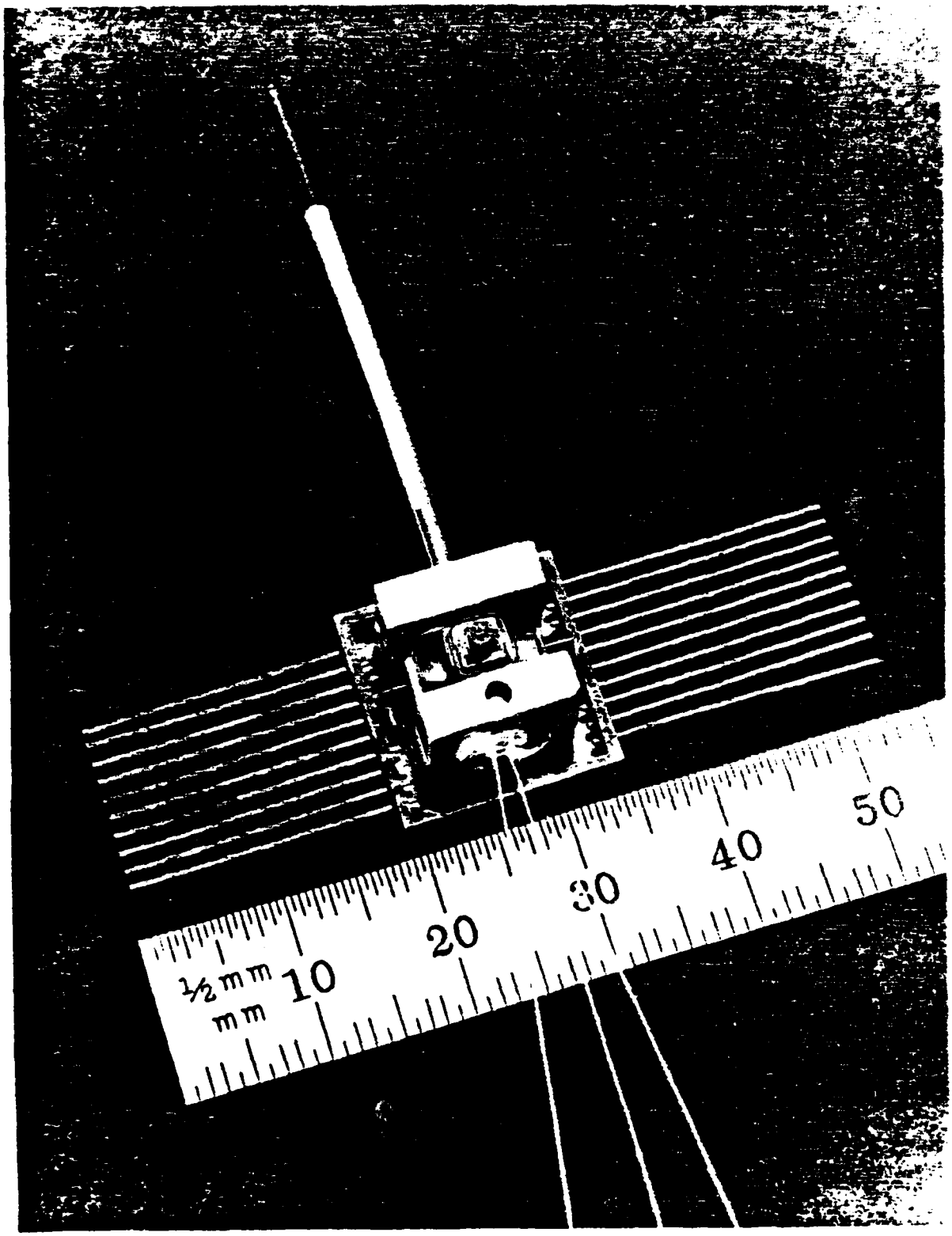

Figure 7.- Operational model of 1 x 3 garnet fiber optic switch.

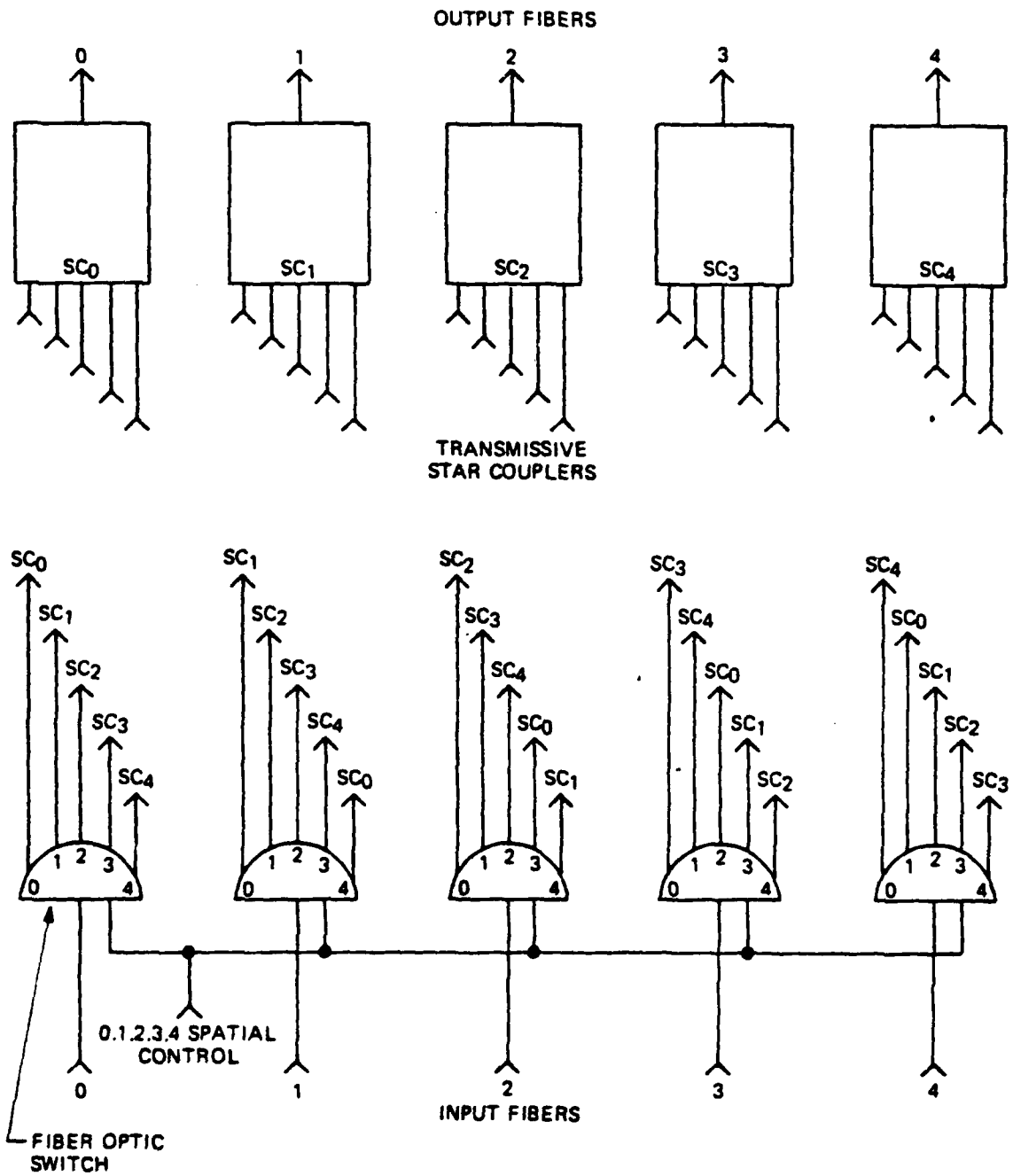

Figure 8.- Residue arithmetic modulo 5 adder.

ALTERABLE GRATING

FIBER-OPTIC SWITCH

SPERRY UNIVAC

DEFENSE SYSTEMS

APPLIED OPTICS

Vol. 20, No. 20

Reprinted from Applied Optics, Vol. 20, page 3566, October 15, 1981

Alterable grating fiber-optic switch

G. F. Sauter, R. W. Honebrink, and J. A. Krawczak

This paper describes a solid state high speed fiber-optic switch based on dynamically alterable magnetic stripe domains that occur naturally in epitaxial films of rare-earth iron garnet. The array of stripe domains acts collectively as a Faraday effect phase diffraction grating that deflects visible and infrared radiation. Electrically derived magnetic fields in the plane of the film steer incident light from an input fiber to one of several output fibers. Reciprocity and wavelength sensitivity can be exploited for systems applications. Both theoretical and experimental results are presented.

I. Introduction

Many authors[1–6] have reported on the fabrication of optical switches that have utility in fiber-optic communications links. This paper reviews the magnetooptic garnet fiber-optic switch. The principle of operation will be described, design criteria presented, experimental results given, and systems potential addressed.

II. Magnetic Stripe Domain Diffraction Gratings

The active component[7] in this optical switch utilizes a dynamically controllable solid state phase diffraction grating that is found in some magnetic materials. Several papers[8,9] have discussed the operating principles of the stripe domain grating structure; thus, only a brief description will be presented here.

One of the natural magnetic states of bismuth garnet epitaxial films on transparent substrates of gadolinium gallium garnet is an array of equal width juxtaposed regions of alternating magnetic vector. This is schematized in Fig. 1 where the relevant magnetic and optical vectors have been included. The width of each stripe w is between 0.5 and 5 μm, the length can extend to centimeters, and the film thickness is usually <20 μm. The parallel and antiparallel nature, $\pm M_\perp$, of the periodic normal components of the magnetization, together with the enhanced Faraday effect in bismuth garnet, produce phase diffraction of an incident plane wave of visible or near-infrared radiation. This is because the direction of the optical electric field is rotated clockwise in up stripes and counterclockwise in down stripes as the wave progresses through the material. Thus, the emerging electric vector fluctuates at the spatial frequency of the magnetic stripe domains. Because the Faraday effect is a manifestation of circular magnetic birefringence, the interaction of the light with the garnet is independent of incident polarization. Figure 2 is a photograph of a stripe array in the ferrimagnetic film, YIG, observed under Faraday microscopy.

The first-order diffracted light appears in the far field at angles of $\pm\theta = \sin^{-1}[\lambda_0/(\Lambda n)]$, where λ_0 is the free-space wavelength of the light, $\Lambda = 2w$ is the periodicity of the grating, and n is the index of the far-field medium. Light intensity in each of the two first-order conjugate beams is governed by the rule

$$\frac{I_1}{I_0} = 0.405 \exp(-\alpha T) \sin^2 FT,$$

where α is the optical absorption of the material, T the film thickness, and F the specific Faraday rotation. As much as 81% of the incident intensity can be passed to the first order if the material is lossless and if the Faraday effect produces an exact ±90° rotation of the optical electric field. Undeflected light provides a zeroth-order component to the output of the epitaxial crystal. In practice present bismuth garnet films exhibit a single-pass diffraction efficiency of 5%[10] at 0.633 μm and 1% in the near infrared. At 1.15 μm the material is virtually transparent.

Because of the continuity of the in-plane component of the magnetization, the grating is alterable, both in orientation and in periodicity, by a magnetic field in the plane of the film. Typically, this field is derived from two orthogonal sets of coils in close proximity to the film. The field strength is similar to what is required for electron beam deflection in cathode ray tubes although much lower electrical power is required since the field volume can be <1 cm^3.

The authors are with Sperry Univac, Defense Systems Division, St. Paul, Minnesota 55165.

Received 8 June 1981.
0003-6935/81/203566-07$00.50/0.

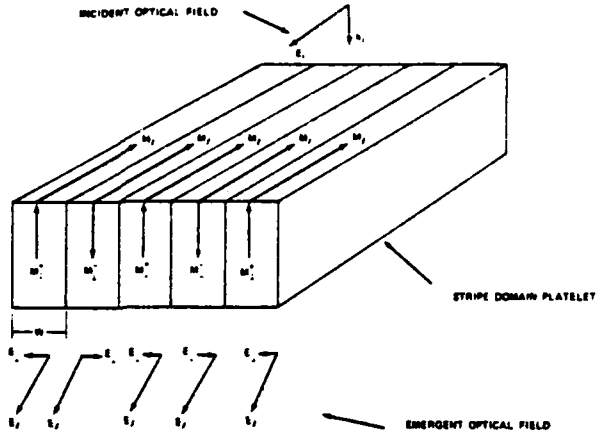

Fig. 1. Pertinent optical and magnetic vectors in a stripe domain material.

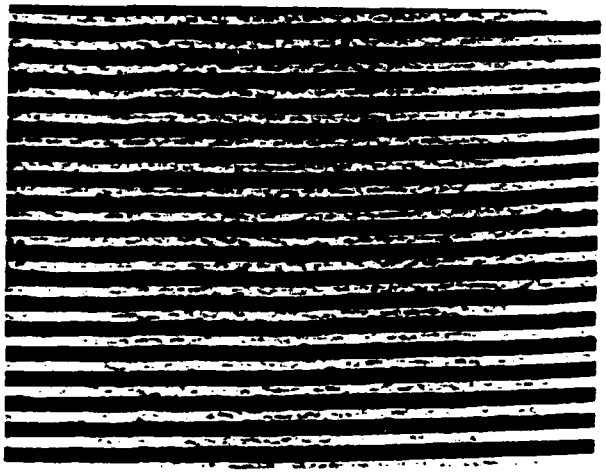

Fig. 2. Stripe domains in YIG. Domain width is 6 μm.

III. Fiber-Optic Switch

Magnetooptic activity at the salient fiber-optic wavelengths, along with magnetic control of an intrinsic grating in garnet films, is the basis for a multiport in-line fiber-optic switch. Figure 3 depicts such a switch using a stripe domain garnet crystal controlled with in-plane fields H_x and H_y. Light from a laser or LED propagating in the input fiber enters the stripe domain grating and is diffracted to the selected output fiber position. The output fibers are arranged in a cone at an angle corresponding to the zero field diffraction position. Having the fibers arranged this way insures that no electrical power is required following the grating rotation to the selected output fiber. It also insures continued communication in the event power is lost. To produce a grating rotation to angle θ the field intensities from the coils are $H_k < H_T = (H_x^2 + H_y^2)^{1/2}$, and $\tan\theta = H_y/H_x$, where H_k is the in-plane saturation field of the garnet crystal. The amplitude of the resultant field is made larger than H_k to saturate the film momentarily. Upon removal of the field, stripe domains form spontaneously in the desired direction.

IV. Theory

To explore the cross talk and signal to noise of such a switch, a model was devised that is based on beam spreading considerations as shown in Fig. 4. Here power P_1 is brought to the input of the film through a conventional bus fiber. Since some of P_1 is absorbed, some is diffracted and some diverges because of the finite thickness of the substrate, a quantity P_2 flows into the output bus fiber. P_2 is given by

$$P_2 = P_1 \exp(-\alpha T) I(r_{10})(1 - 2\eta)\frac{A_2}{A_{10}},$$

where A_2 is the area of the output beam intercepted by the bus fiber, A_{10} is the total area of the emergent beam at the bus fiber intercept, $I(r)$ is the intensity distribution of the beam, and η is the plus or minus first-order diffraction efficiency of a lossless stripe domain crystal.

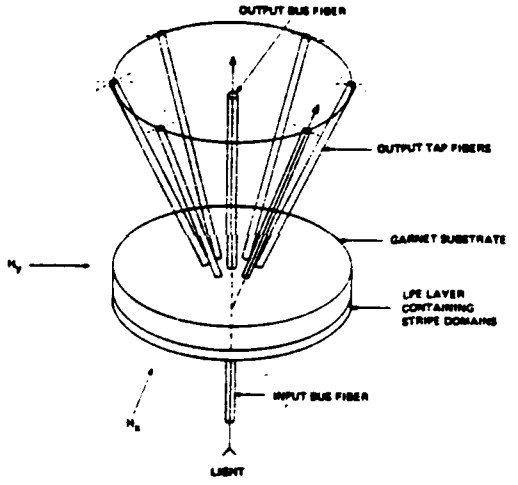

Fig. 3. Stripe domain fiber-optic switch.

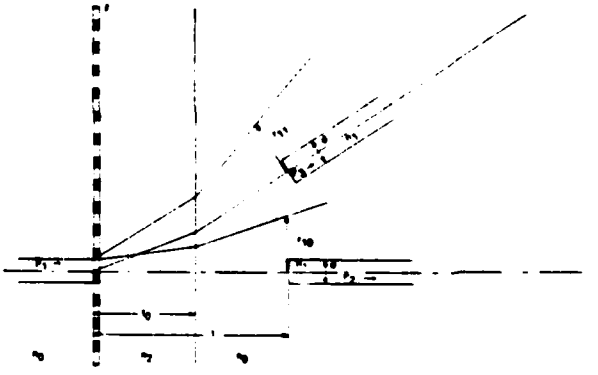

Fig. 4. Geometric optics model of garnet fiber-optic switch.

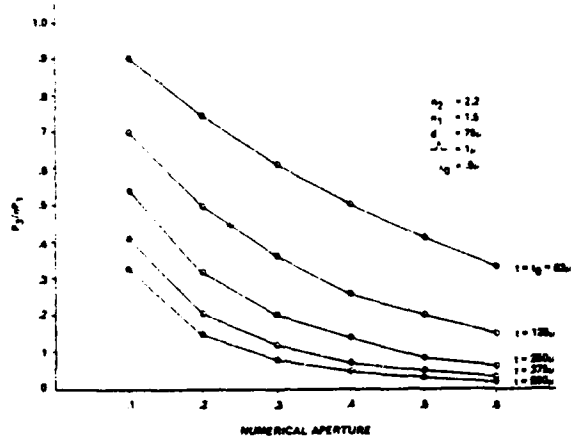

Fig. 5. Numerical aperture dependent power transfer from bus to tap.

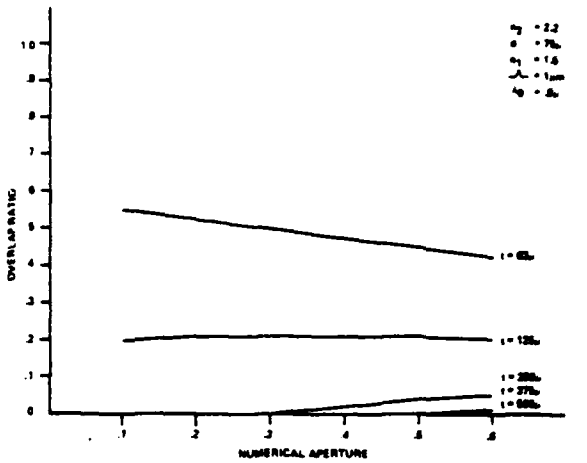

Fig. 6. Numerical aperture dependent zeroth-order overlap at the taps.

Analysis of the geometry reveals that

$$r_{10} = \frac{d}{2} + t_0 \tan\left(\sin^{-1}\frac{\text{N.A.}}{n_2}\right) + (t - t_0)\tan\left(\sin^{-1}\frac{\text{N.A.}}{n_0}\right),$$

where n_2 is the index of the garnet, n_0 is the index of the surrounding medium, N.A. is the numerical aperture of the fibers, and d is the fiber diameter. The first-order light also diverges before encountering the output tap fiber. Thus the actual switched power captured by P_3 is given by

$$P_3 = P_1\eta \exp(-2T) I(r_{11}) \frac{A_3}{A_{11}}.$$

A_3 and A_{11} are analogous to A_2 and A_{10}, and

$$\begin{aligned} r_{11} = {} & \left[\frac{d}{2} + t_0 \tan\left[\sin^{-1}\left(\frac{\text{N.A.}}{n_2} + \frac{\lambda_0}{\Lambda n_2}\right)\right] - t_0 \tan\left(\sin^{-1}\frac{\lambda_0}{\Lambda n_2}\right)\right] \\ & \times \left[\cos\left(\sin^{-1}\frac{\lambda_0}{\Lambda n_0}\right)\right] + \left[(t - t_0)/\cos\left(\sin^{-1}\frac{\lambda_0}{\Lambda n_0}\right)\right. \\ & - \frac{d}{2} - t_0 \tan\left[\sin^{-1}\left(\frac{\text{N.A.}}{n_2} + \frac{\lambda_0}{\Lambda n_2}\right)\right] \\ & + t_0 \tan\left(\sin^{-1}\frac{\lambda_0}{\Lambda n_2}\right)\left]\left[\tan\left[\sin^{-1}\left(\frac{\text{N.A.}}{n_0} + \frac{\lambda_0}{\Lambda n_0}\right)\right]\right. \\ & \left. - \sin^{-1}\left(\frac{\text{N.A.}}{n_2} + \frac{\lambda_0}{\Lambda n_2}\right)\right]. \end{aligned}$$

For example, suppose that P_1 has a Gaussian distribution in the output bus fiber plane and r_{10} and r_{11} are taken as 4σ (approximately $10^{-4} I_0$). Then

$$I(r_{10})\frac{A_2}{A_{10}} \propto 1 - \exp\left[\frac{-2d^2}{r_{10}^2(t)}\right].$$

$$I(r_{11})\frac{A_3}{A_{11}} \propto 1 - \exp\left[\frac{-2d^2}{r_{11}^2(t)}\right].$$

Thus,

$$P_2(t) = P_1\eta \exp(-\alpha T)\left\{1 - \exp\left[\frac{-2d^2}{r_{10}^2(t)}\right]\right\}.$$

$$P_3(t) = P_1\eta \exp(-\alpha T)\exp\left[\frac{-2d^2}{r_{11}^2(t)}\right].$$

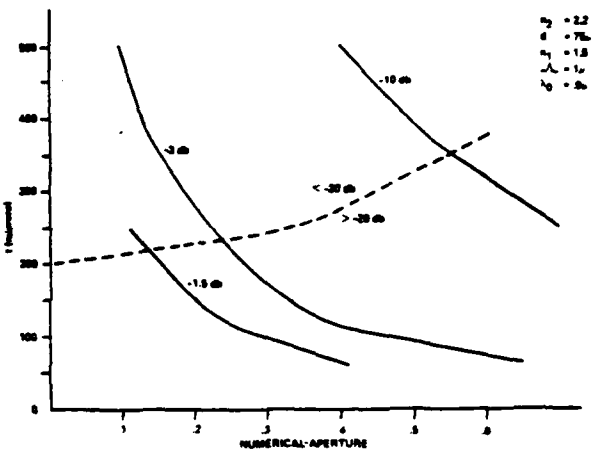

Fig. 7. Numerical aperture dependent cross talk/insertion loss tradeoff.

For a uniform intensity beam distribution

$$P_2(t) = P_1 \exp(-\alpha T)(1 - 2\eta)\frac{d^2}{4r_{10}^2}.$$

$$P_3(t) = P_1 \exp(-\alpha T)\eta\frac{d^2}{4r_{11}^2}.$$

From this model a set of curves was obtained that can be used to predict the performance of a garnet fiber-optic switch with practical fibers. Specifically the calculations assume a free-space wavelength of 0.9 μm, a garnet index of 2.2, an orientable grating with periodicity Λ, 75-μm diam fibers, and a uniform intensity beam profile.

Figure 5 shows the fraction of the power $P_3/\eta P_1$ coupled from the input fiber to the output tap fiber as a function of numerical aperture for various thicknesses of the stripe domain crystal. Figure 6 shows the overlap ratio as a function of numerical aperture of the ellipse formed by the entrance of the output fiber and the circle

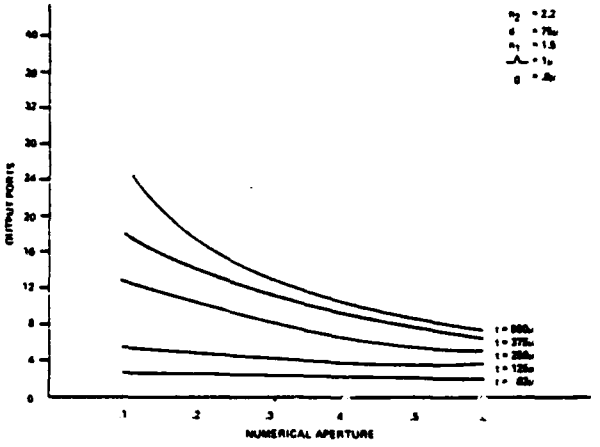

Fig. 8. Numerical aperture dependent fan out.

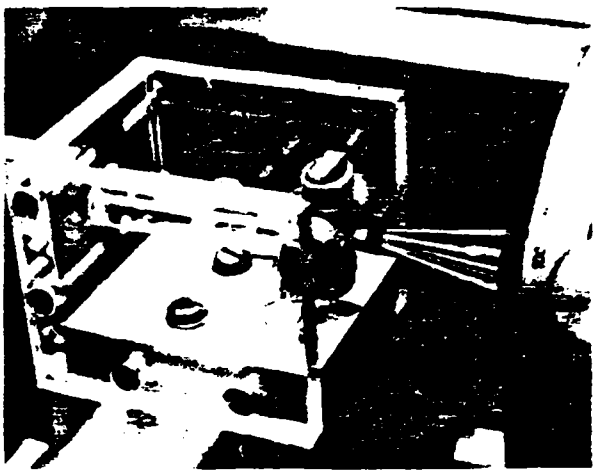

Fig. 9. Experimental apparatus.

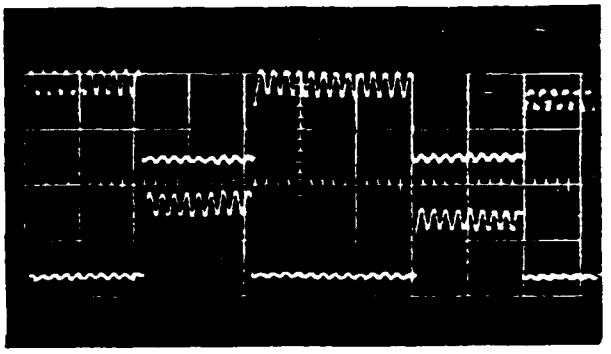

Fig. 10. Tap fiber signals.

formed by the zeroth-order beam as it intersects the crystal substrate surface. This overlap ratio multiplied by the power remaining in the zeroth-order beam constitutes cross-talk noise in the nonselected output fibers. Figure 7 illustrates the same data of Figs. 5 and 6, plotted to show possible design points under the constraints of allowed insertion loss and cross-talk power, e.g., a 3-dB switch with less than −20 dB of cross-talk noise requires a numerical aperture <0.24 and a crystal thickness (LPE layer plus substrate) >225 μm. These are realizable values. Another source of cross-talk noise is from one output fiber to another. Figure 8 shows the number of output ports that can be placed on a crystal under the constraint of no overlap of the ellipses formed by the diffracted beam at the crystal substrate surface. For this example, eight output ports could be accommodated.

V. Experiments

Figure 9 shows a working model of a one input and two output in-line fiber-optic switch. The plastic cone holds the two output fibers in place at the zero applied field diffraction angle of the particular crystal used. The two output fibers are 90° apart. An intensity modulated He–Ne laser beam was focused on the input end of a 62.5-μm core fiber with a 10× objective lens. The input fiber was attached normal to the crystal with an index matching fluid. The output signal from each of the 62.5-μm core output fibers was detected with photodiodes and amplified. The x,y coils were alternately gated with 1-msec pulses to switch from one fiber to the other. Figure 10 shows the signals obtained from the two channels.

Experimental data on the coupling efficiencies of the input-to-output bus fiber and the input-to-tap fiber, as a function of input-to-output fiber separation, were obtained from the apparatus of Fig. 9, with 0.18-N.A. 75-μm core fibers, and a crystal with a grating constant, $\Lambda = 3.4$ μm. These data are superposed on theoretical expectations for a Gaussian power distribution in Figs. 11 and 12, respectively. In Fig. 13 the measured SNR as a function of input-to-tap fiber separation shows the positive effect of reducing the grating constant (or increasing the optical wavelength). Since the diffracted beam is at a greater angle the tap fibers do not intercept as much of the zeroth-order power. Thus the SNR can be improved substantially.

Recently, a multiport tap switch was constructed packaged in a double width dual in-line header and capable of operating at the more suitable 0.85-μm wavelength. The package consists of one input fiber, one bus line output fiber, two tap fibers, the crystal, and an x,y set of drive coils. Figure 14(a) shows the parts of the switch prior to assembly. The coil form was constructed from nylon and contains cylindrical ferrite rods on each pole for field enhancement. The coils were designed to switch in 1 μsec with a 1-A current pulse. The three output fibers are held in place with a mechanical ferrule and a 75-μm thick disk with three 125-μm etched holes for proper fiber alignment. Figure 14(b) is a close-up of the assembled switch containing a garnet crystal with a stripe domain periodicity of 3.4 μm, while Fig. 14(c) shows the experimental apparatus for positioning the various elements of the switch. Results of measurements on this switch are compiled in Table I.

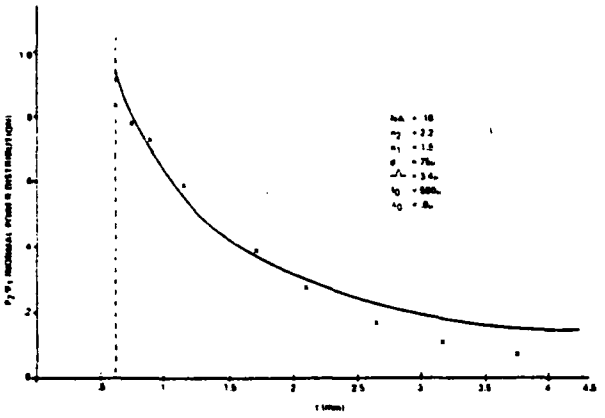

Fig. 11. Theoretical and experimental bus-to-bus power transfer.

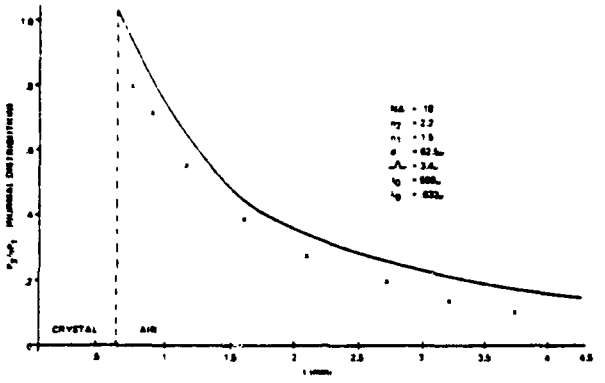

Fig. 12. Theoretical and experimental bus-to-tap power transfer.

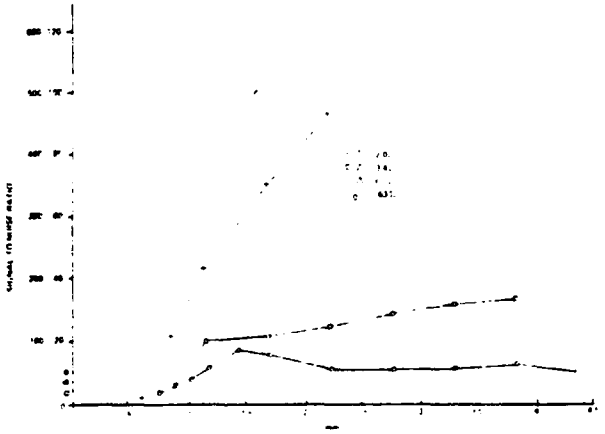

Fig. 13. Tap fiber signal-to-noise ratio.

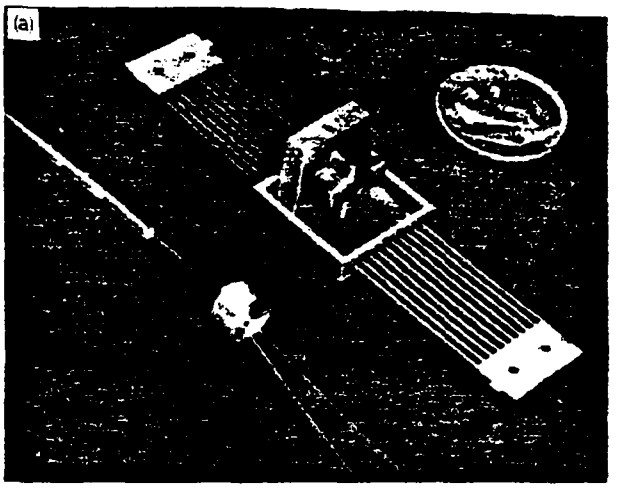

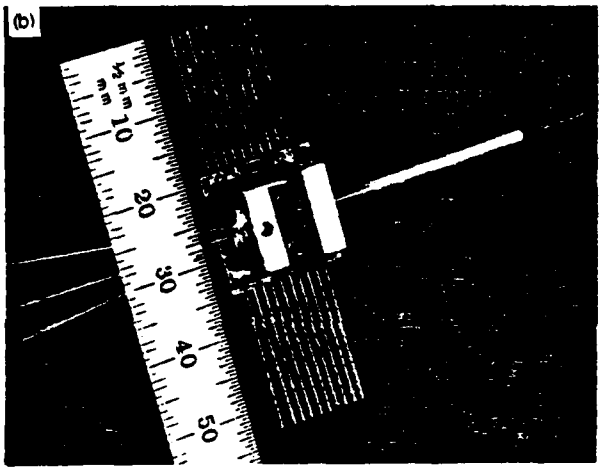

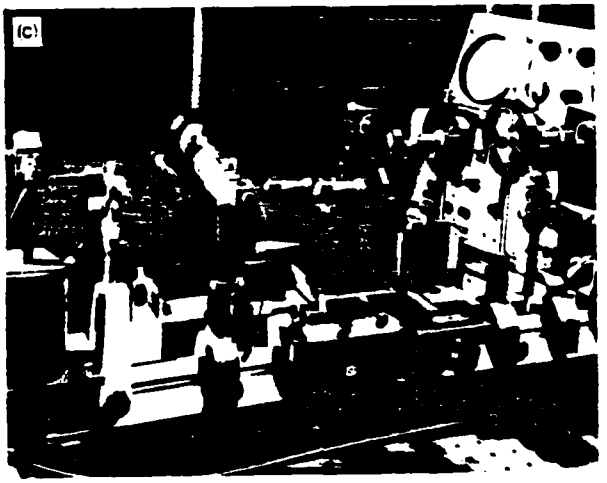

Fig. 14. Operational switch: (a) exploded view; (b) assembled view; and (c) apparatus.

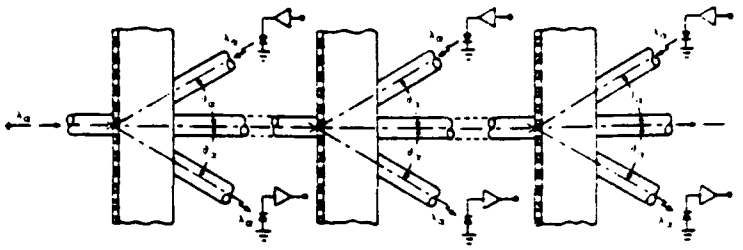

Fig. 15. Bus organized bidirectional system.

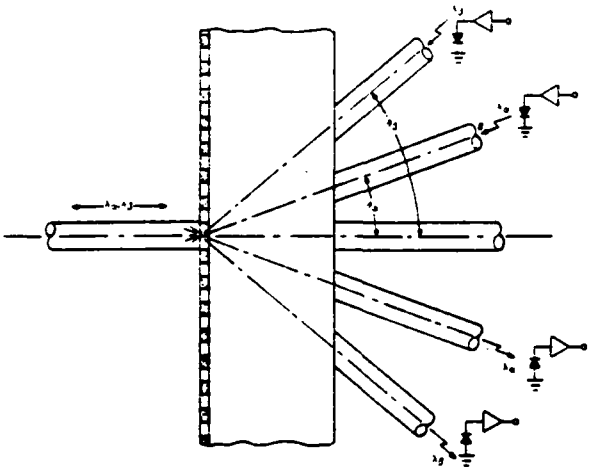

Fig. 16. Wavelength MUX and DEMUX.

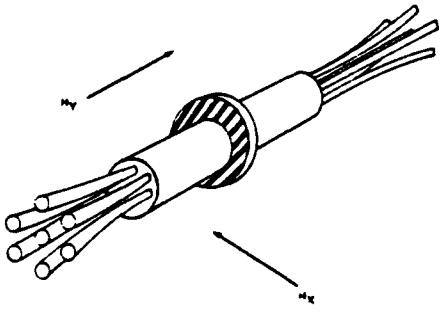

Fig. 17. Gradient-index–lens interface.

Table I. Design Results

	Predicted	Measured
Fraction of power available coupled to bus fiber	0.62	0.53
Fraction of power available coupled to tap fiber	0.55	0.51
Signal-to-noise ratio	16:1	8:1
Switching conditions	1 A @ 1 μsec	0.6 A @ 2 μsec

VI. Systems

In its present form the switch is in a receive only configuration and accepts just one optical wavelength. To provide two-way communications additional components must be added. Since the grating is reciprocal a signal transmitted from one of the output tap ports will propagate along the input fiber back to the source. Several possible operating configurations are shown in Figs. 15–17. Figure 15 shows tap fibers at the conjugate beam positions in a bus cascaded switch arrangement with bidirectionality. Multiplexing and demultiplexing can also be realized, as depicted in Fig. 16. Different wavelengths are mapped into distinctly different θs by the grating. In Fig. 17 a two-way switch[11,12] based on the combination of a garnet film with input and output Selfoc lenses is suggested. This would facilitate packaging, reduce zeroth-order cross talk, and allow nearly all first-order light to be picked up by the output tap fibers in single or multiwavelength systems.

VII. Summary

An optical switch based on alterable magnetic stripe domains in bismuth garnet films has been described. Its advantages include (1) solid state nonmechanical nature; (2) operation at important fiber-optic wavelengths; (3) low electrical drive power; (4) power required only during switching; (5) switching times in the hundreds of nanoseconds; and (6) high fan out. Theoretical and experimental data have been presented, and several system configurations have been mentioned.

The authors would like to thank Gary Nelson and Bill Harvey of Sperry Univac for supplying the bismuth garnet films and also, Dick Soref, Don McMahon, and Mike Kestigian of Sperry Research Center for helpful discussions.

This work was sponsored in part by the U.S. Army Research Office, Research Triangle Park, N.C. Information contained herein does not necessarily reflect the position or policy of the U.S. Government, and no official endorsement should be inferred.

References

1. R. A. Soref and D. H. McMahon, Opt. Lett. 5, 147 (1980).
2. R. E. Wagner and J. Cheng, Appl. Opt. 19, 2921 (1980).
3. K. Mitsunaga, K. Murakami, M. Masuda, and J. Koyama, Appl. Opt. 19, 3837 (1980).
4. M. L. Dakss, U.S. Patent 3,990,780 (1976).
5. Communications Spectra, in Opt. Spectra 44 (Dec. 1980).
6. W. J. Tomlinson, R. E. Wagner, A. R. Strnad, and F. A. Dunn, Electron. Lett. 15, 192 (1979).
7. R. A. Soref, W. B. Spillman, and M. Kestigian, Proc. Natl. Electron. Conf. 33, 188 (1979).
8. T. R. Johansen, D. I. Norman, and E. J. Torok, J. Appl. Phys. 42, 1715 (1971).
9. G. B. Scott and D. E. Lacklison, IEEE Trans. Magn. MAG-12, 291 (1976).
10. R. A. Soref and M. Kestigian, RADC-TR-F 19628-79-C-0086, 79 (1980).
11. R. A. Soref, Sperry Research Center, Sudbury, Mass.; private communication.
12. W. J. Tomlinson, Appl. Opt. 19, 1127 (1980).

END

FILMED

2-83

DTIC